

**Stress, strain, deformation mechanisms,  
fluid pressure and fluid flow  
in deforming sedimentary rocks :  
what we can learn from integrated studies  
of folded strata**

Professor Olivier LACOMBE

---

**How to go farther than the simple geometrical  
and kinematic description of folds in the upper continental crust ?**

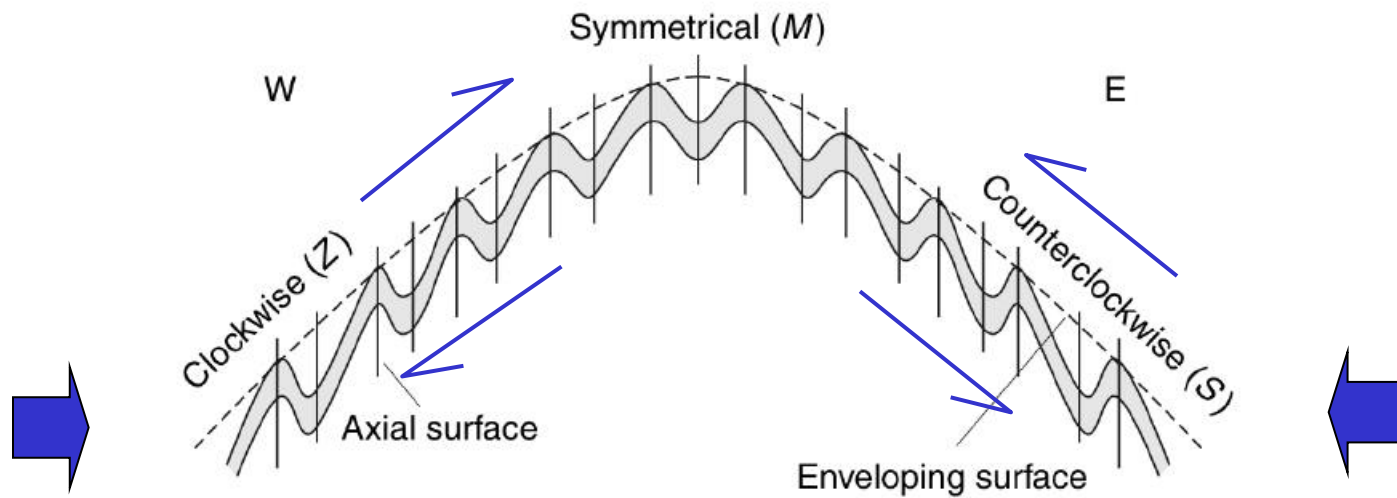






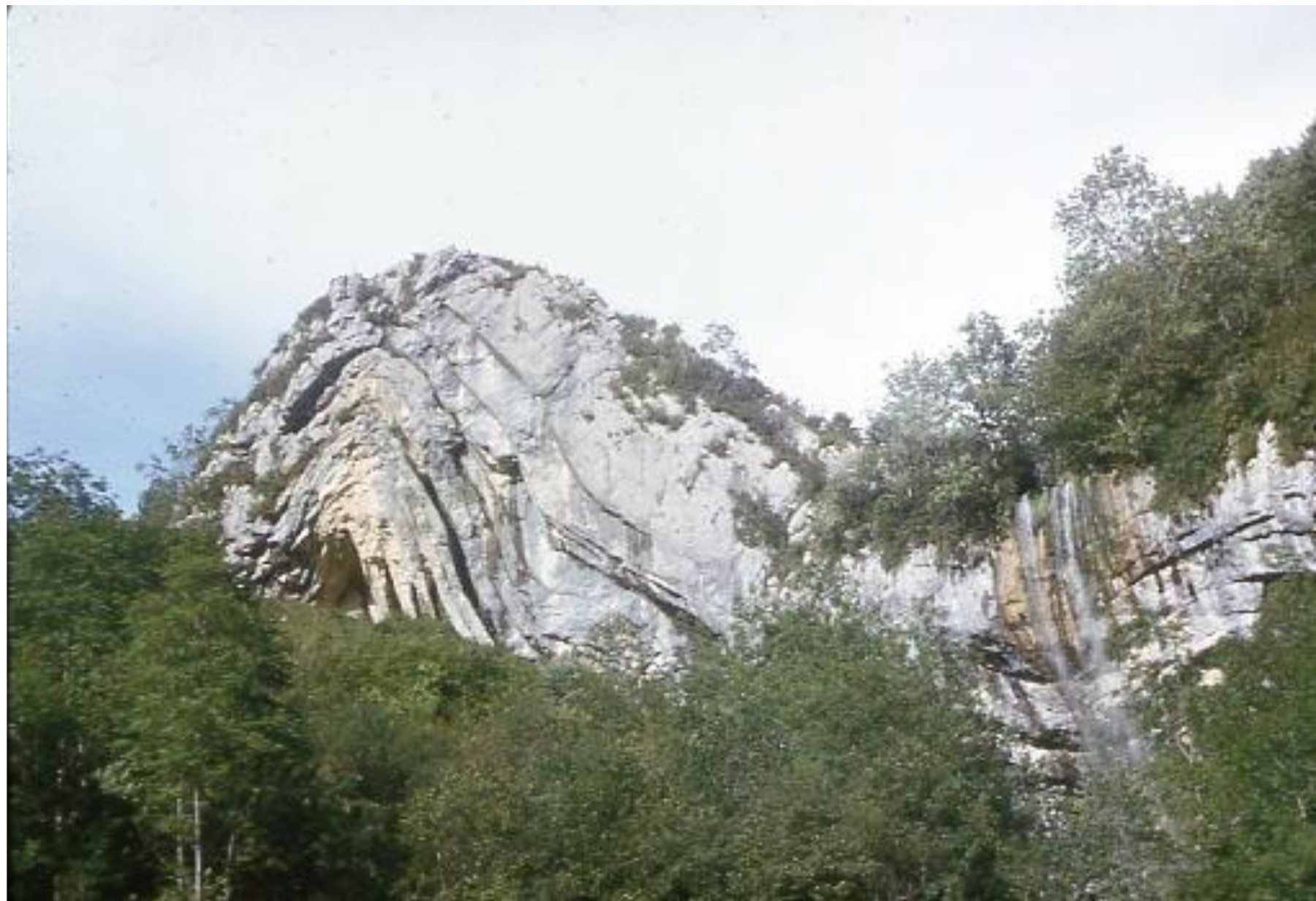


# Disharmony



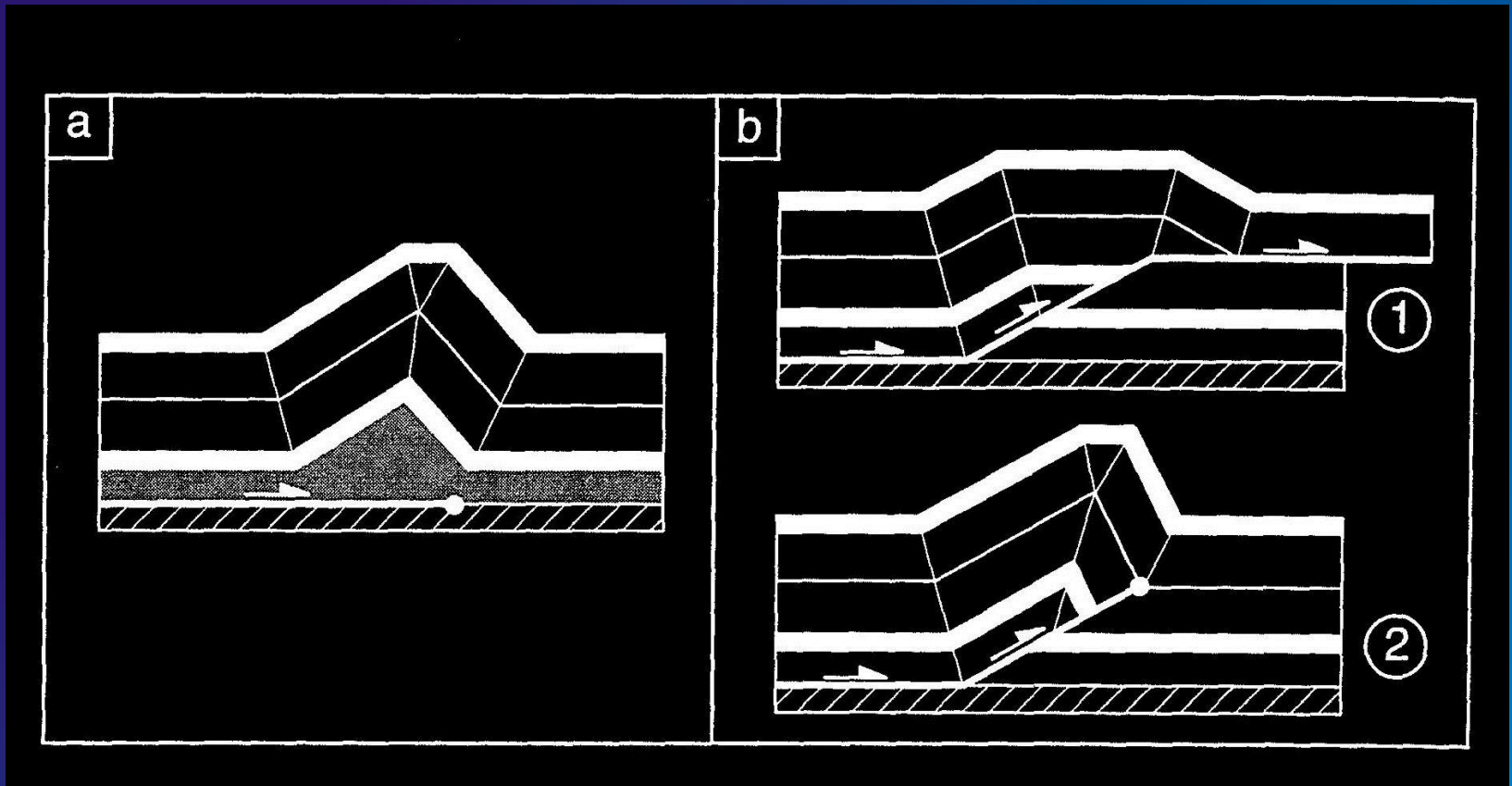












*« detachment fold » : strata are folded in order to accommodate sliding along the flat and deformation within the décollement level*

*« fault-bend fold » : folding above a ramp connecting obliquely two décollement levels*

*« fault-propagation fold » folding develops contemporaneous with ramp propagation*



## Décollement fold (Tadighoust, Ht Atlas, Maroc)

Courtesy D. Frizon de Lamotte





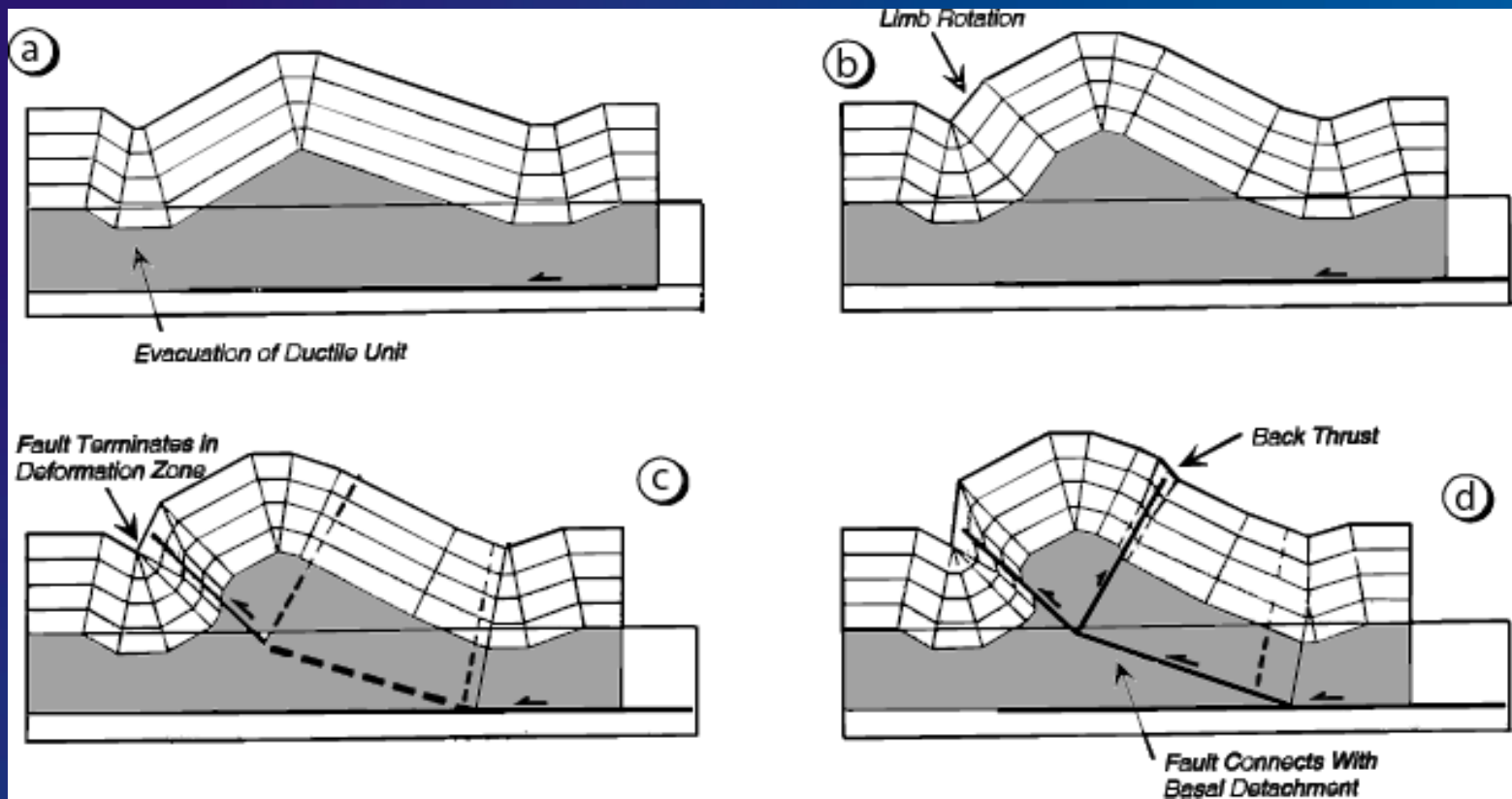
Courtesy D. Frizon de Lamotte



Faulted décollement fold (Tadighoust, Ht Atlas, Maroc)

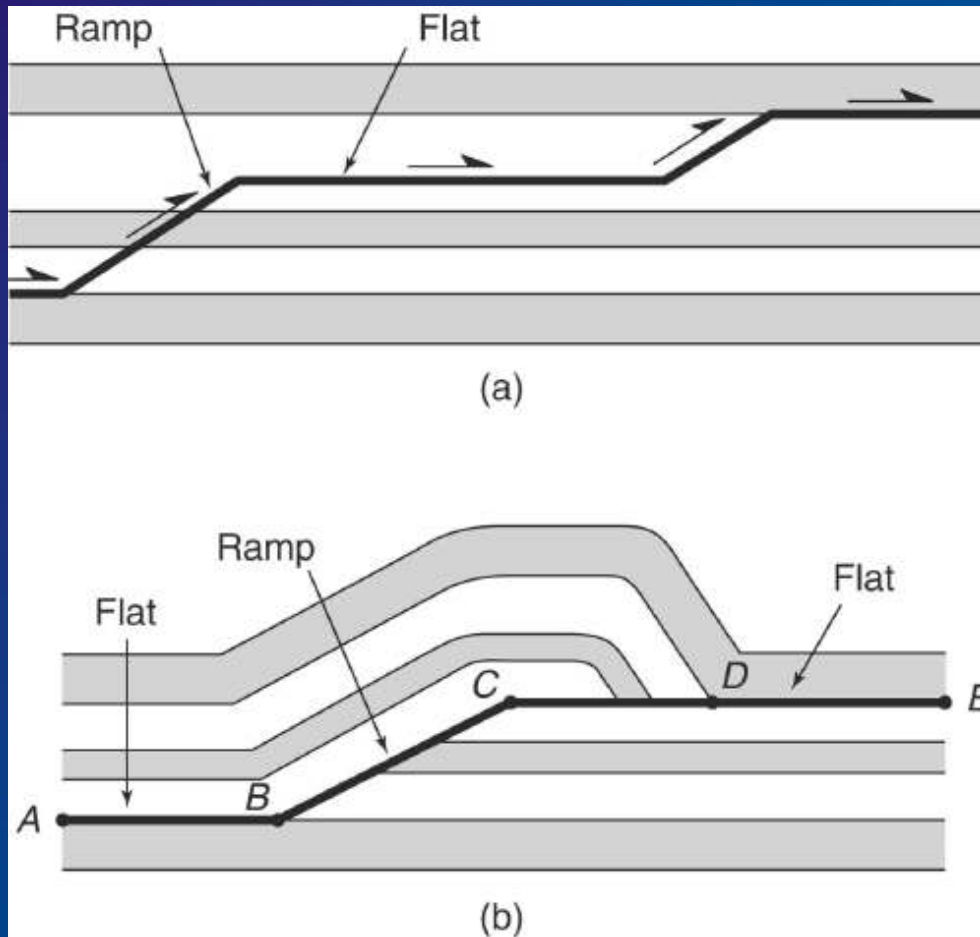
Courtesy D. Frizon de Lamotte



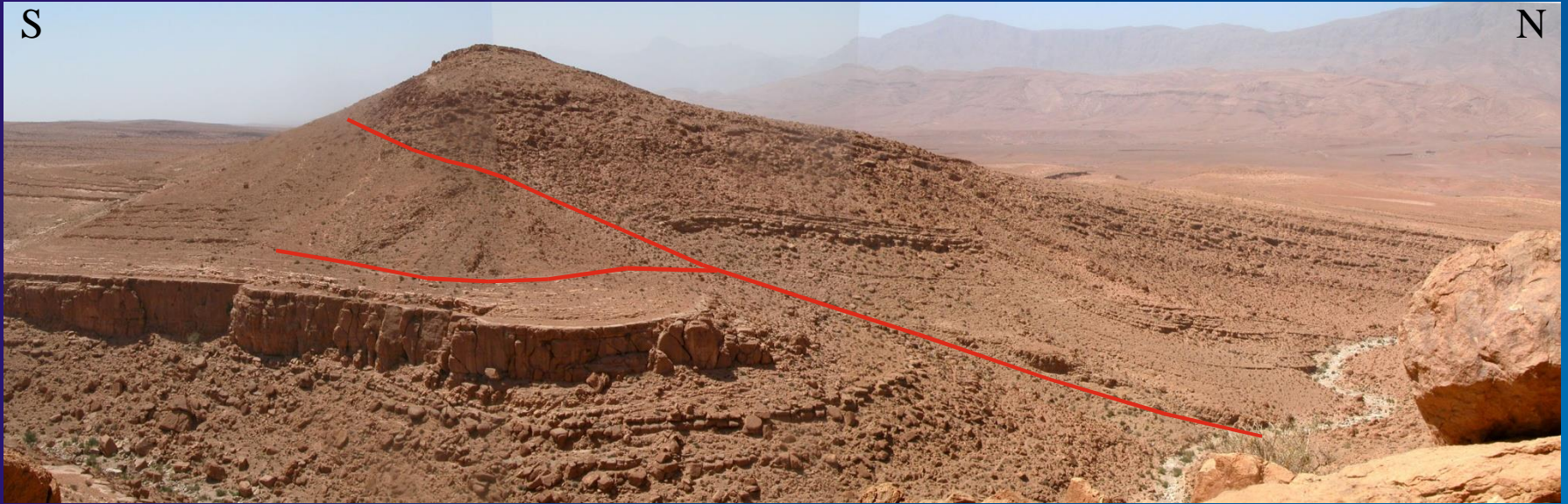


Development of late thrusts (Mitra, 2003)

# Fault-bend fold







Fault-bend fold, Tadighoust, Ht Atlas, Maroc.





*ramp*

*ramp*

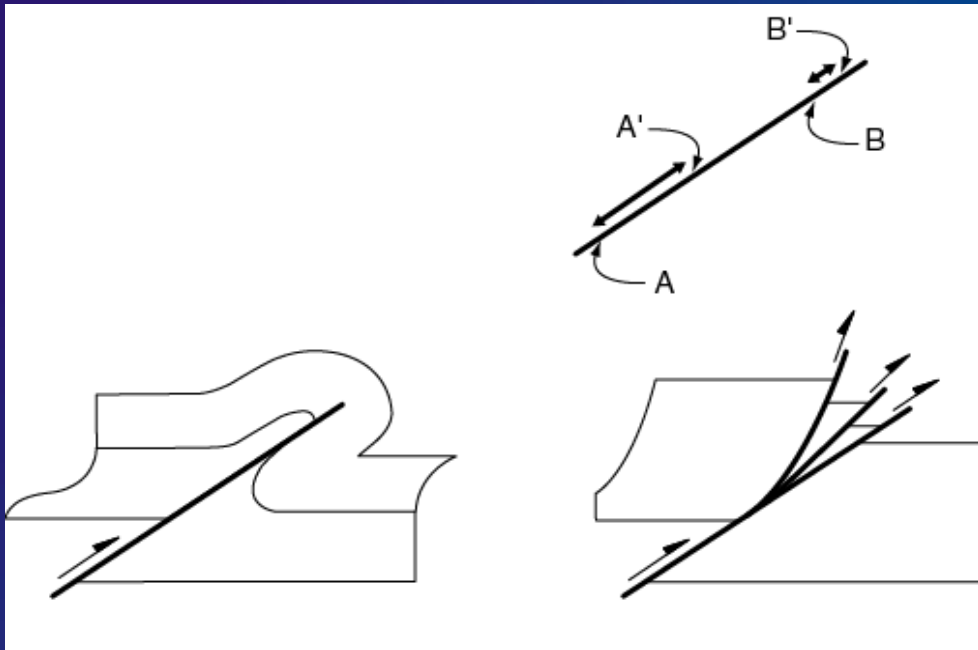
*flat*

*flat*

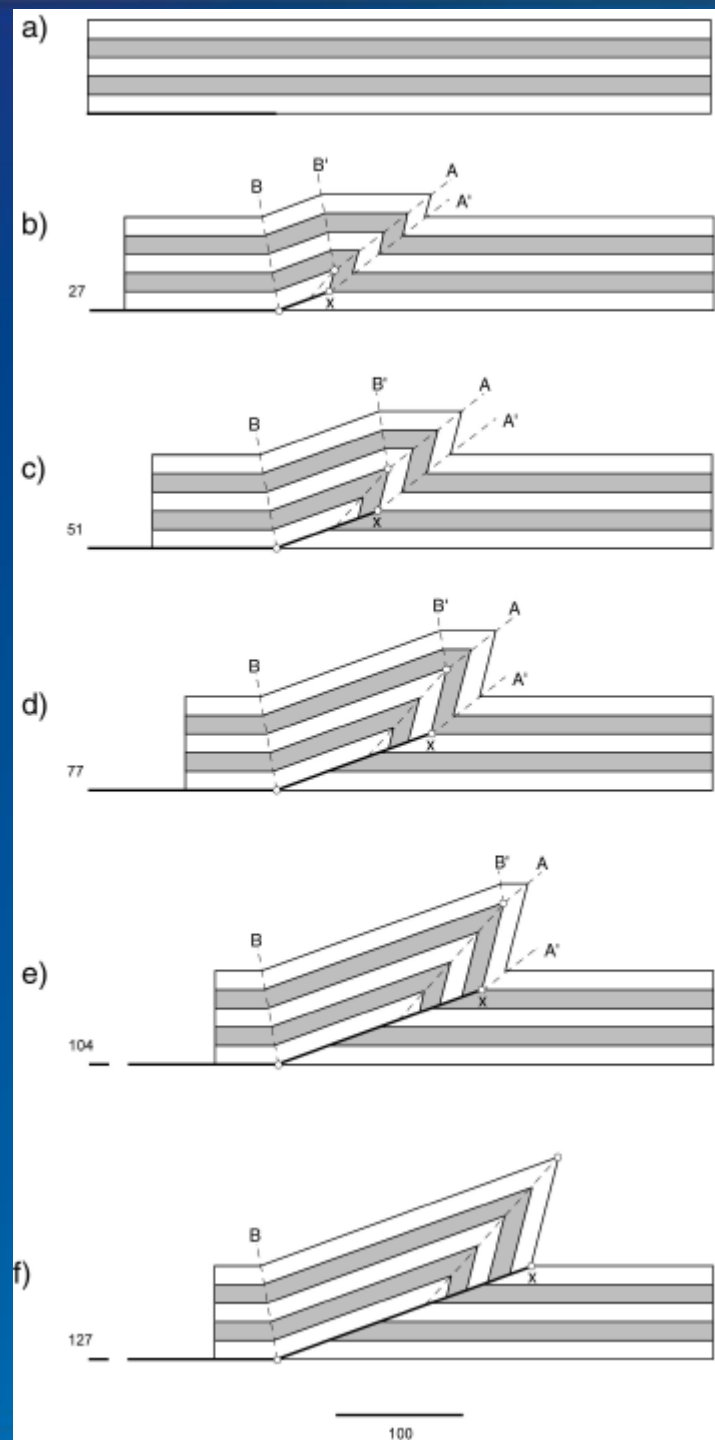
*flat*

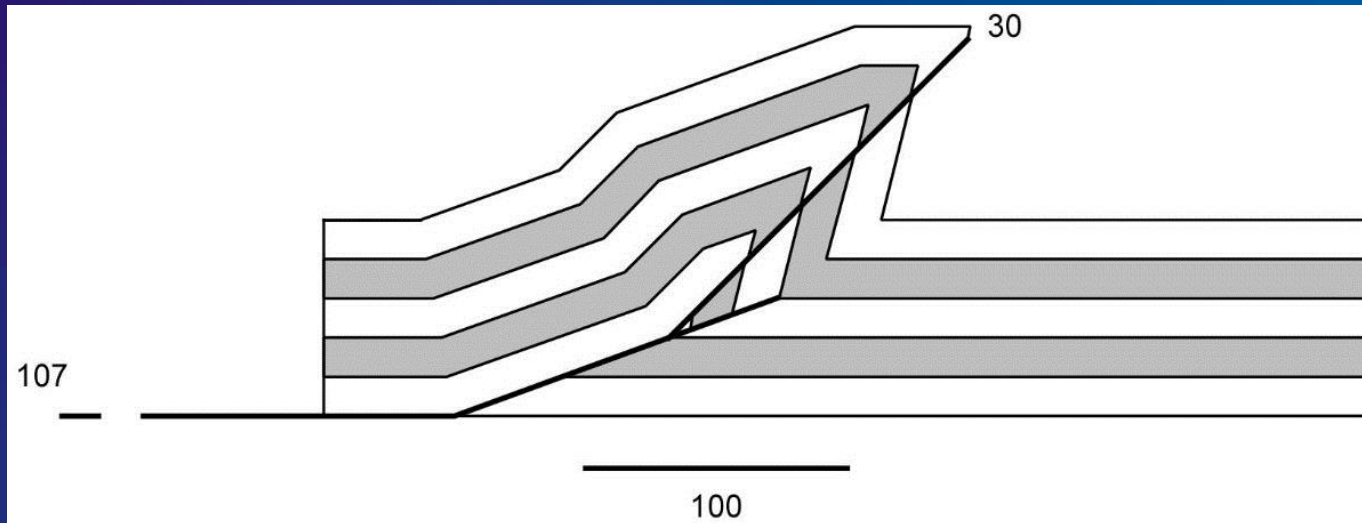


# Fault-propagation fold (Suppe, 1985)



How to accommodate a displacement gradient  
along a fault ?  
(modified after Dahlstrom, 1969)





Possible secondary evolution : rupture of  
the forelimb and development of a footwall  
syncline  
(Mercier et al., 1997)

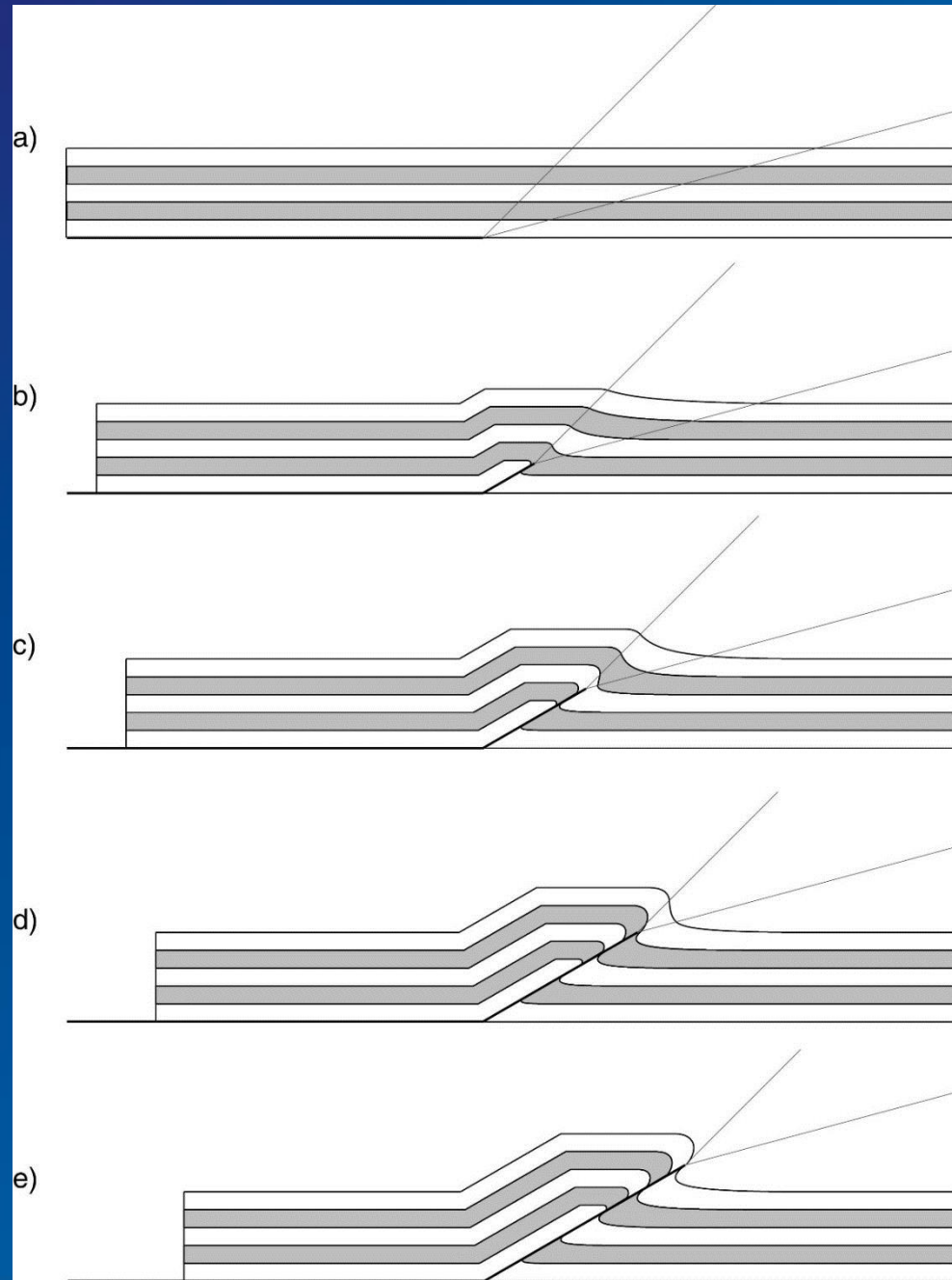


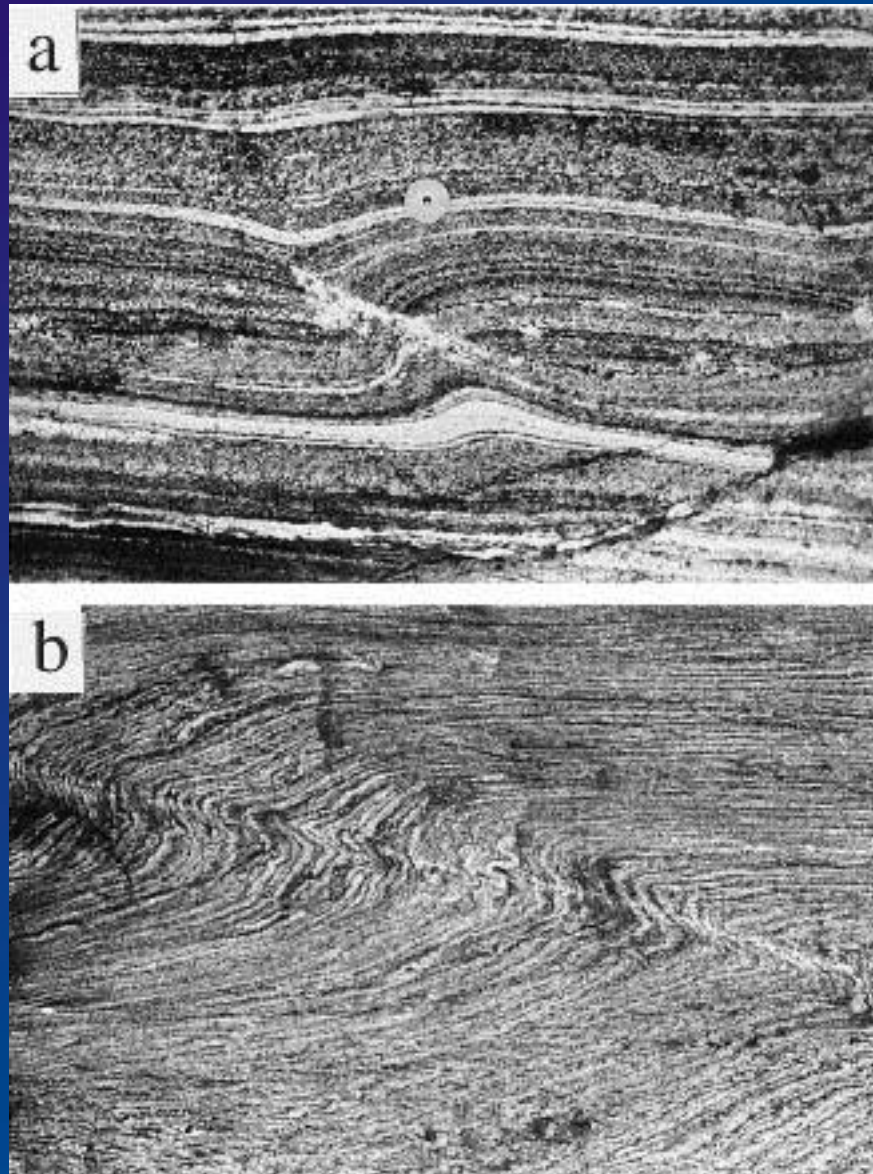
## Trishear folding :

Formation of a syncline and an anticline at the front of the fault.  
This fault then cuts across the forelimb of the fault-related fold.

Thickening and progressive rotation  
of the forelimb

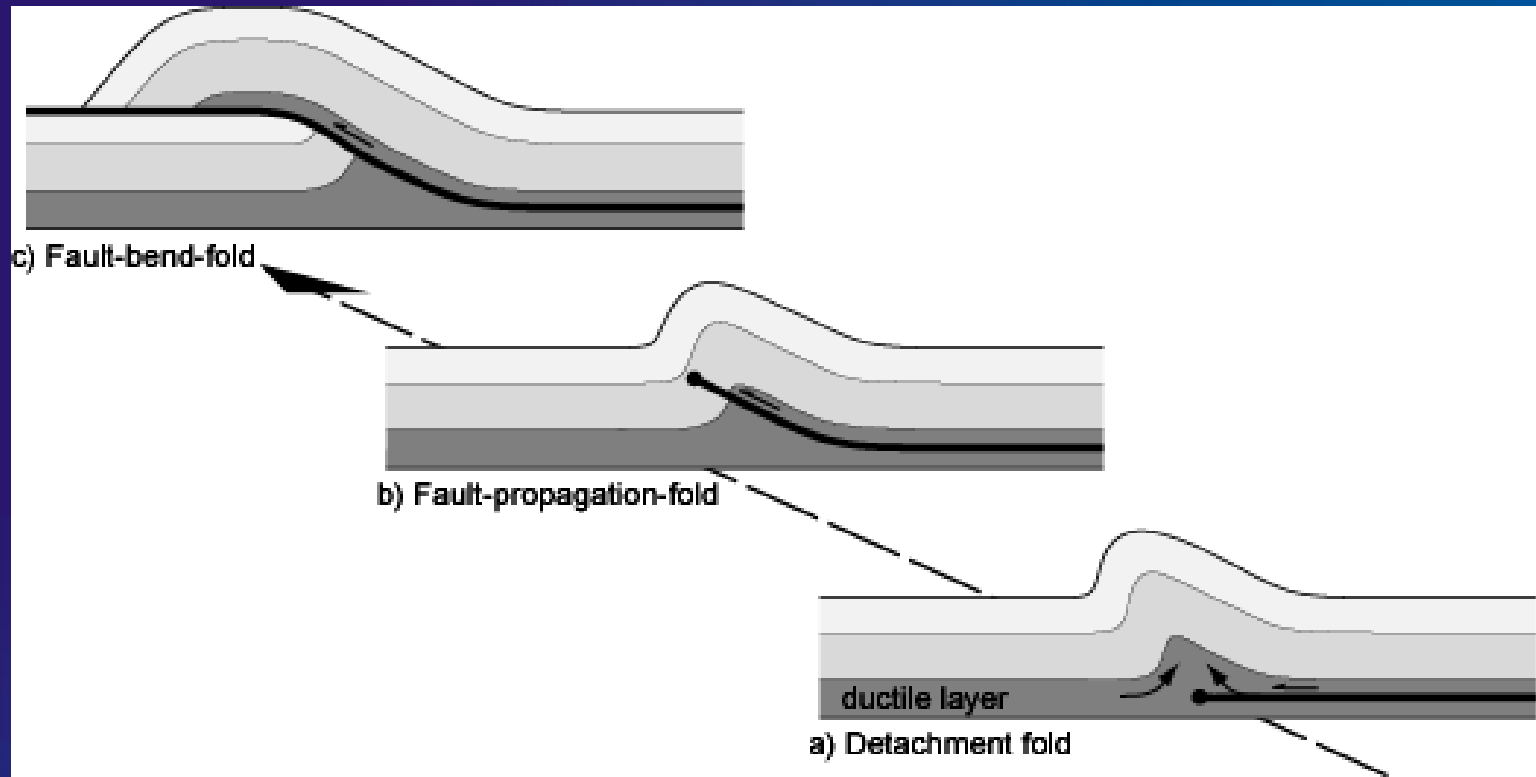
The backlimb has a simple « kink »  
geometry.





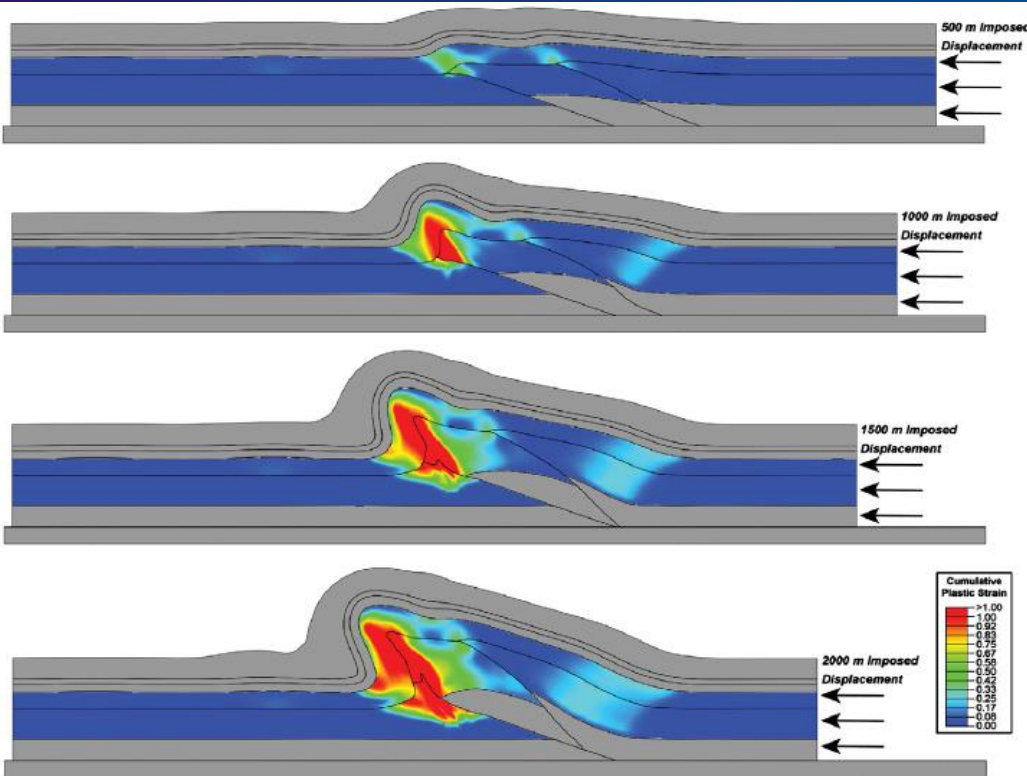
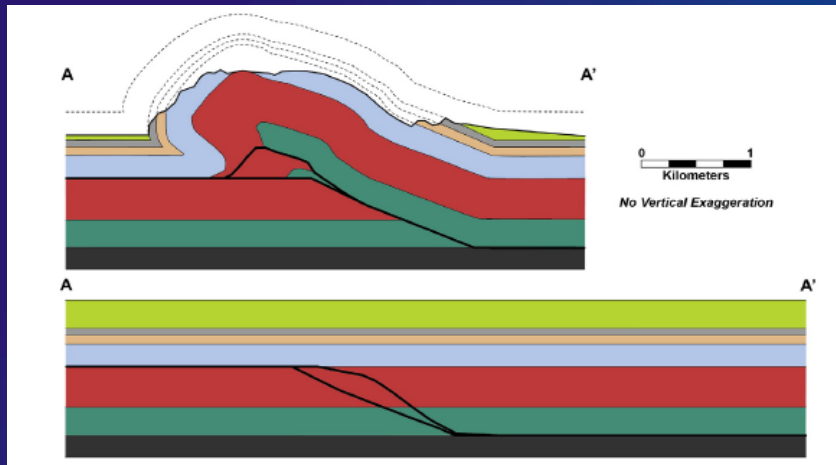
Example of forelimb thickening





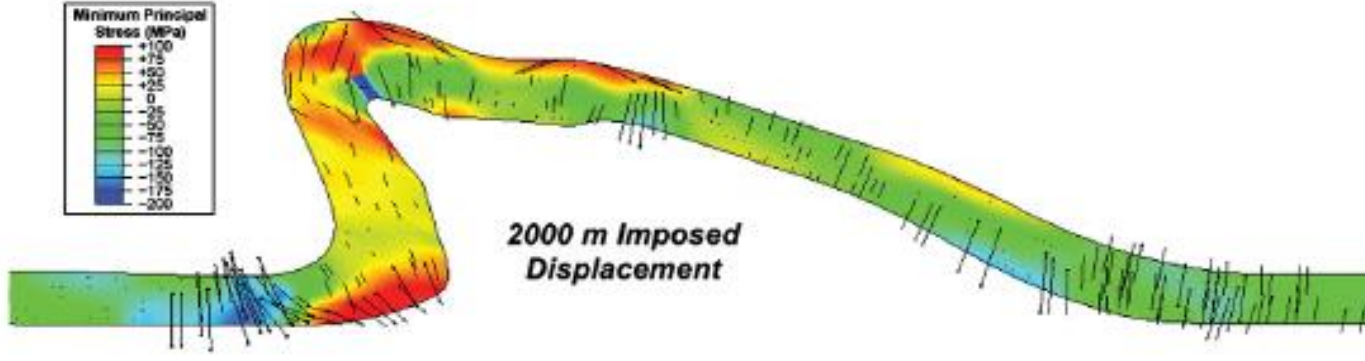
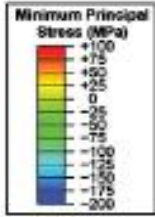
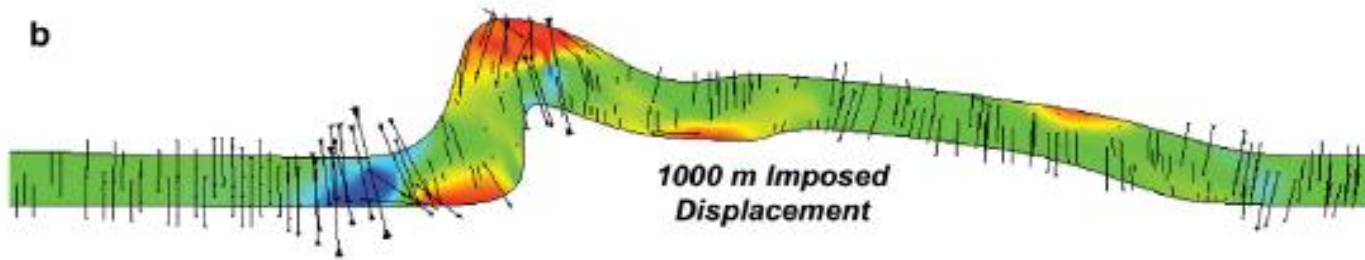
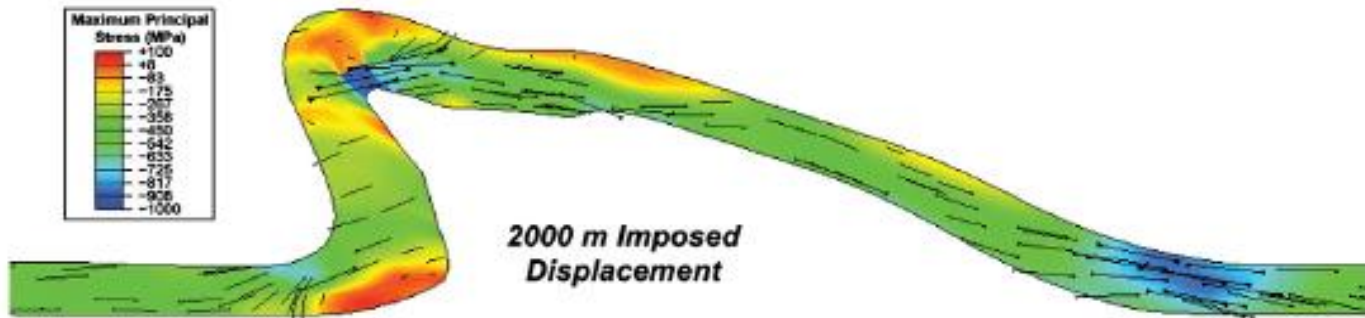
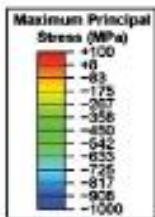
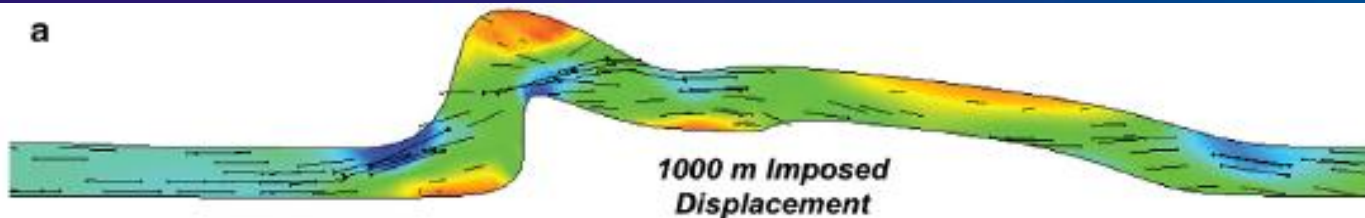
Unified model suggesting that instead of different processes, folding modes illustrate different stages of evolution of a single fold (Molinaro, 2004; Sherkati, 2004)

(Smart et al., 2012)



Geomechanical modeling can predict the onset of failure and the type and abundance of deformation features along with the orientations and magnitudes of stresses. This approach enables development of forward models that incorporate realistic mechanical stratigraphy, include faults and bedding-slip surfaces as frictional sliding interfaces, reproduce the overall geometry of the fold structures of interest, and allow tracking of stress and strain through the deformation history.

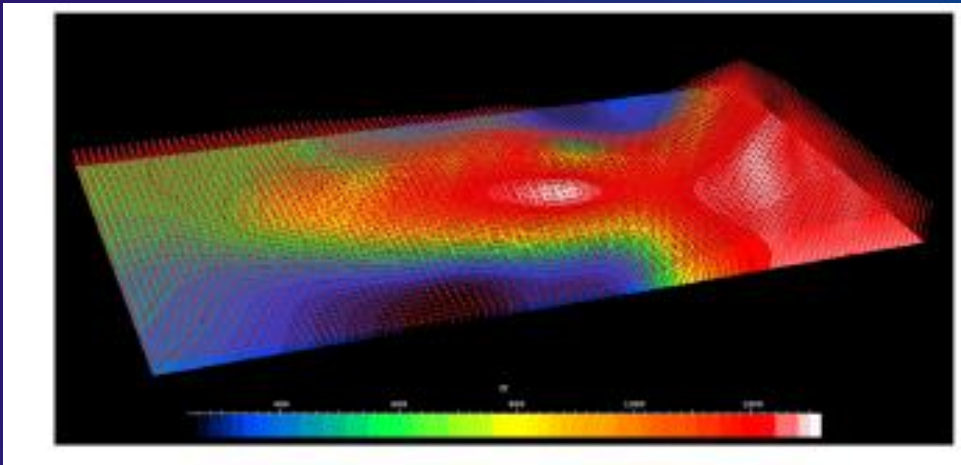
The use of inelastic constitutive relationships (e.g., elastic-plastic behavior) allows permanent strains to develop in response to the applied loads.



(Smart et al., 2012)



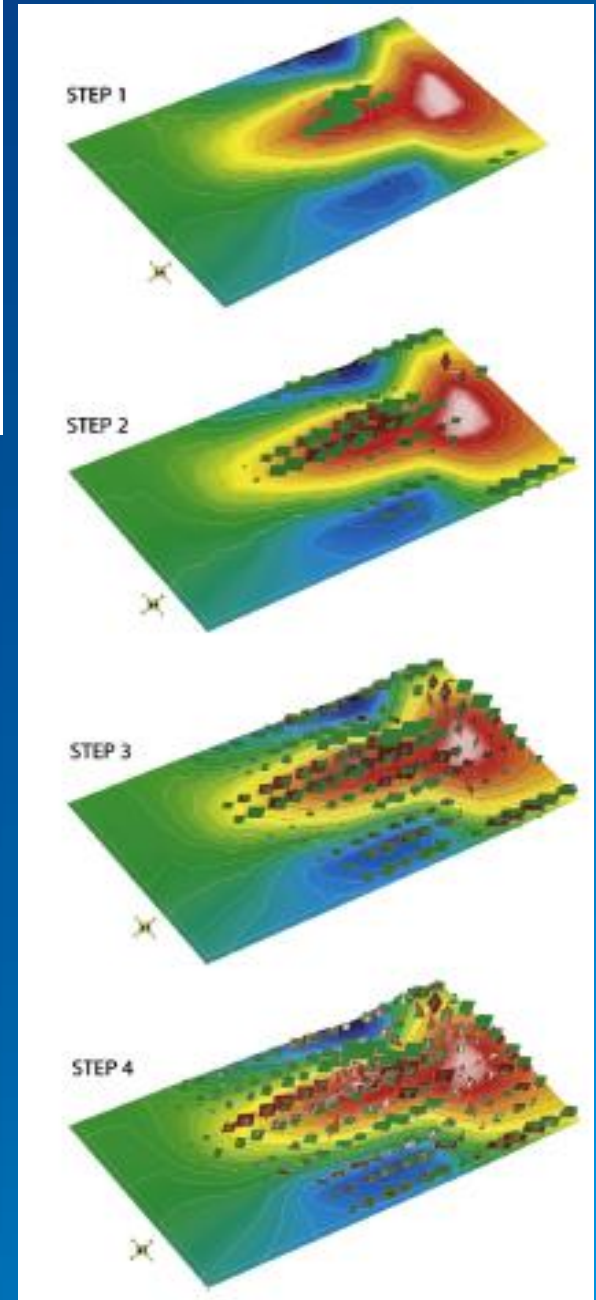
(Sassi  
et al., 2012)



The 3D restoration of a fold provides the external displacement loading conditions to solve, by the finite element method, the forward mechanical problem of an idealized rock material with a stress-strain relationship based on the activation of pervasive fracture sets.

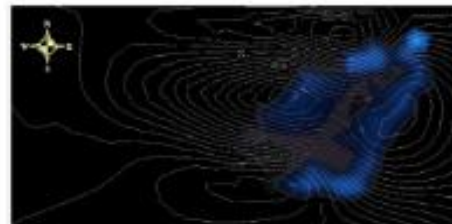
In this elasto-plasticity constitutive law, any activated fracture set contributes to the total plastic strain by either an opening or a sliding mode of rock failure.

Inherited versus syn-folding fracture sets development can be studied using this mechanical model.



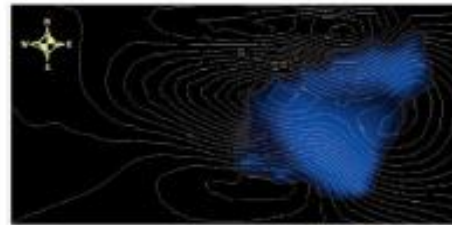
(Sassi  
et al., 2012)

### SLIDING MODE FRACTURES

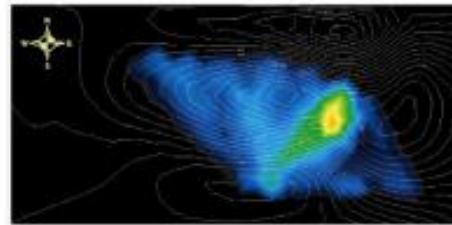


Fracture class  
azimuth

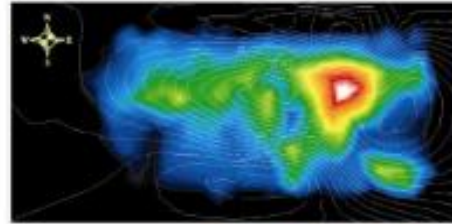
NS



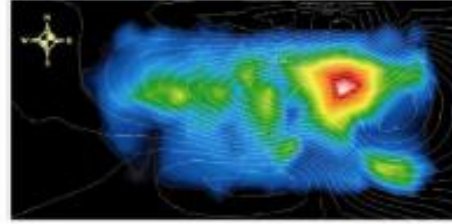
NE-SW



EW

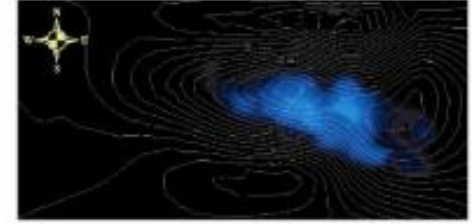
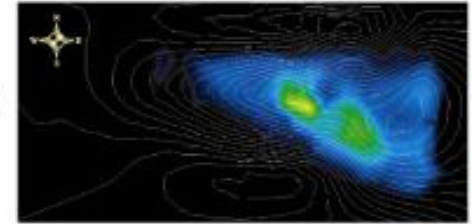
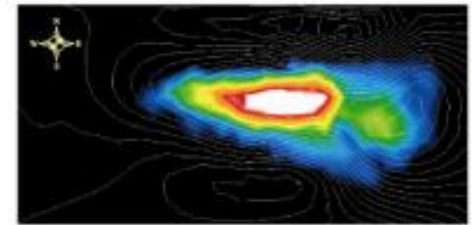
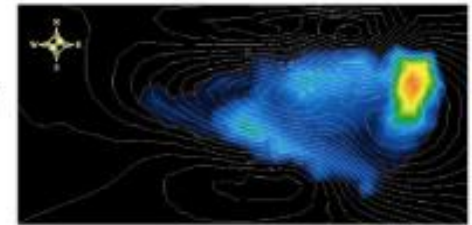
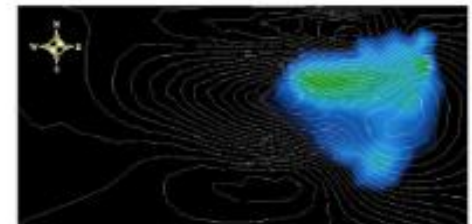


NW-SE



N120

### OPENING MODE FRACTURES



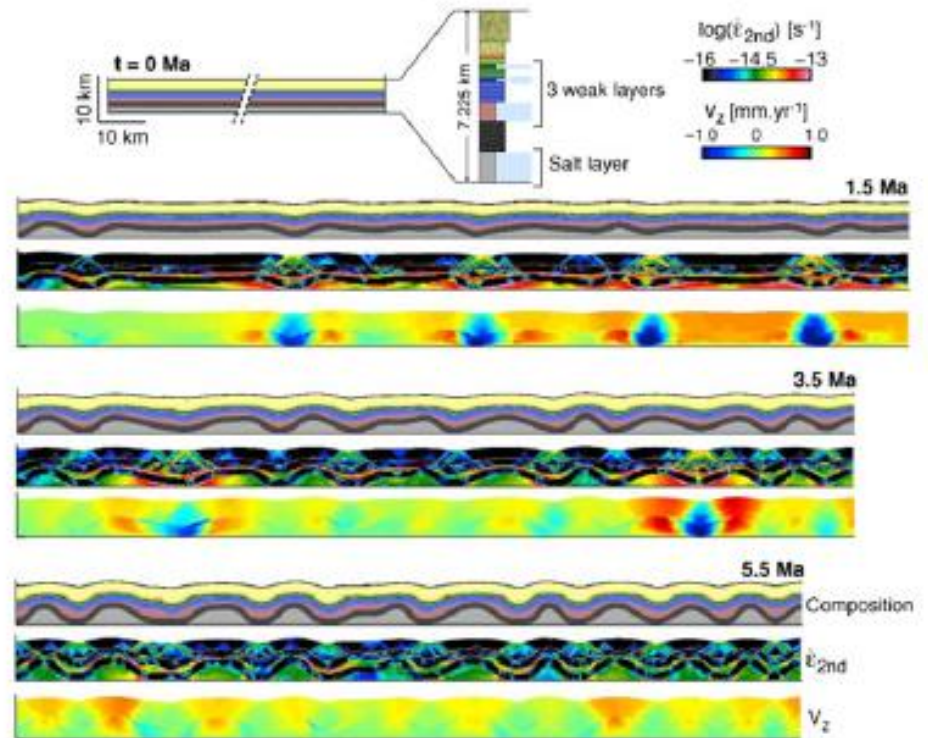
Scale of irreversible deformation

## Mechanism of cover folding

### Stratigraphy and mechanical layering (Fars region)



## Mechanical modelling of cover folding





The study of fold evolution is typically based on analytic and numerical models that are used to investigate possible kinematic scenarios of folding, based on the present-day geometry of folded strata and geometrical assumptions such as thickness and length preservation.

Although this approach has proven to be useful to propose consistent geometrical models of folding, it is mainly macroscopic, and the successive deformation mechanisms that accommodate internal strain within folded strata (fractures and faults at the mesoscale, pressure-solution cleavage and grain-scale deformation (e.g. mechanical compaction, twinning in calcite grains) at the microscopic scale remain to be properly linked to such geometrical models.

Geomechanical modeling has been a significant improvement by allowing prediction of the onset of failure and the type and abundance of deformation features along with the orientations and magnitudes of stresses.

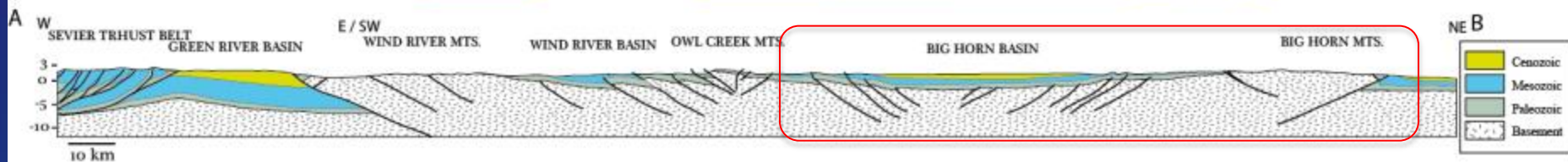
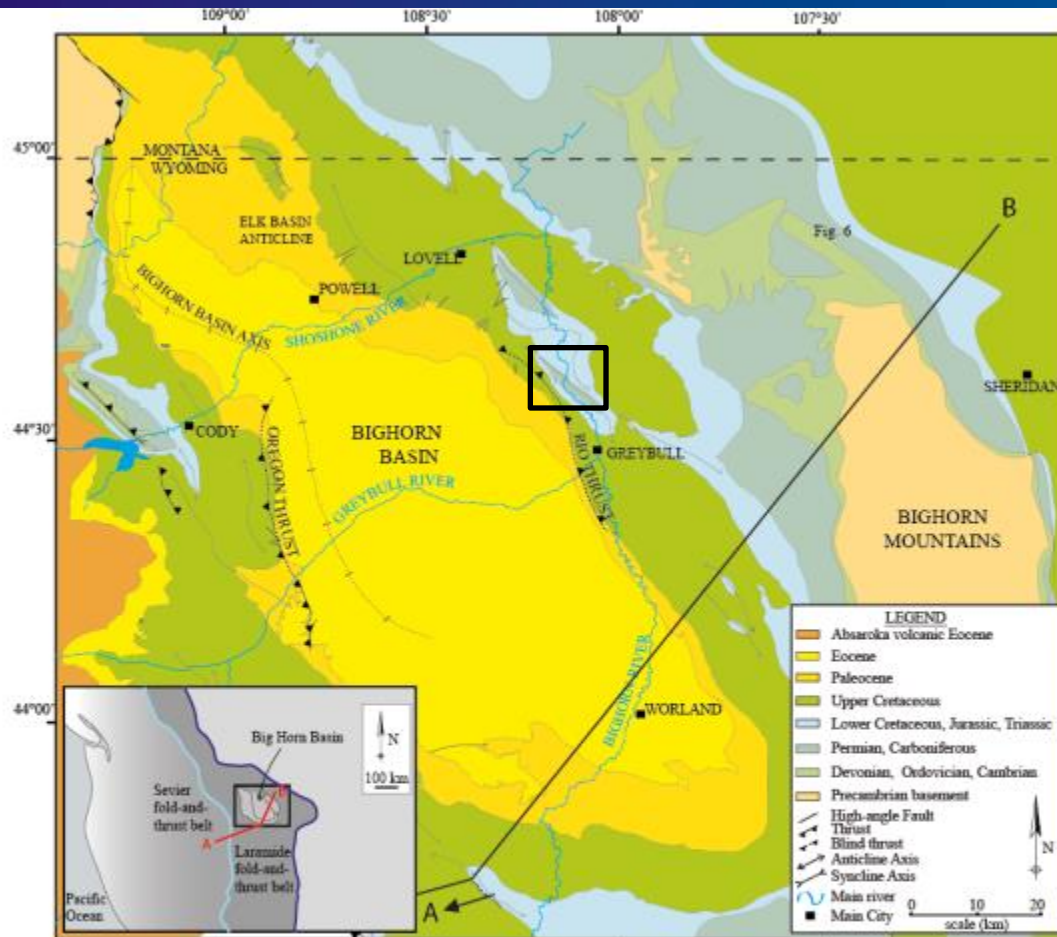
While the appraisal of the mechanical behaviour of folded strata is an essential aspect to understand and simulate the evolution of folded/faulted formations, only a few attempts have been made to bridge the gap between the macroscopic scale and the microscopic scale and to provide quantities like strain or strain to be compared with outputs of geomechanical models.

Aim at unraveling the history of strain acquisition and at linking macroscale and microscale mechanisms of deformation active during folding

**Structural and microstructural evolution  
of Sheep Mountain Anticline ( Wyoming, USA)**



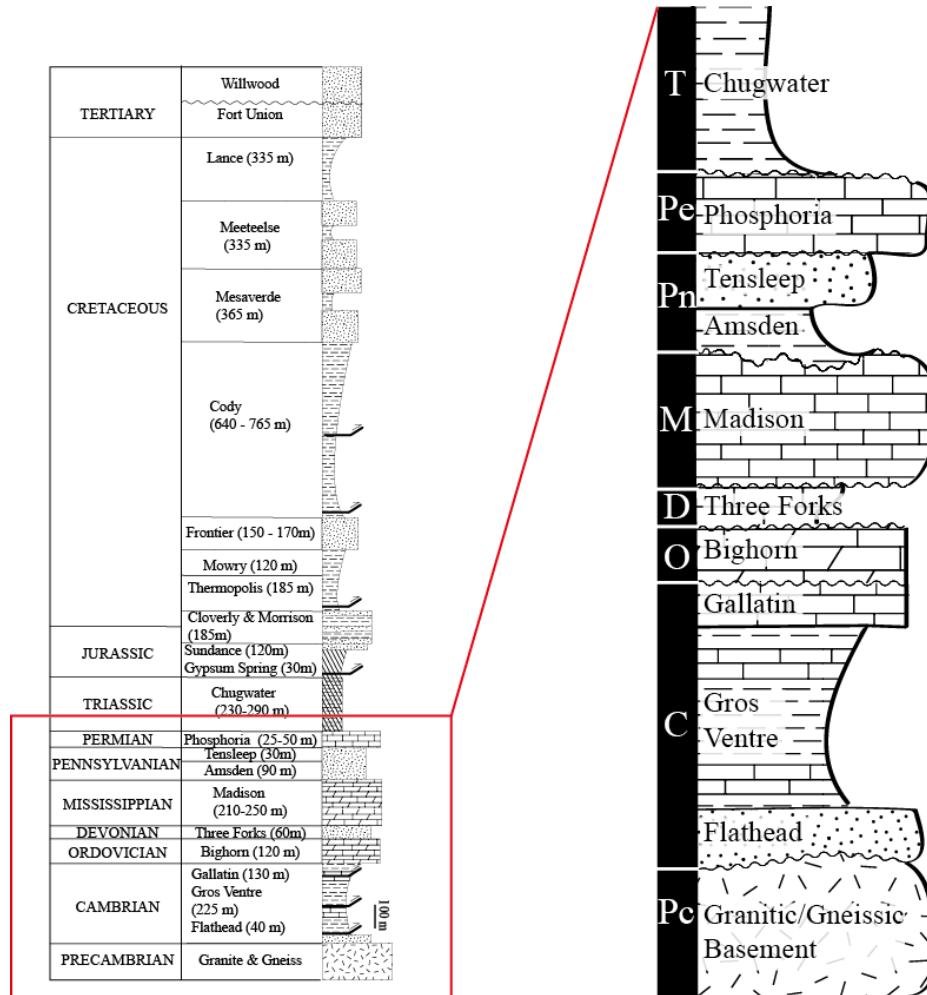
# The Bighorn Basin, and the Sevier and Laramide orogenies

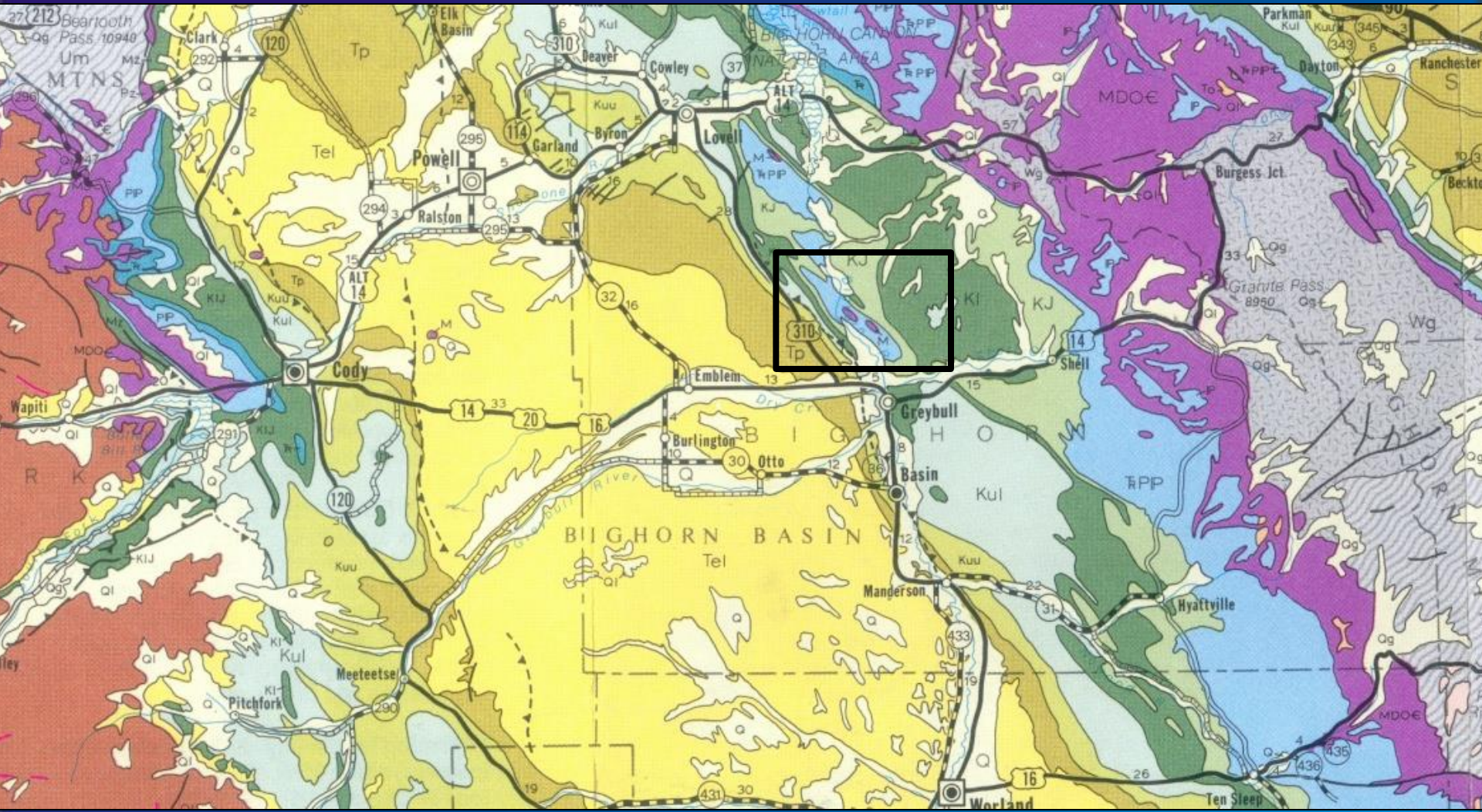






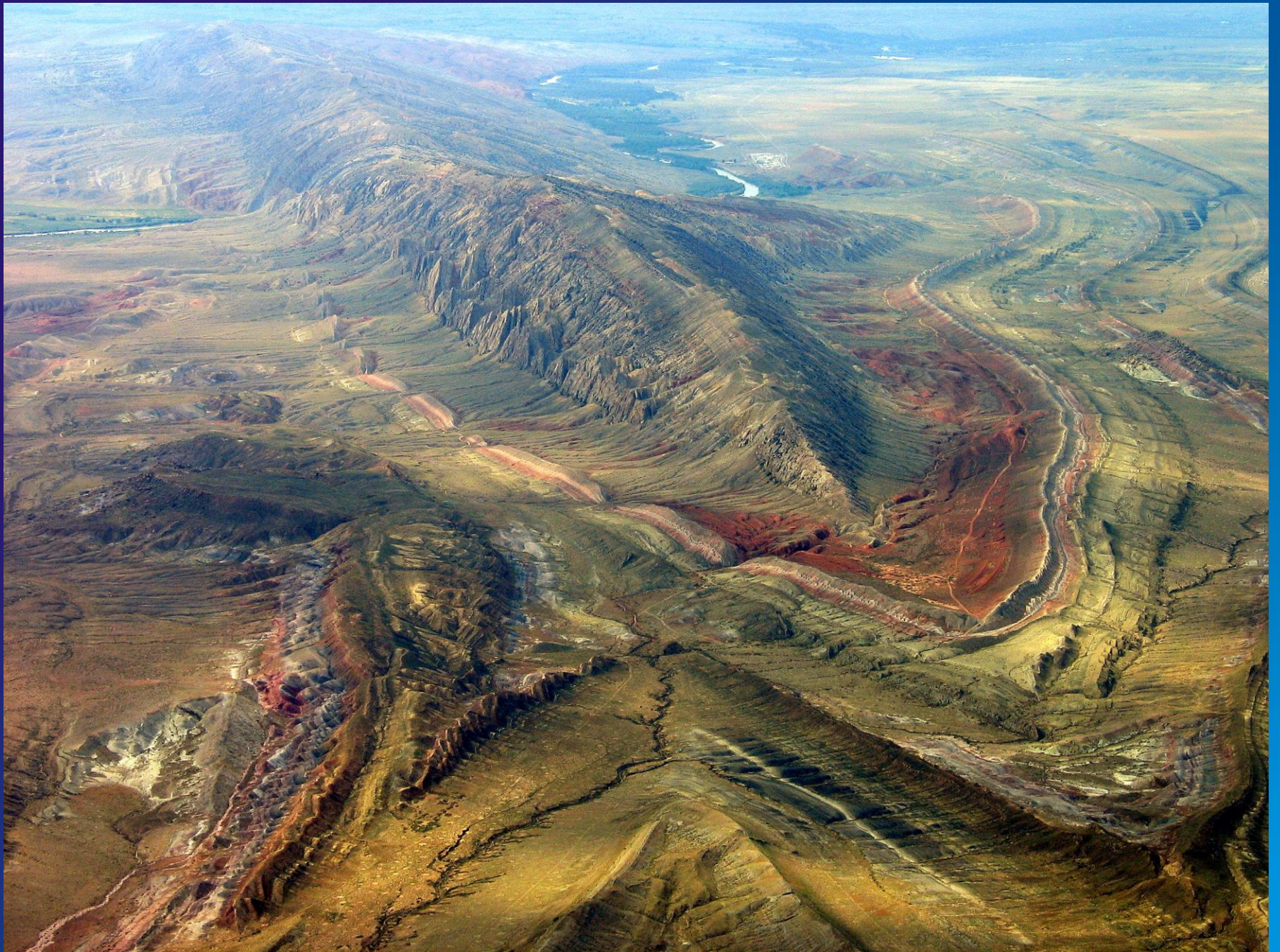
# Stratigraphic units of the Bighorn Basin





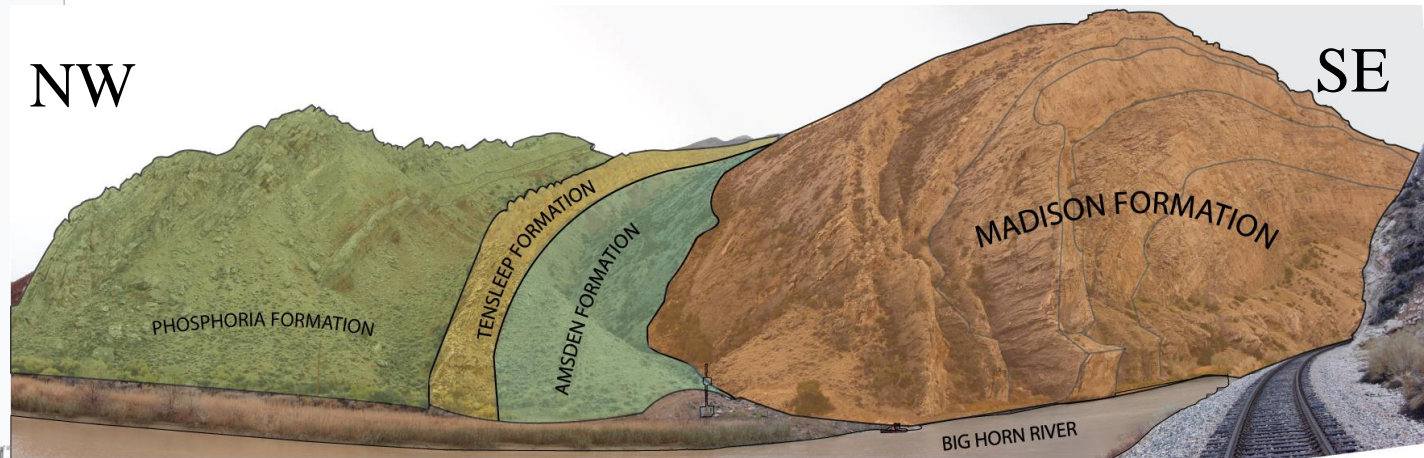
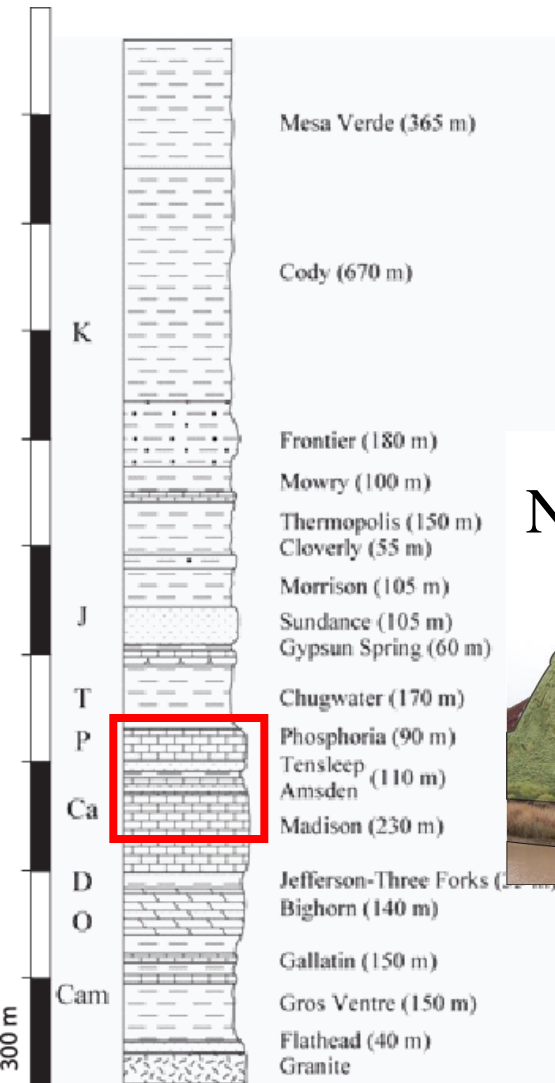
10 km







# Stratigraphy of Sheep Mountain Anticline

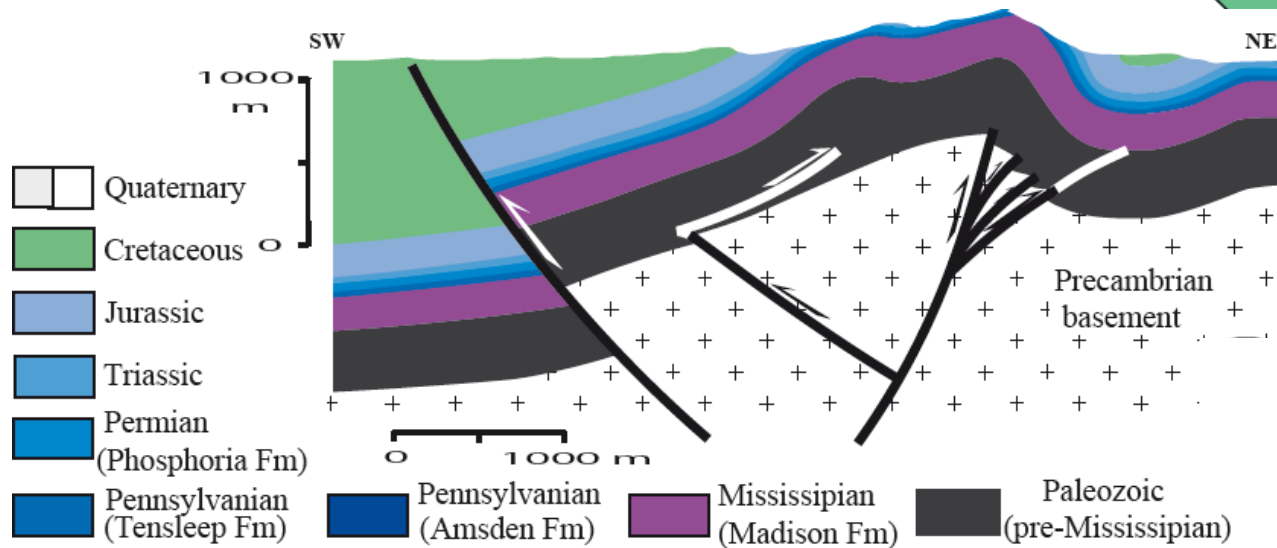
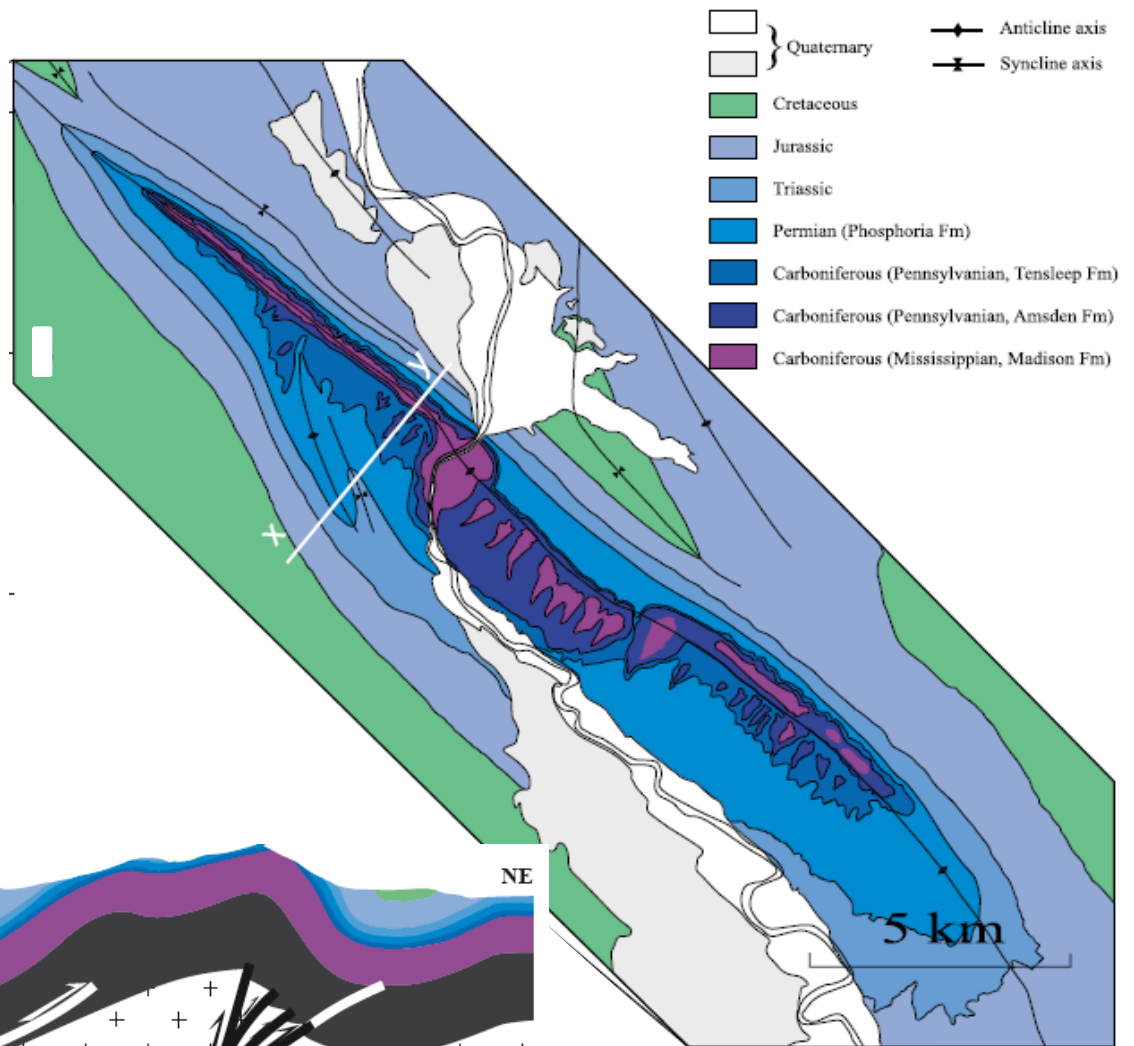


- 300 meters of exposed competent formations (mainly carbonates)
- Shaly stratigraphic series (3000m thickness)





(Amrouch et al.  
Tectonics, 2010)





Investigating folding at the microscale :  
anisotropy of rock physical properties  
and calcite twinning in folded strata

# Anisotropy of sedimentary rocks

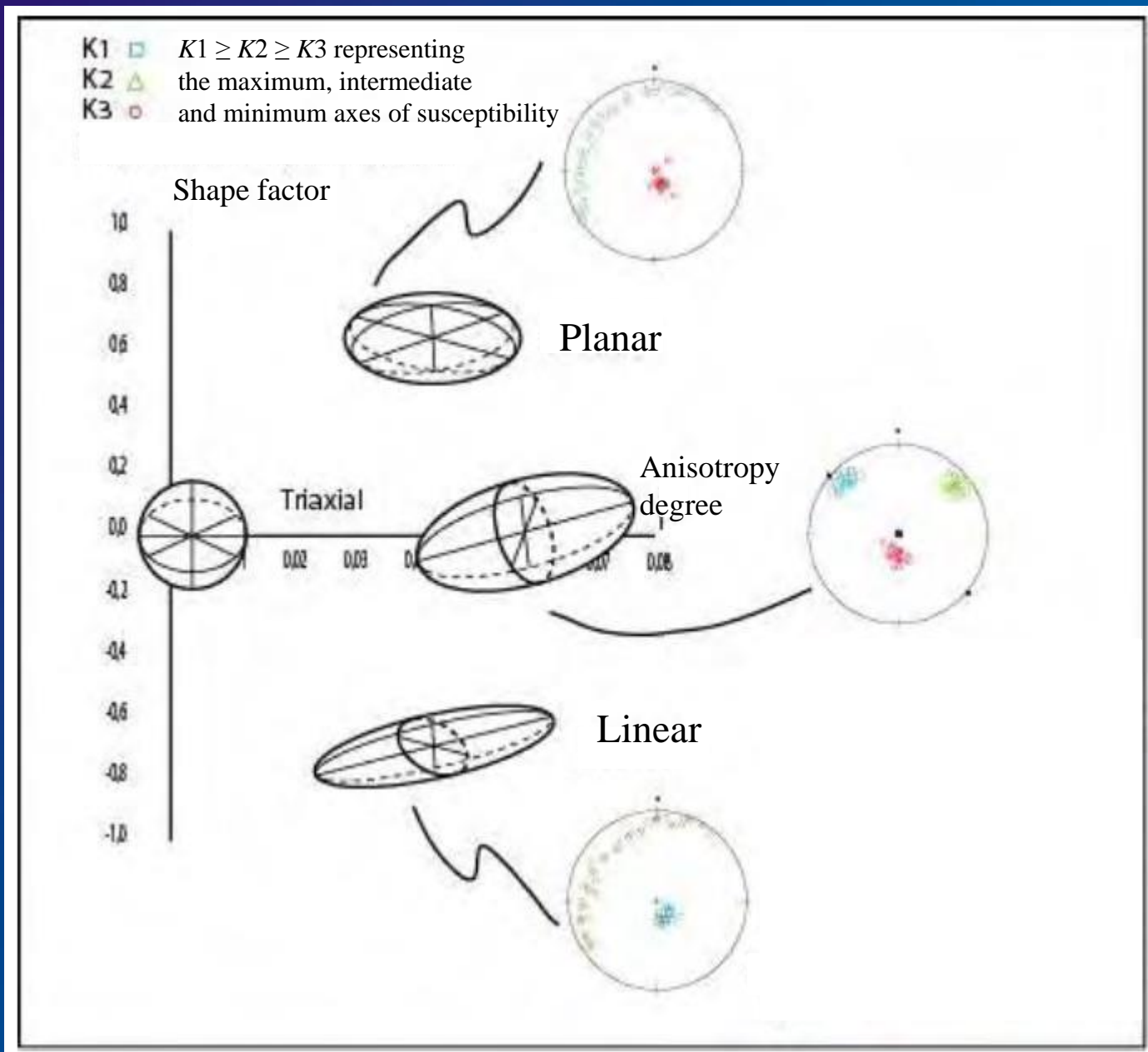
The anisotropic behaviour of sedimentary rocks with respect to a particular physical property (elasticity, magnetic susceptibility, electrical conductivity and permeability) is determined by both matrix properties and pore space distributions.

The matrix of a sedimentary rock can be anisotropic because of preferred mineral orientation, water currents during deposition or pressure solution in response to an anisotropic stress field during loading.

The pore space distribution can be anisotropic because of the sedimentation processes controlled by gravity, which often result in transversely isotropic rocks, depositional processes driven by water currents, and the presence of preferentially oriented cracks within or between the minerals

# AMS

The measurement of AMS helps characterize penetrative tectonic fabrics in deformed rocks because AMS is sensitive to even slight preferred orientations of magnetic minerals.

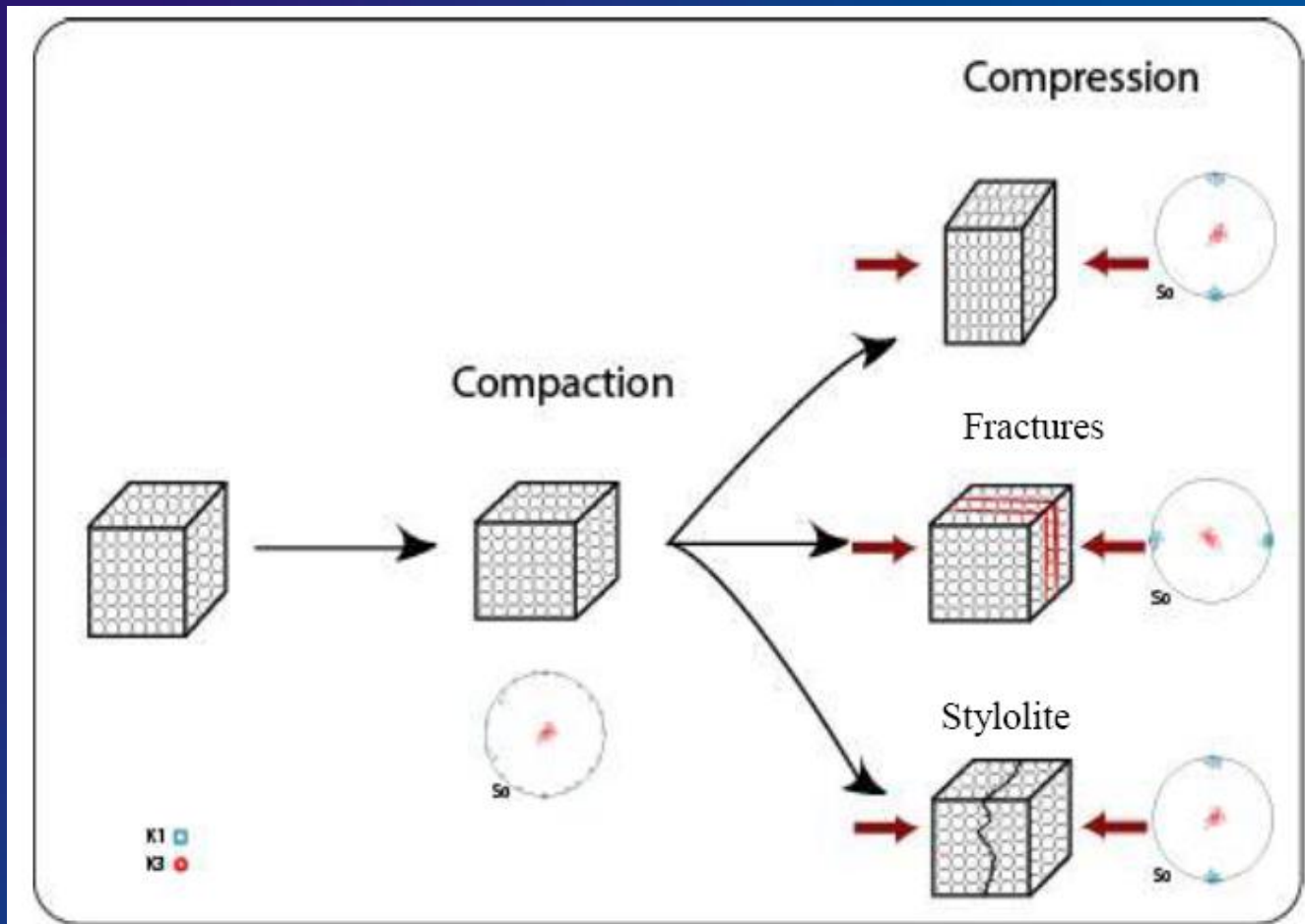




In sedimentary rocks, magnetic susceptibility  $K_m$  originates primarily from three distinct sources: (1) the dominant diamagnetic minerals (quartz or calcite), (2) the paramagnetic minerals (clays and other Fe-bearing silicates) and (3) diluted ferromagnetic minerals (magnetite, hematite and pyrrhotite), depending on their relative proportion.

Generally,  $K_m$  ranges between low negative values and low positive values (from  $-10 \times 10^{-6}$  SI to  $10 \times 10^{-6}$  SI). In Fe-bearing silicate rocks  $K_m$  covered susceptibilities up to  $500-1000 \times 10^{-6}$  SI whereas ferromagnetically dominated rocks are generally characterized by values higher than  $1000 \times 10^{-6}$  SI. The lack of paramagnetic minerals tends to decrease the limit of influence of ferromagnetic fraction on magnetic susceptibility.

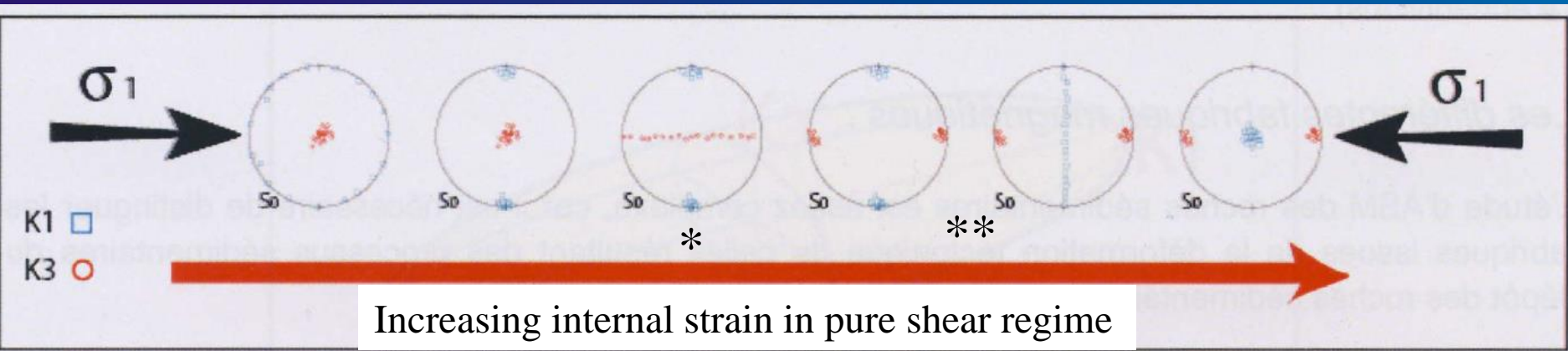
# AMS



The interpretation of AMS fabrics is strongly dependent on the carrier of the magnetic signal

# AMS

The magnetic fabric is typically defined using the orientation of either the magnetic foliation, that is, the plane containing the  $K1$  and  $K2$  axes when  $K1 \approx K2 \gg K3$ , or the magnetic lineation, that is, the direction of the  $K1$ -axis.



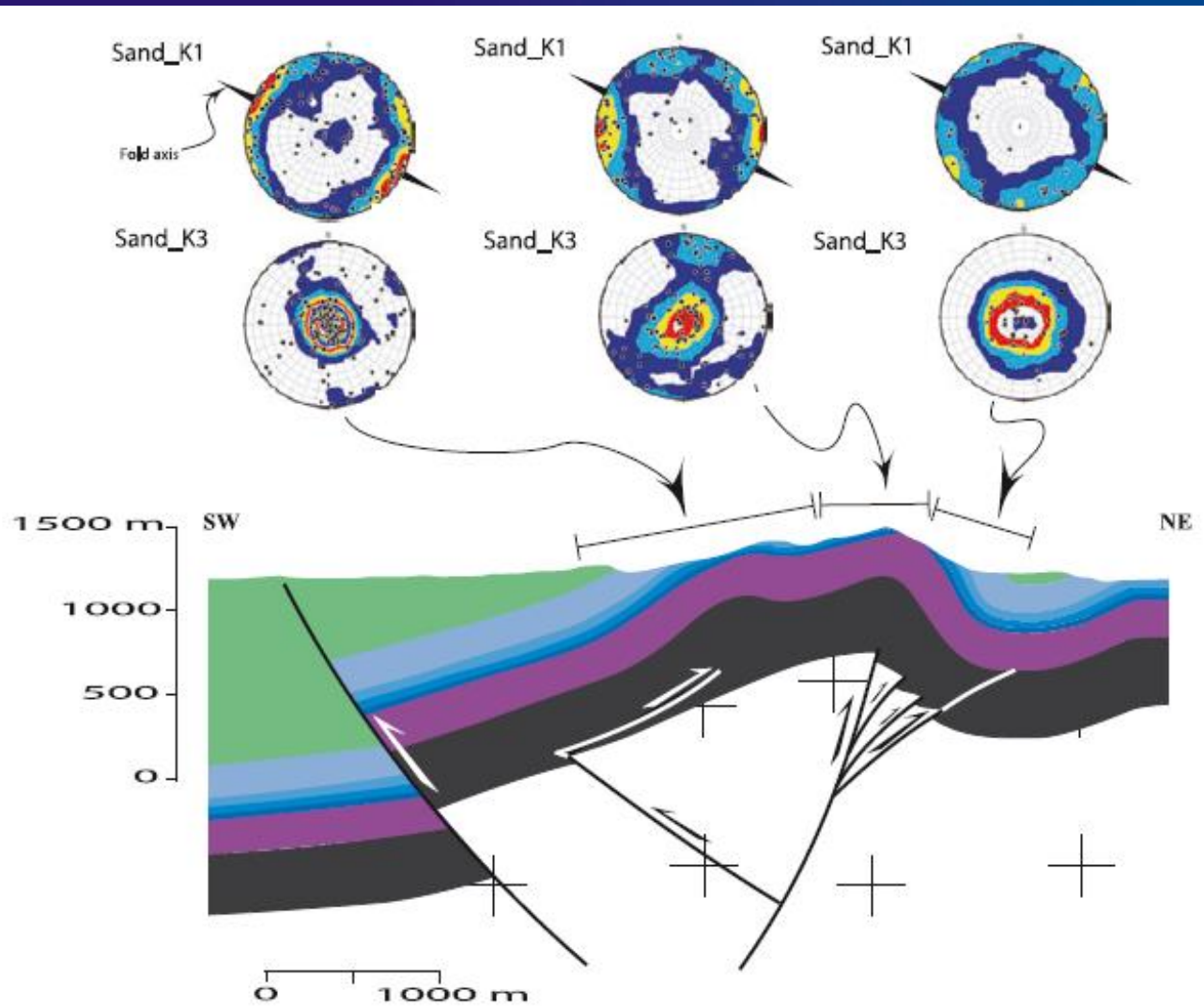
\* Intermediate fabric : magnetic lineation  $K1$  still contained within the bedding but clustered at right angle to the shortening direction, whereas the  $K3$  is leaving the pole to bedding and exhibits a girdle distribution around  $K1$ .

\*\* Tectonic fabric characterized by  $K3$  parallel to the shortening direction.  $K1$  is either parallel to the intersection between the bedding and the incipient cleavage or exhibits a girdle around  $K3$



While the correlation between the orientations of principal AMS axes and principal strain axes tends to be very consistent, the correlation between the magnitudes of principal AMS axes and corresponding principal strain axes is not.

# AMS (sandstones)

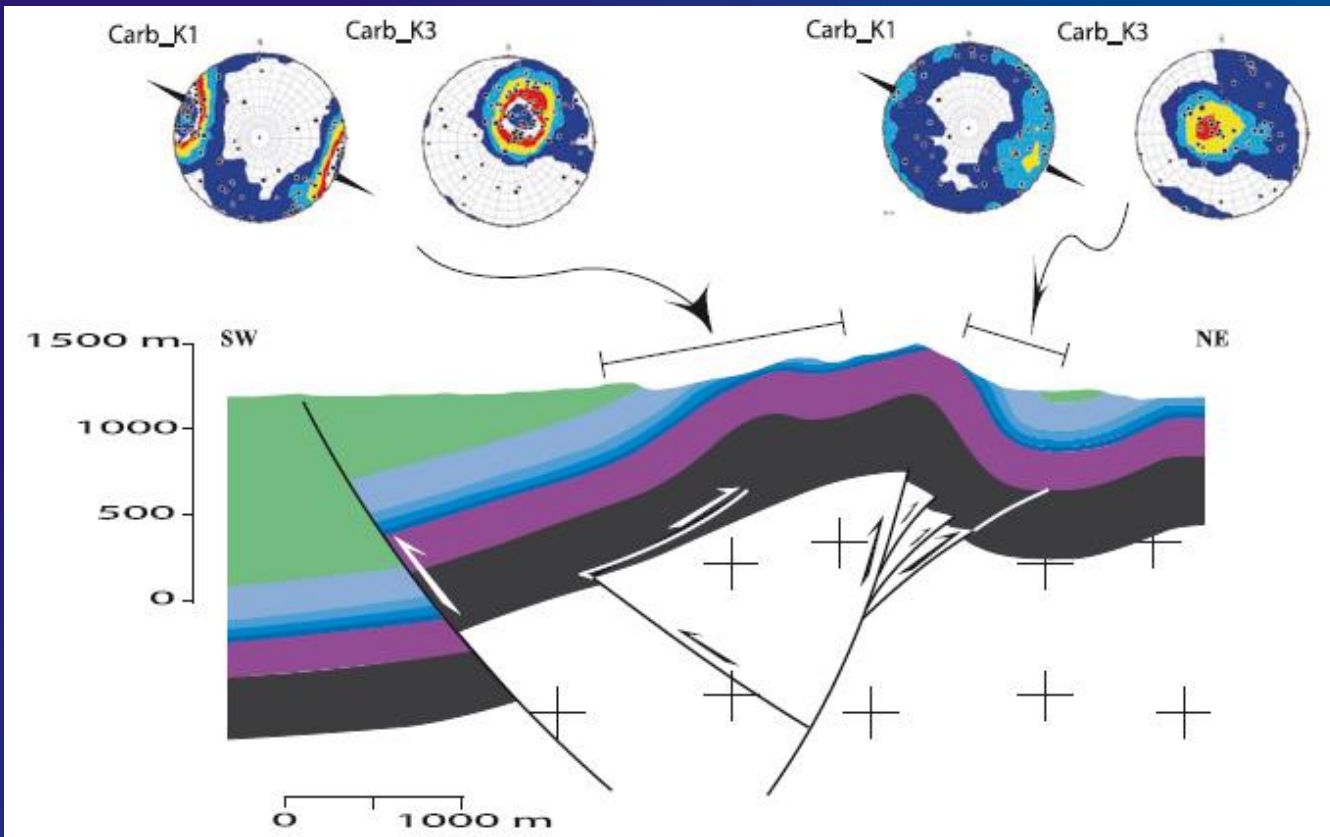


Forelimb : planar oblate fabrics with the maximum axes K1 scattered in the plane of bedding, the minimum axes K3 being on average normal to it. --> sedimentary fabrics.

Backlimb : similar fabric but with significantly more clustering of K1 close to the direction of fold axis in the plane of bedding. Fabrics mixing both shortening direction and pole of bedding → tectonic (sandstones deformed by prefolding LPS).

Hinge : linear fabric with a girdle distribution of K3; competition between intermediate and true tectonic fabrics. Inferred shortening direction, normal to the magnetic lineation and parallel to the K3 girdle

# AMS (carbonates)



Forelimb : K1 scattered in the plane of bedding with a weak maximum close to the fold axis orientation, and K3 clustered either along the pole of bedding or perpendicular to it. Similarly to sandstones, combination of relict sedimentary fabrics with intermediate and tectonic fabrics locally.

Backlimb : well defined cluster of K3, which significantly deviates from the pole of bedding, and very well clustered K1 axes. Similarly to sandstones, K1 mean axis is trending  $\sim N120^\circ$ , close to the trend of the fold axis.  $\rightarrow$  fabric associated to the regional shortening direction. Obliquity of the magnetic foliation with respect to bedding plane  $\rightarrow$  bed-parallel shearing instead standard LPS



## APWV

At laboratory conditions (no confining pressure) the anisotropic behaviour of rocks with respect to the propagation of  $P$  waves is mainly controlled by microstructures (at  $\mu\text{m}$  scale) leading to a reduction of the inter- or intragranular cohesion. Such microstructures can be the pore network, the microfractures and the contacts between grains.

Considering the simple case of an elliptic pore space, the maximum velocity will be observed in the direction of long axis of the pore. In the case of a planar distribution of cracks or pressure solution cleavage planes,  $P$ -wave velocity is greatly reduced along the direction normal to the plane.

A preferred orientation of intergranular contacts will be characterized by a maximum velocity normal to it.

However, one must keep in mind that the resulting acoustic fabric is a composite of these fabrics.

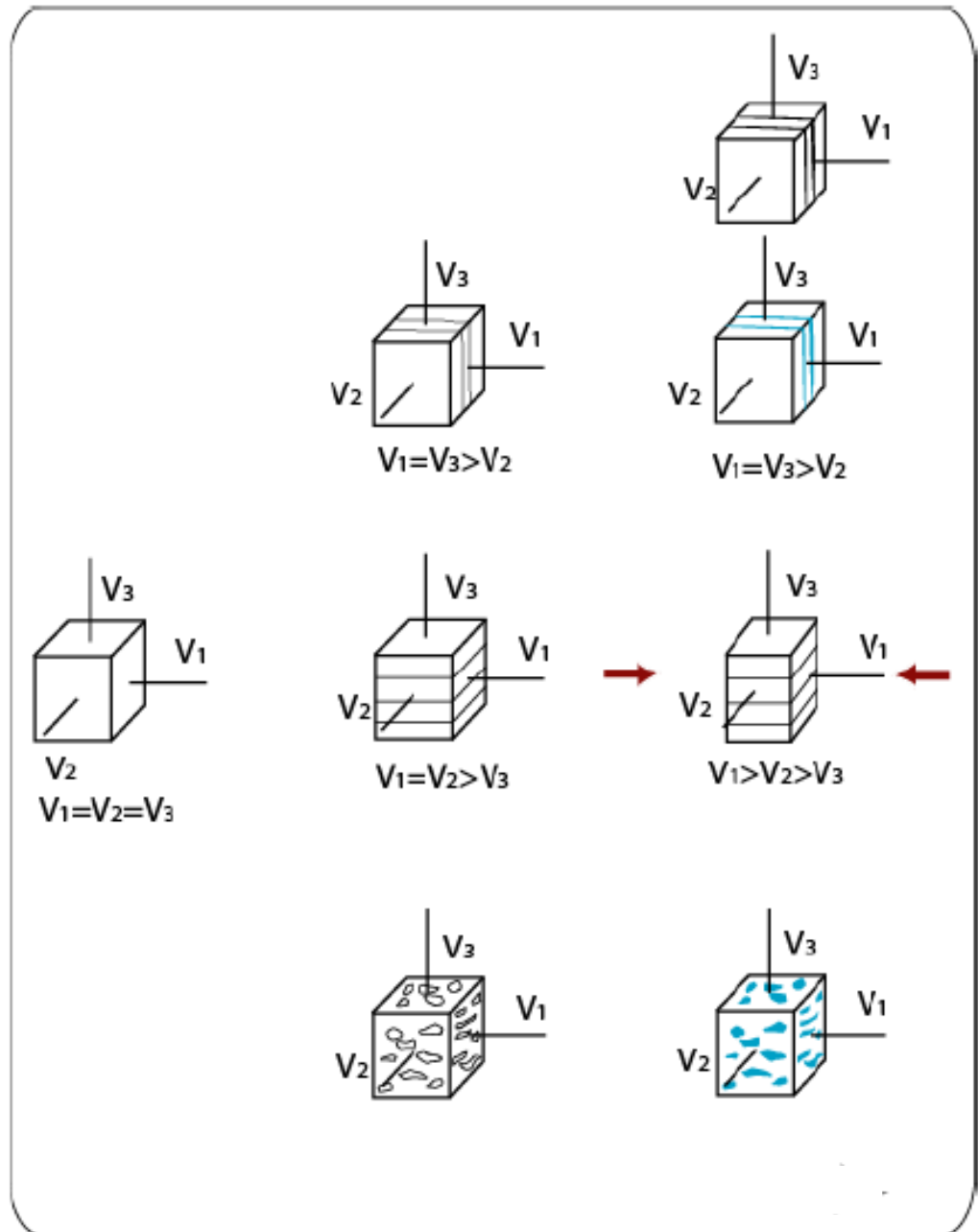
## APWV

There is an overall tendency for the mean velocity to be higher in the carbonates than in the sandstones, and, within the same lithology, to be lower in high porosity samples. These classical trends are generally explained by the fact that velocities range between the velocities of the mineral grains (intrinsically higher in calcite than in quartz) and those of the mineral-pore fluid filled (air or water) assemblage.

A significant decrease of anisotropy after water saturation, with a concomitant increase of velocity can be matched with a model of velocity anisotropy controlled by the porosity and its shape.

A rock made of an anisotropic matrix and an isotropic pore space will be characterized by velocity and anisotropy increase when it is saturated with incompressible material (water).

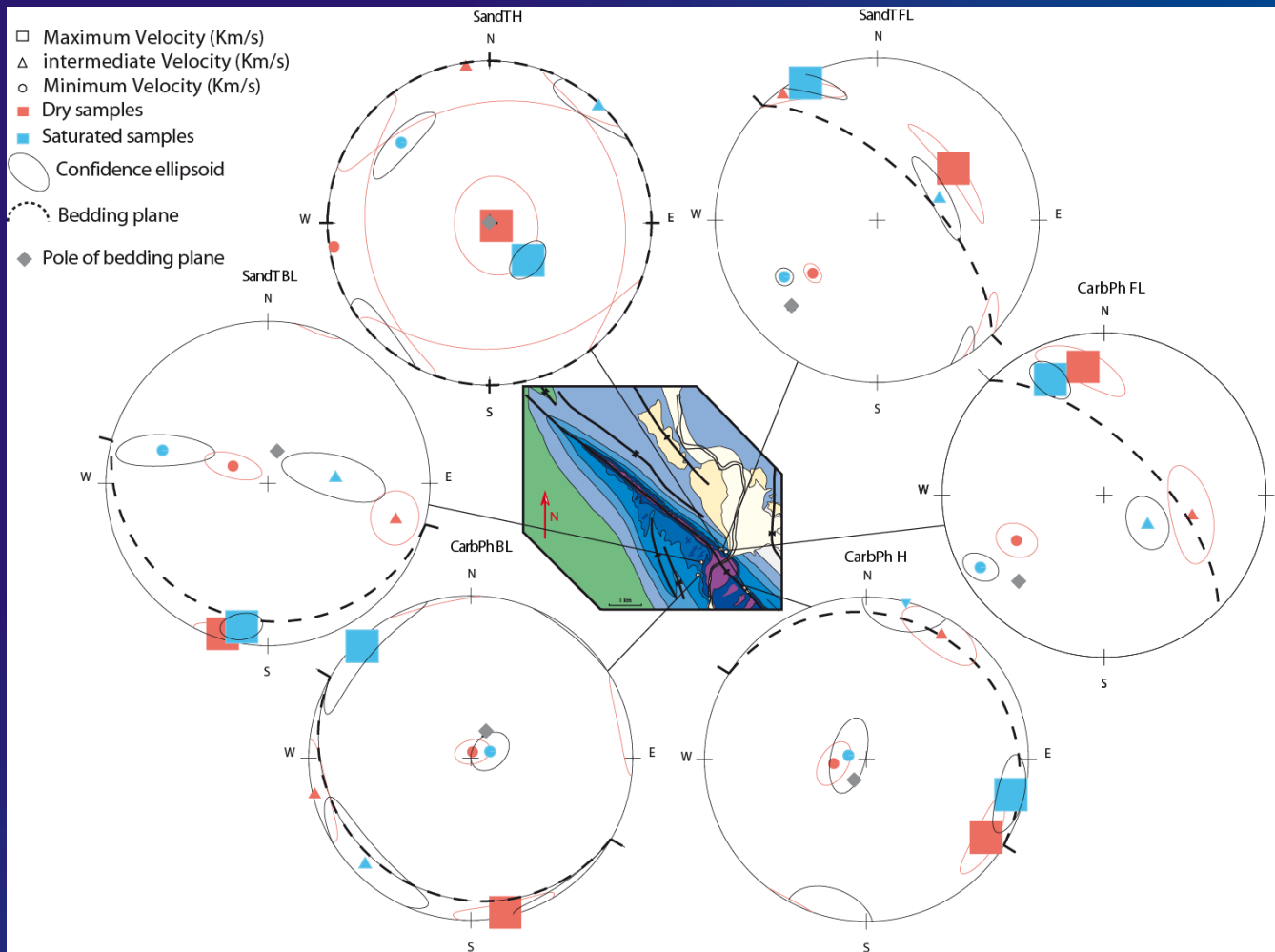
# APWV





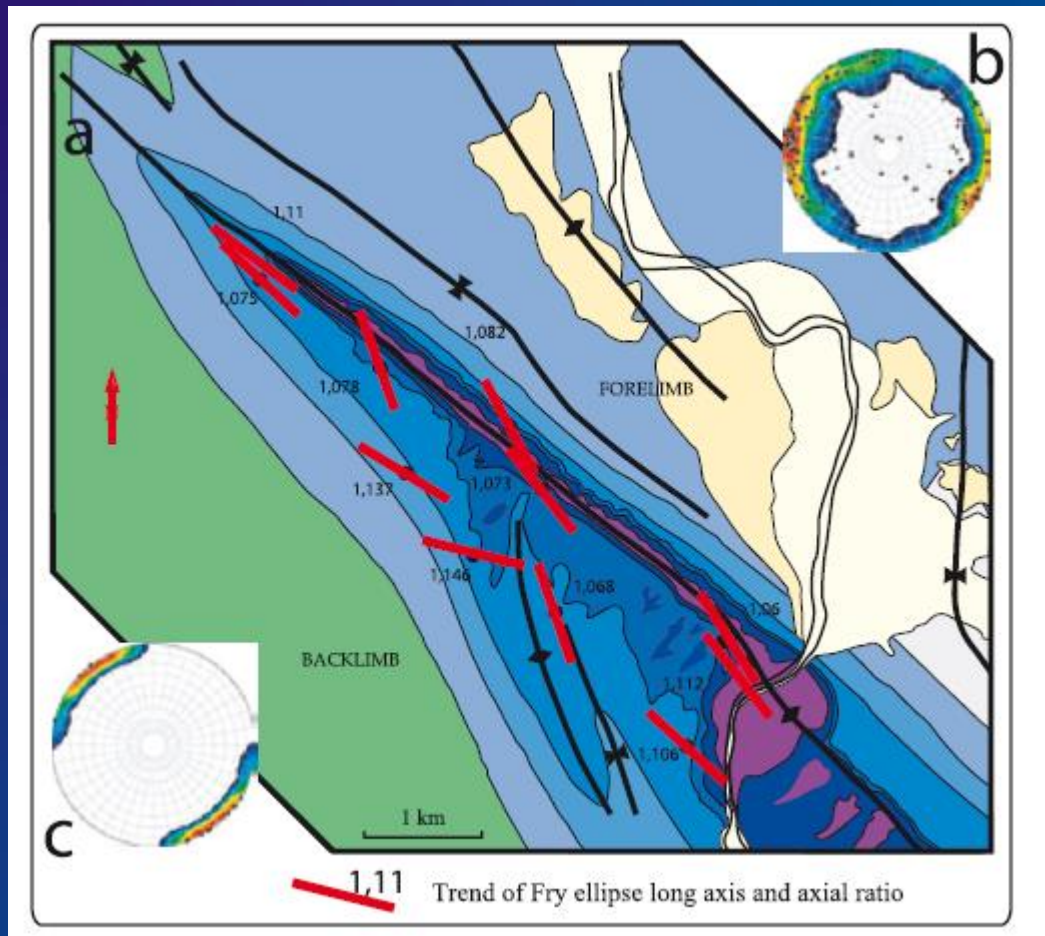
# APWV

(Amrouch et al., 2010)



Forelimb : Deformation is preferentially revealed by the porosity, which is systematically oriented with its long axis parallel to the fold axis. APWV indicates that the anisotropy is dominated by an anisotropic pore network embedded into an almost isotropic matrix.

Backlimb : APWV fabrics are grain-supported, showing that the matrix is more anisotropic in the backlimb than in the forelimb. The direction of anisotropy is roughly related to the plane of bedding indicating that APWV fabrics could also be linked to early stage LPS deformation.



Strain axes deduced from Fry method at Sheep Mountain anticline: (a) Geological map of Sheep Mountain Anticline with long-axis trends and axial ratios of individual bedding-parallel Fry ellipses at sampling locations throughout the study area and (b) trends of all the  $K_1$  axes of AMS fabrics measured from the same samples used for Fry analysis. (c) The lower-hemisphere stereonet illustrates the long axes of bedding parallel Fry ellipses in the study area

# Summary

## Forelimb :

AMS : Preservation of sedimentary magnetic fabrics, weak anisotropy

APWV : anisotropy dominated by anisotropic pore network embedded into an almost isotropic matrix.

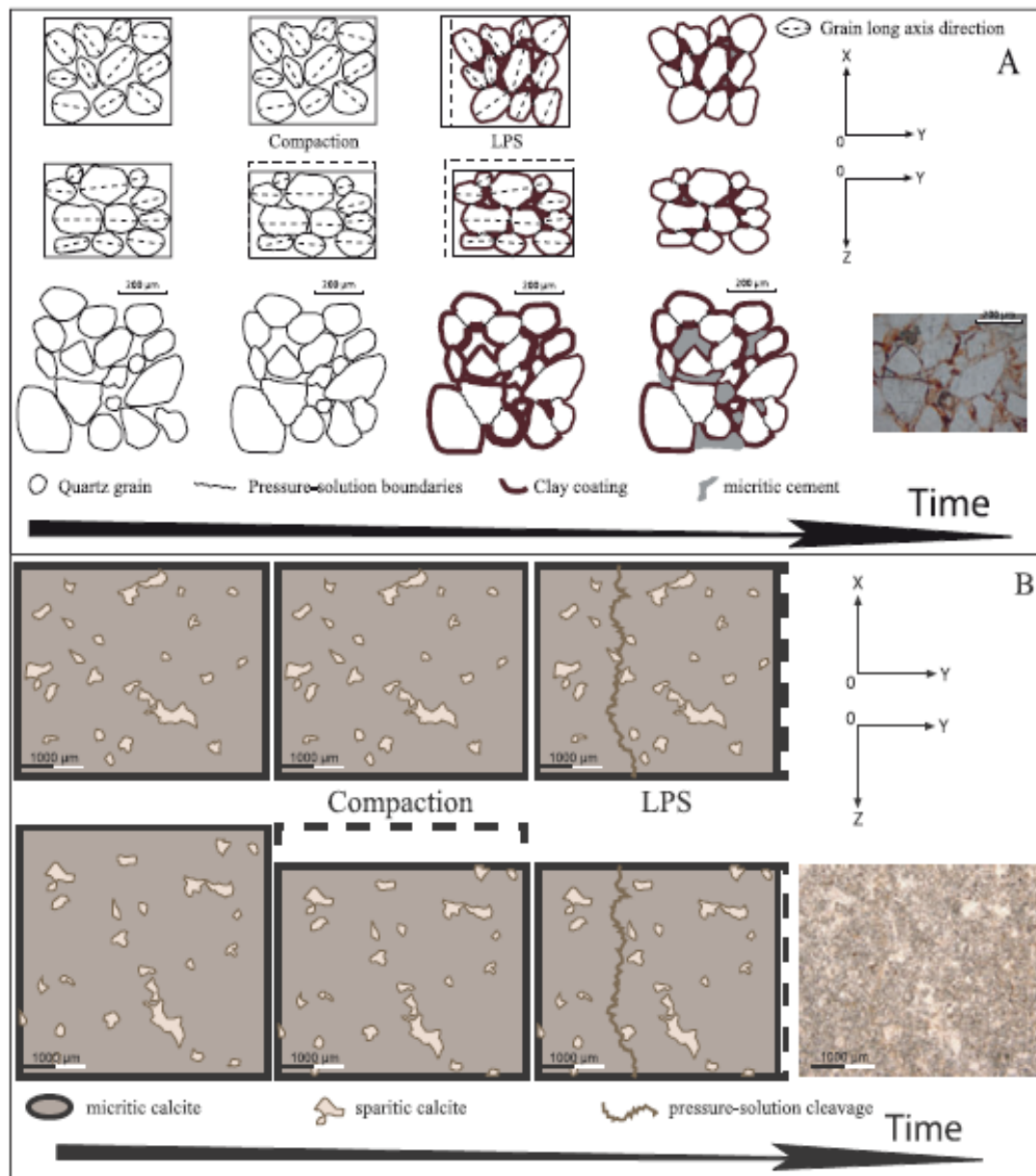
## Backlimb :

AMS : true tectonic strain at the matrix scale (sandstones : pre-folding LPS, carbonates : bedding-parallel shear).

APWV : grain-supported fabrics, showing that the matrix is more anisotropic in the backlimb than in the forelimb. Direction of anisotropy roughly related to bedding indicating that APWV fabrics could also be linked to early stage LPS deformation.

→ succession of microscopic deformation mechanisms active before and during folding





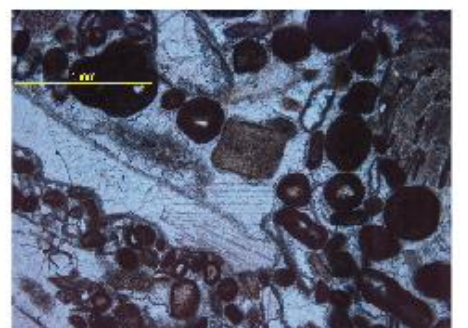
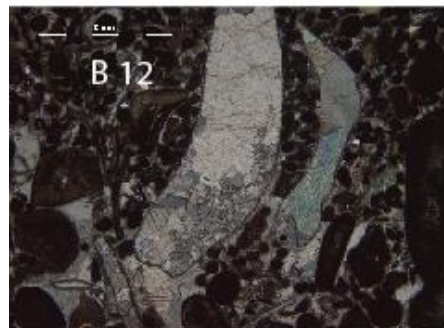
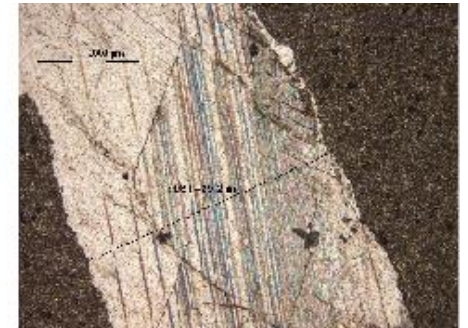
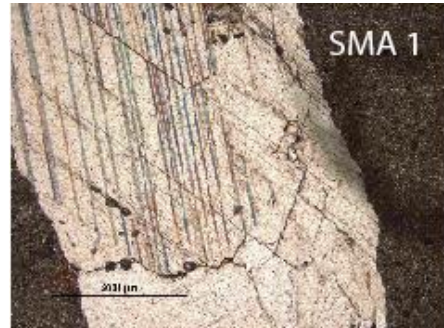
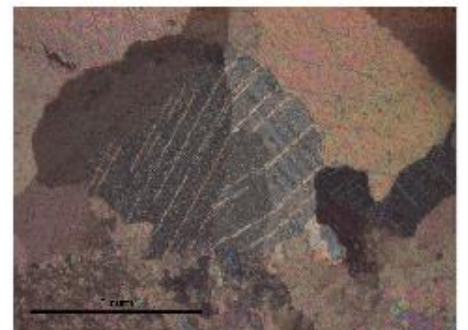
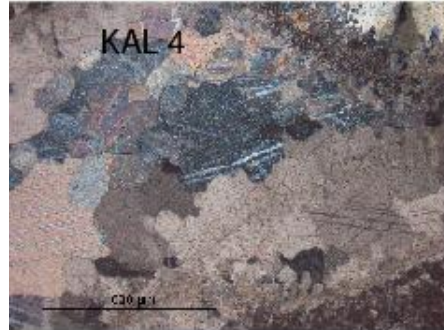
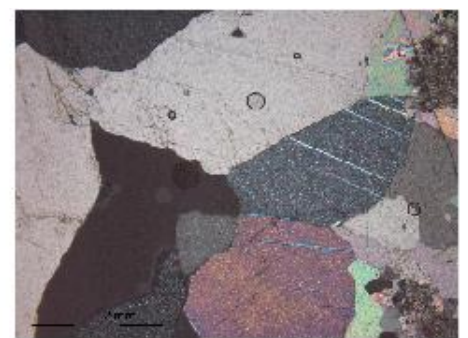
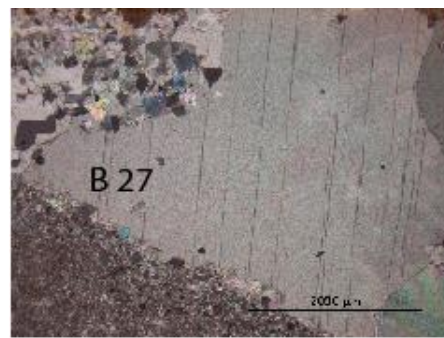
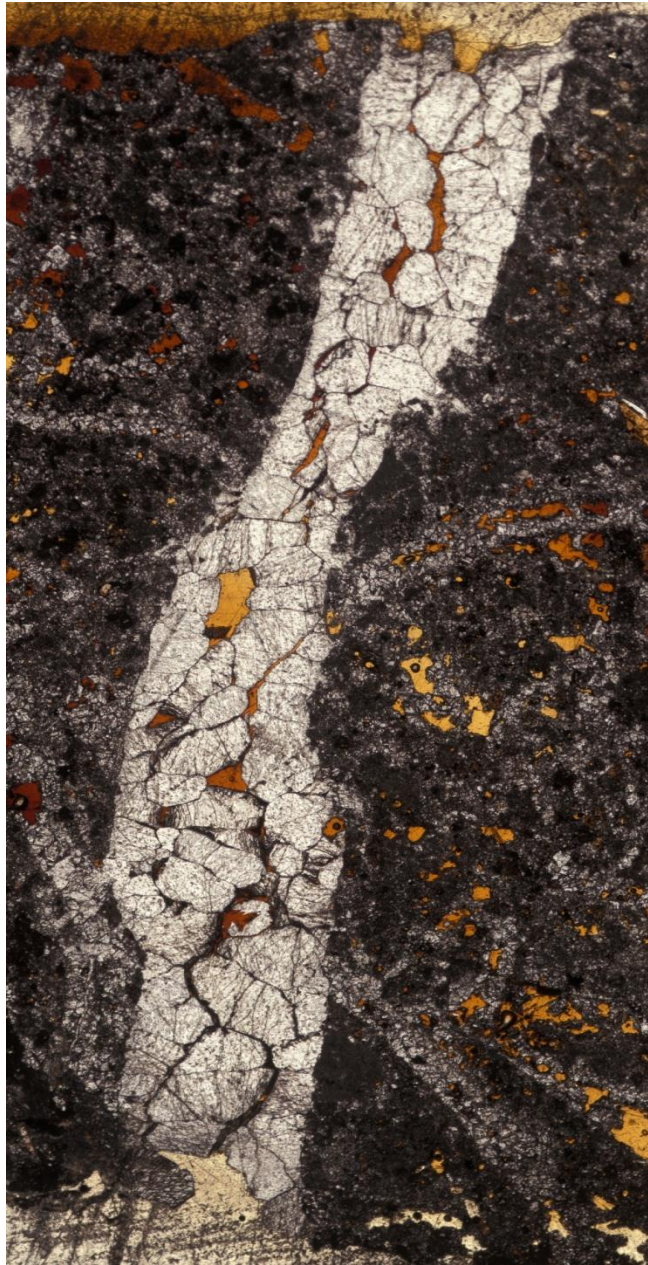
Sketches of different stages of formation/deformation of a sedimentary rock until a final state illustrated by the microphotographs of polished thin sections observed in natural light. (a) Sandstones (Amsden); (b) Carbonates (Phosphoria).  $XY$  plane is the bedding plane ( $X$ : Strike;  $Y$ : dip),  $YZ$  is the plane perpendicular to the bedding plane.

(Amrouch et al., 2010)

The macroscopic asymmetry of the NE-verging SMA, likely related to underlying basement thrust, is also clearly marked at the mesoscopic and the microscopic scales. Structural observations made at the microscopic scale in part of a fold may therefore be relevant to the fold scale.

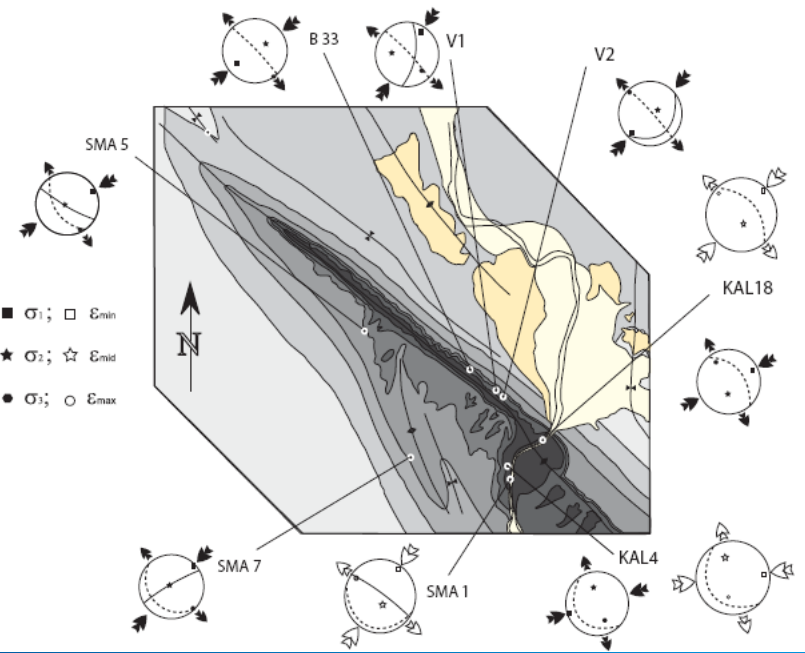
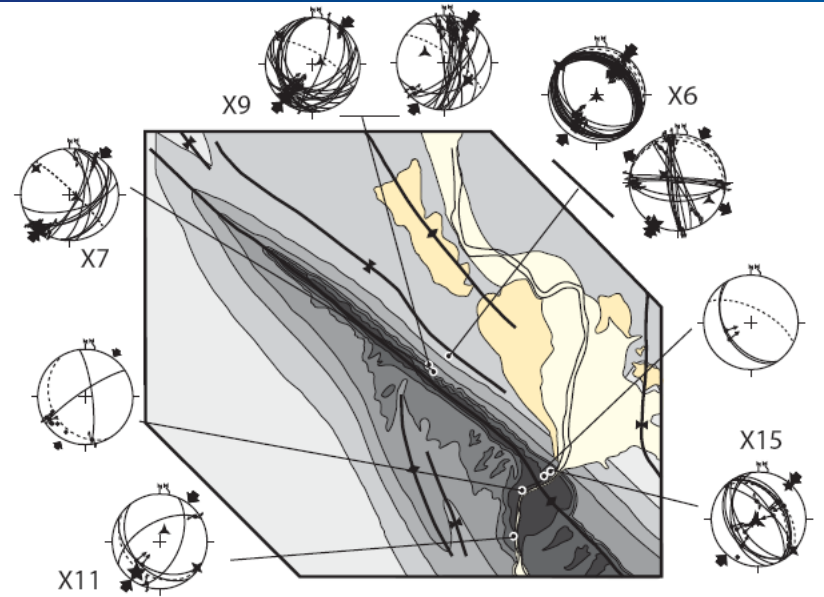
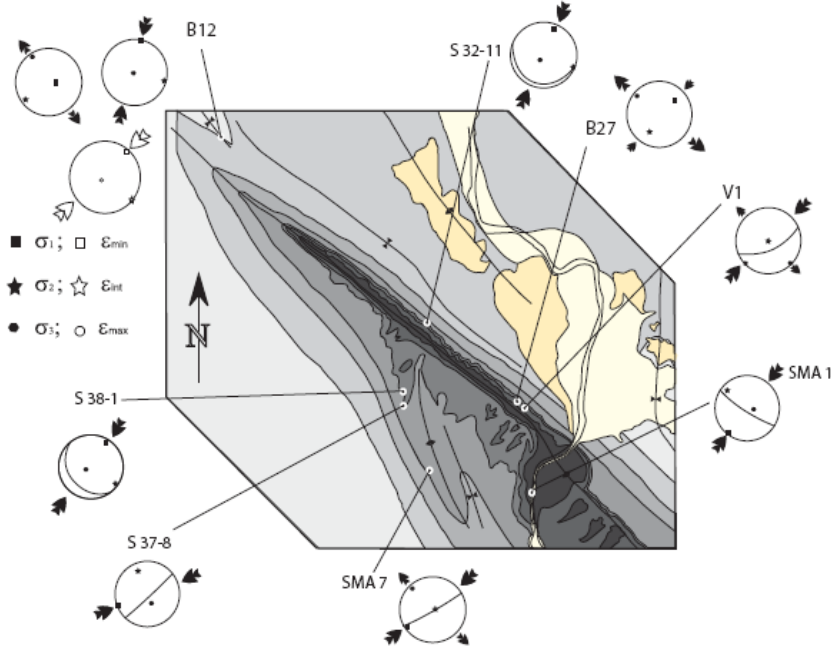
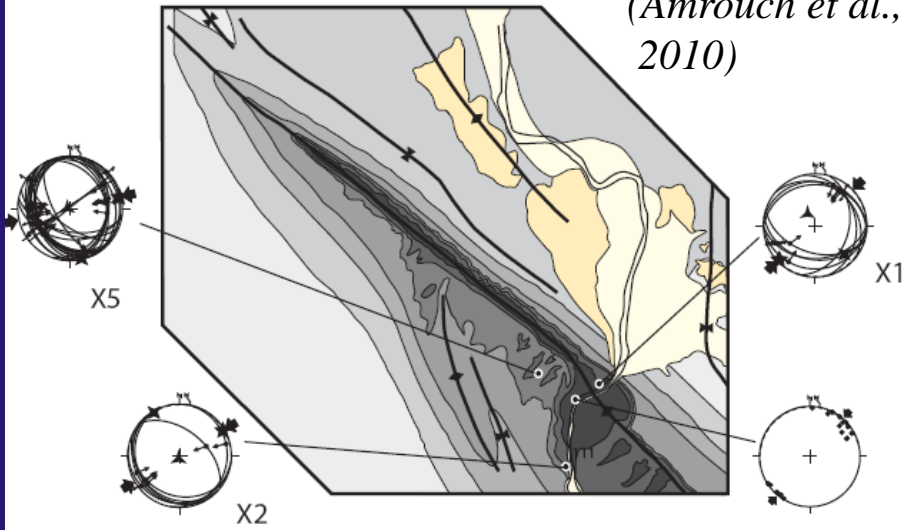
Calcite twinning in folded strata

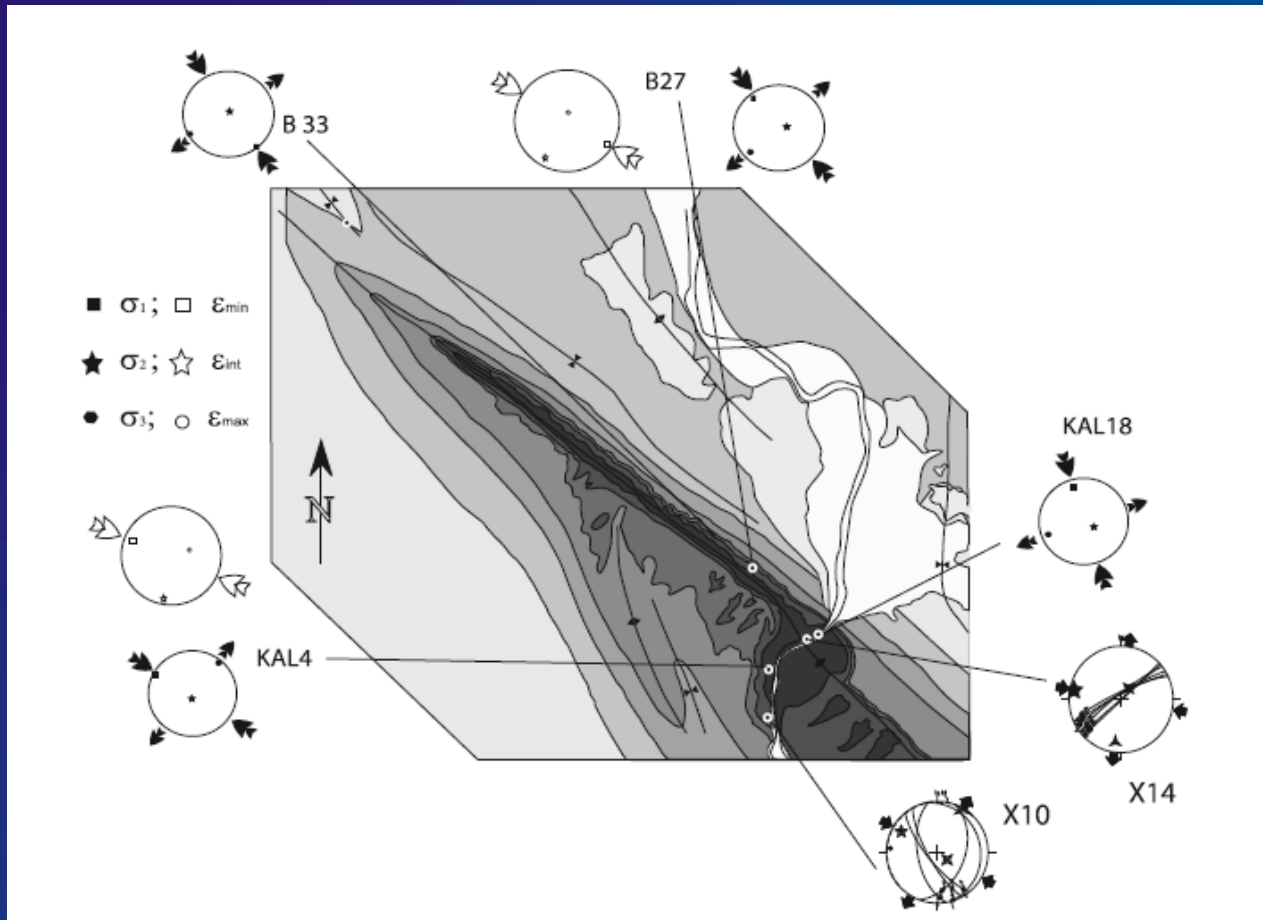






(Amrouch et al., 2010)

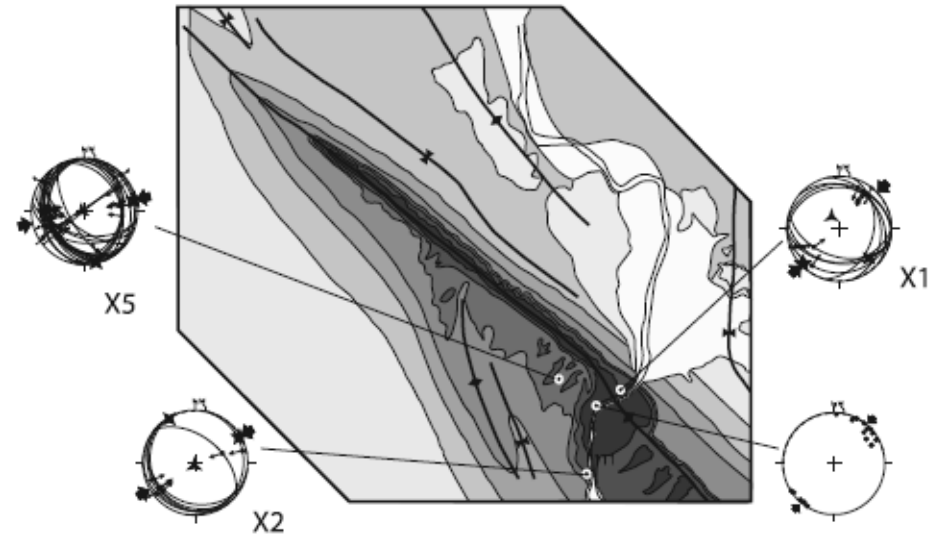
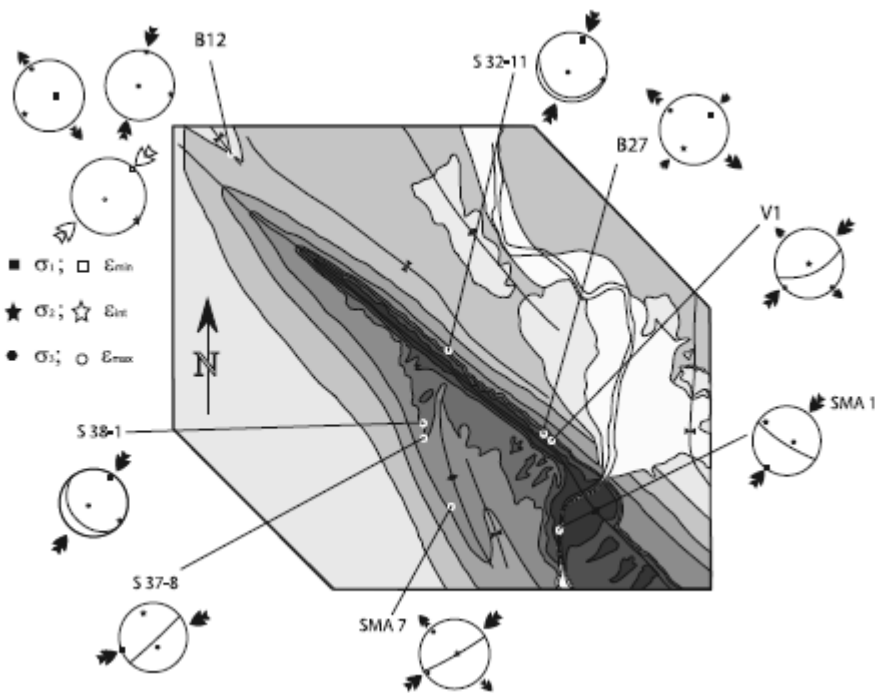




Pre-folding stage : strike-slip stress regime under a NW-SE horizontal compression



# Early-folding stage: Paleostress /strain orientations related to Laramide LPS.

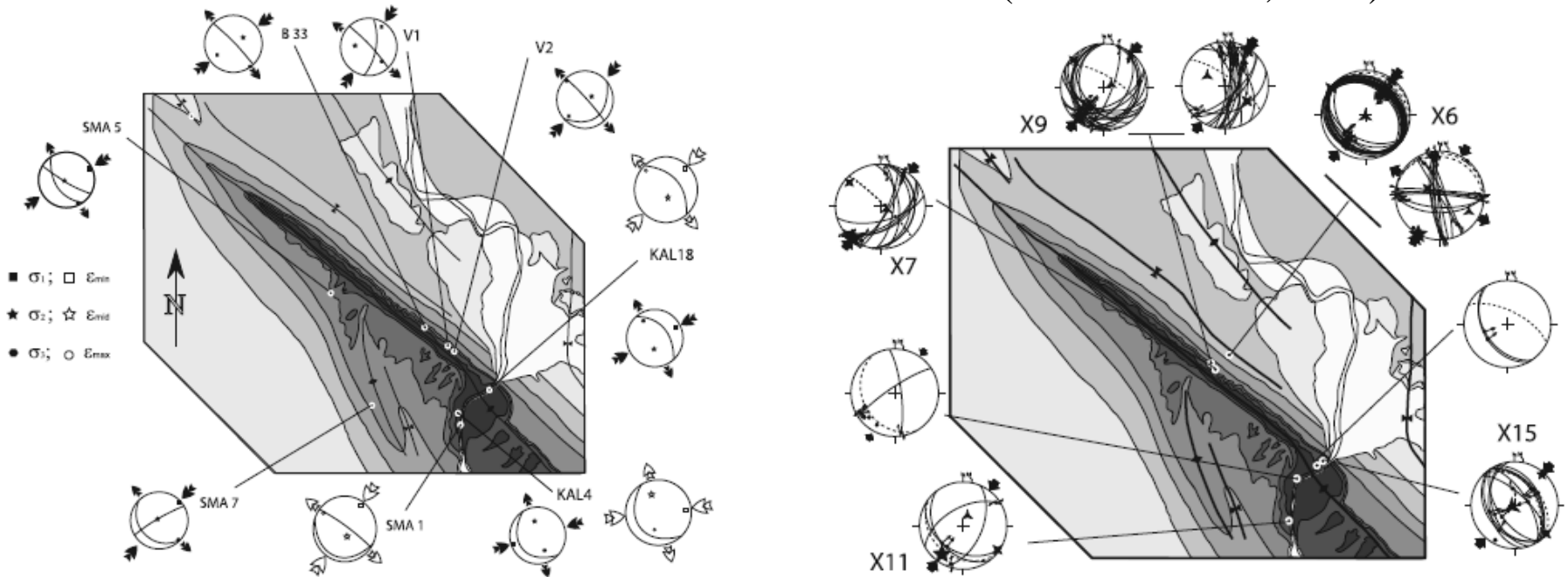


(Amrouch et al., 2010)

Laramide Layer-Parallel Shortening (LPS). The compression was oriented NE to ENE either in a strike-slip or in a compressional regime.

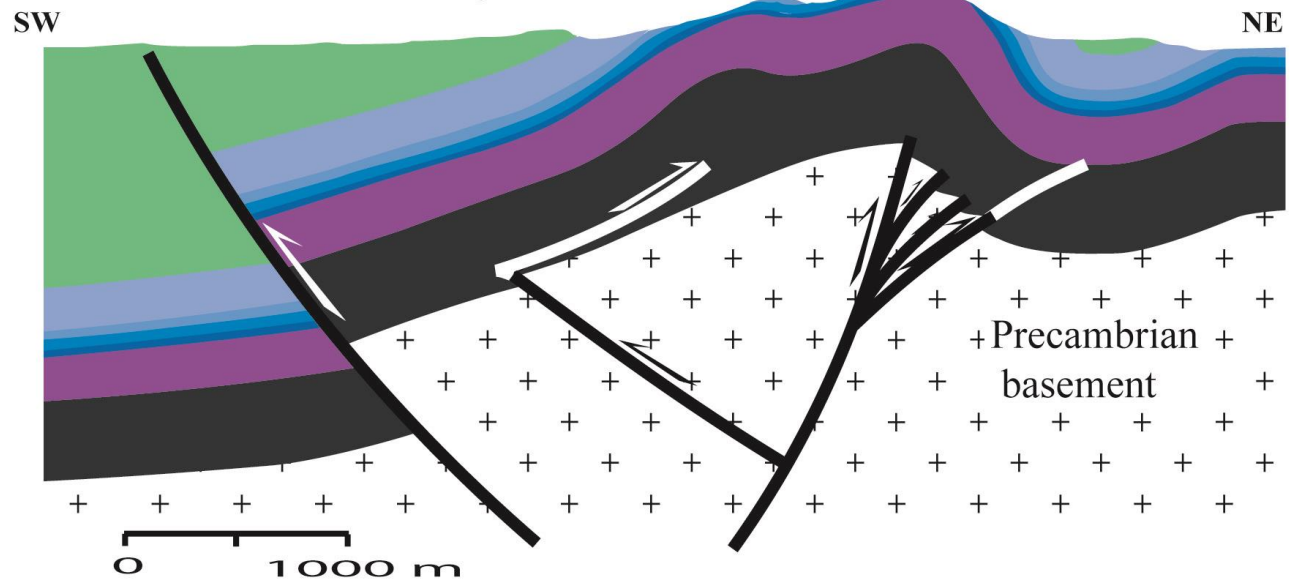
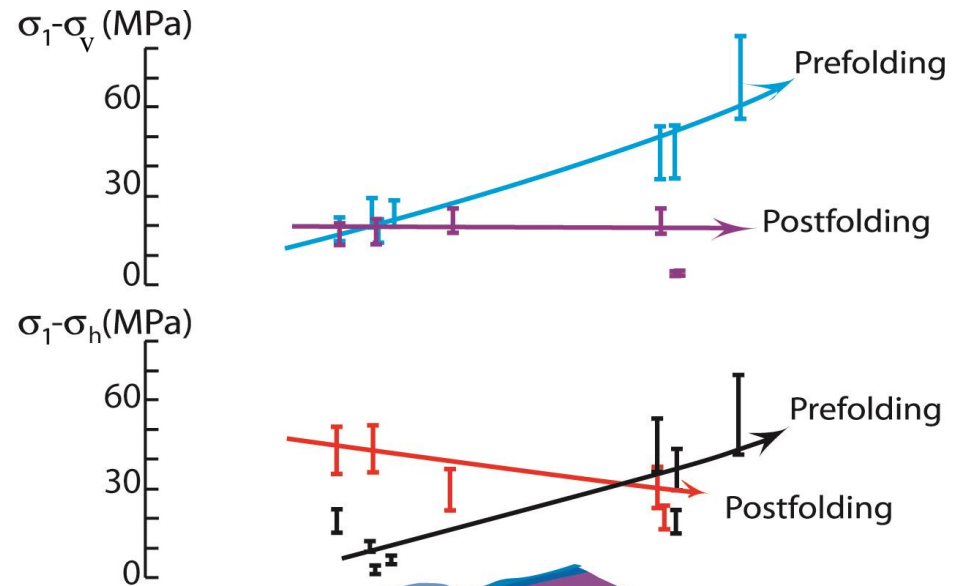
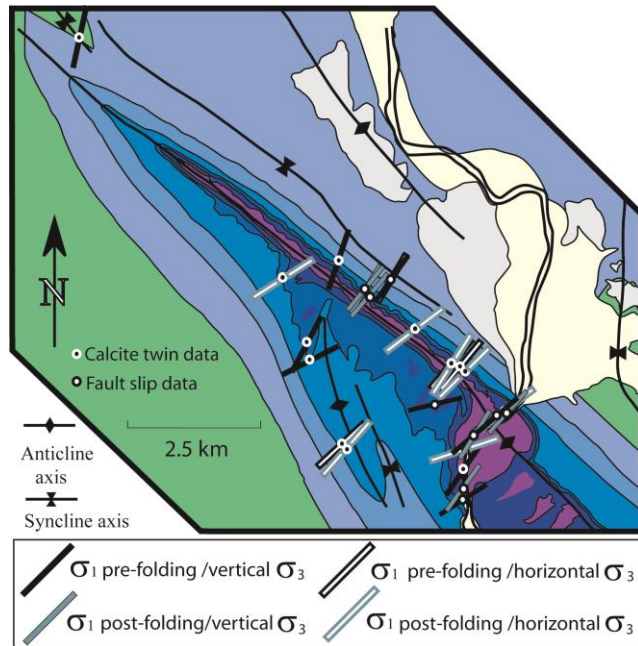
# Late-folding stage: paleostress / strain orientations related to Laramide late stage fold tightening.

(Amrouch et al., 2010)



Faults and calcite twins reveal a late fold tightening stage, associated with a strike-slip stress regime and a paleo- $\sigma_1$  axis also oriented NE.

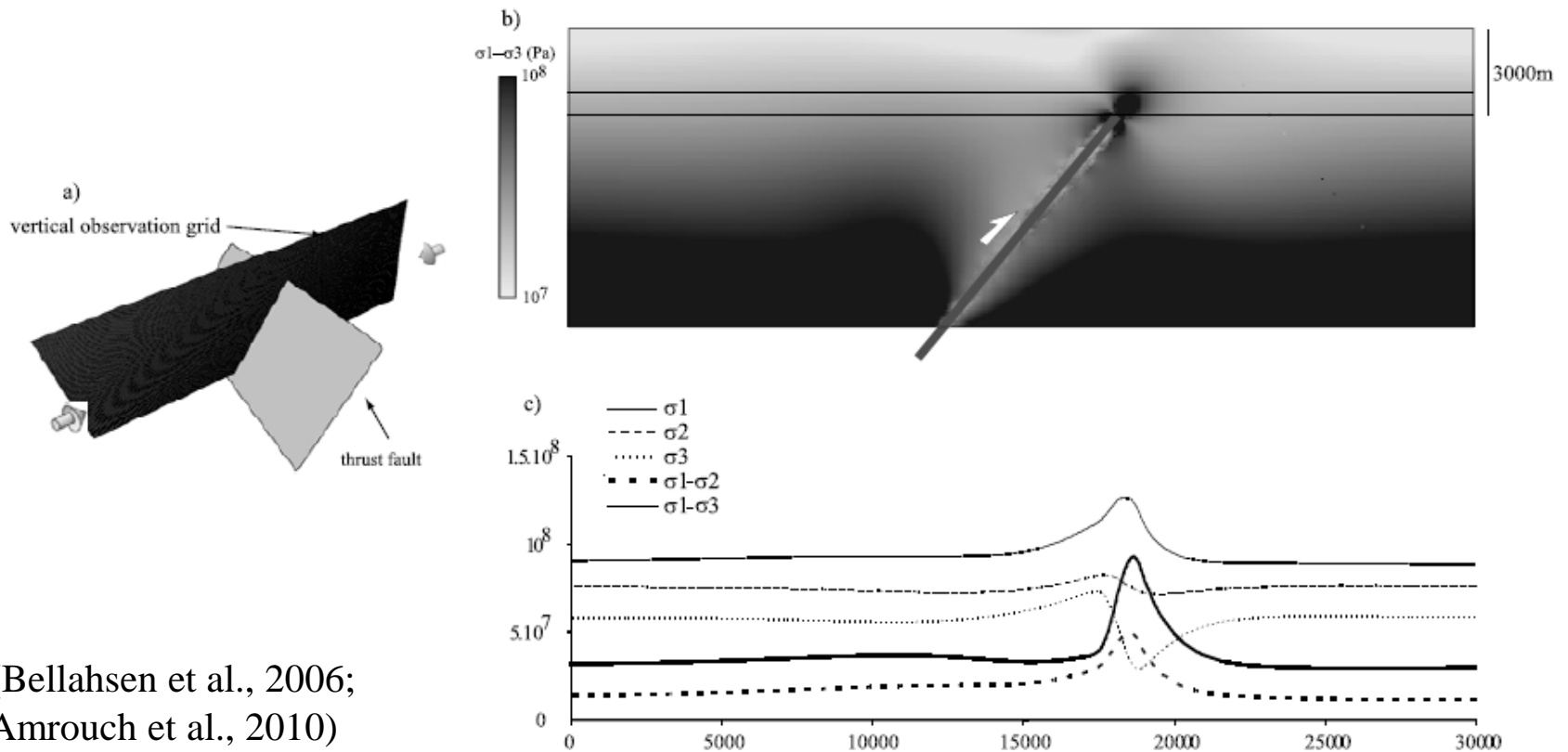
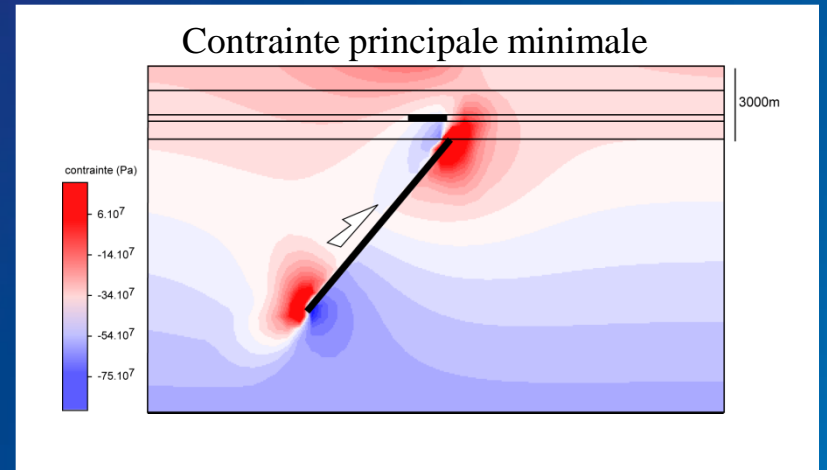
# Early-folding and late-folding Laramide paleo-differential stress magnitudes from calcite twinning paleopiezometry



(Amrouch et al., 2010)



Stress perturbations in the sedimentary cover  
at the tip of the underlying basement fault  
starting to move during Laramide stress  
build-up



(Bellahsen et al., 2006;  
Amrouch et al., 2010)

The estimated paleo- principal stress magnitudes are in the range of 20-60 MPa for  $\sigma_1$  and -3-10 MPa for  $\sigma_3$  in the limestone rocks deformed at 1000-2000m depth.

These estimates of are amongst the very few ones available for upper crustal paleo-stresses at the particular time of tectonic deformation (e.g. Taiwan, Lacombe, 2001).

Being related to ongoing deformation, and averaged over the duration of the Laramide event, they are theoretically hardly compared to modern stresses measured in situ which are rather representative of ambient instantaneous stresses.

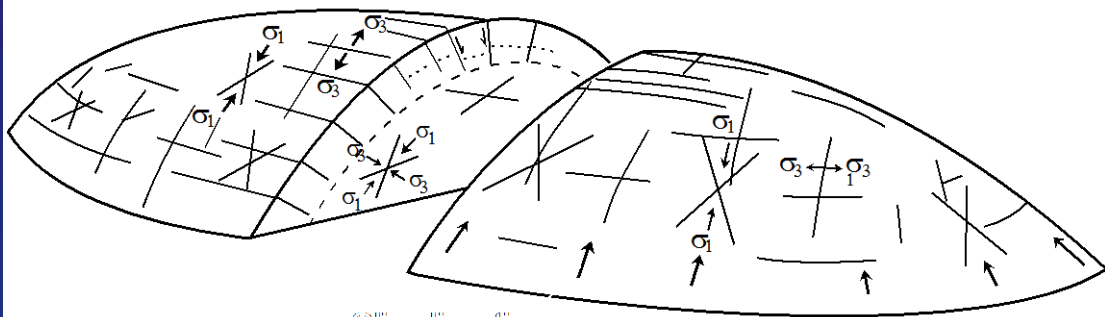
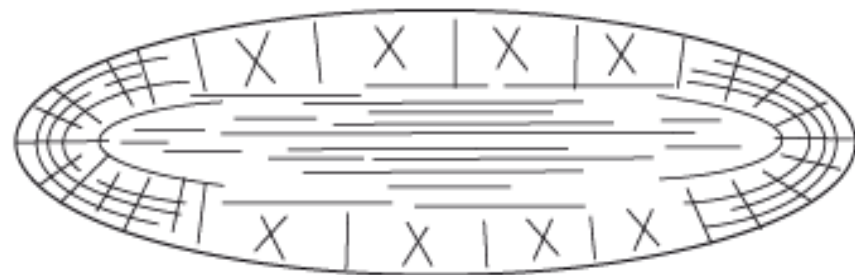
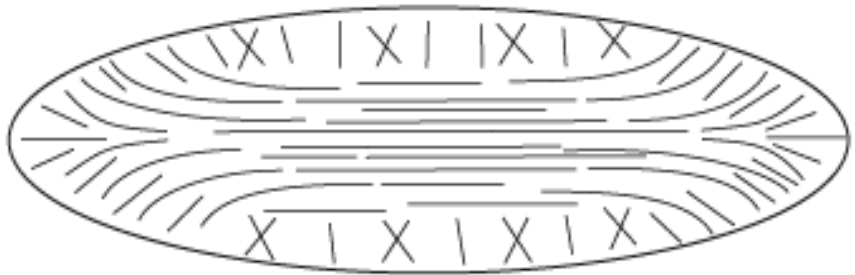
They are nevertheless of the same order than the modern principal stress values determined in strike-slip or compressional stress regimes at various places e.g., at the SAFOD pilot hole (Hickman and Zoback, 2004)

Investigating folding at the mesoscale :  
fracturing in folded strata

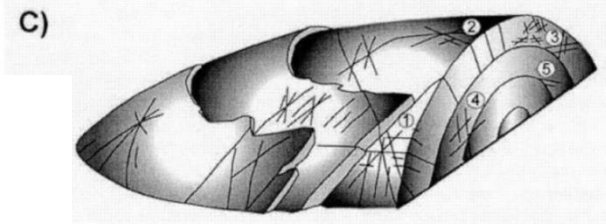
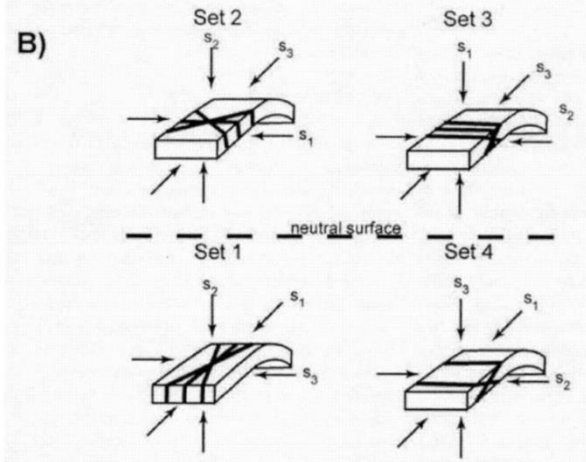
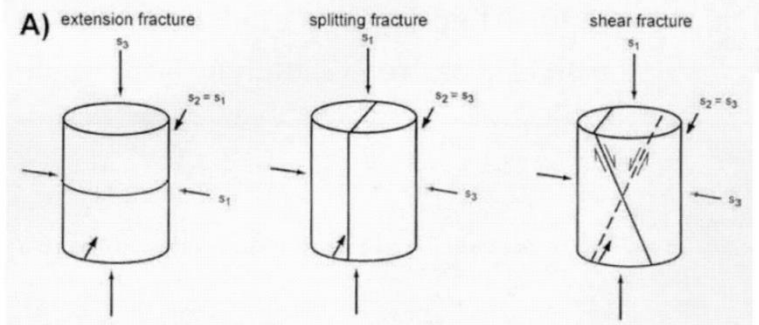


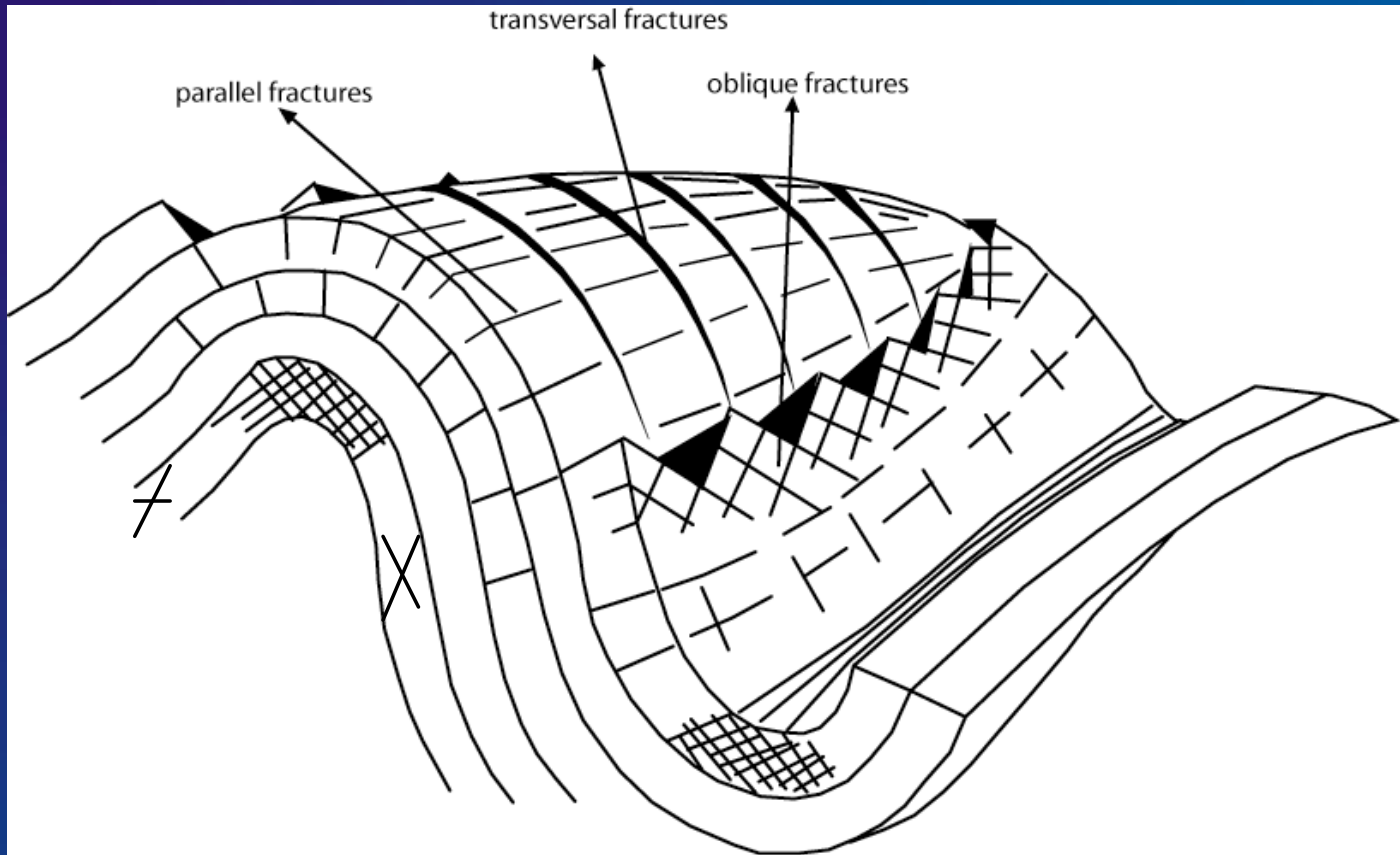
Fold geometry and kinematics have for a long time been recognized as the most important factors that control fracturing. Stearn & Friedman (1972) proposed a pioneering classification of fold-related fractures, including an axial extensional set running parallel to the fold axis, a cross-axial extensional set oriented perpendicular to the fold axis and two sets of conjugate shear fractures oblique to the fold axis with their obtuse angle intersecting the trend of the fold axis.

Since then, numerous studies have attempted to relate the development of mesostructures to either the structural domains of the fold or to quantitatively estimated curvature of strata

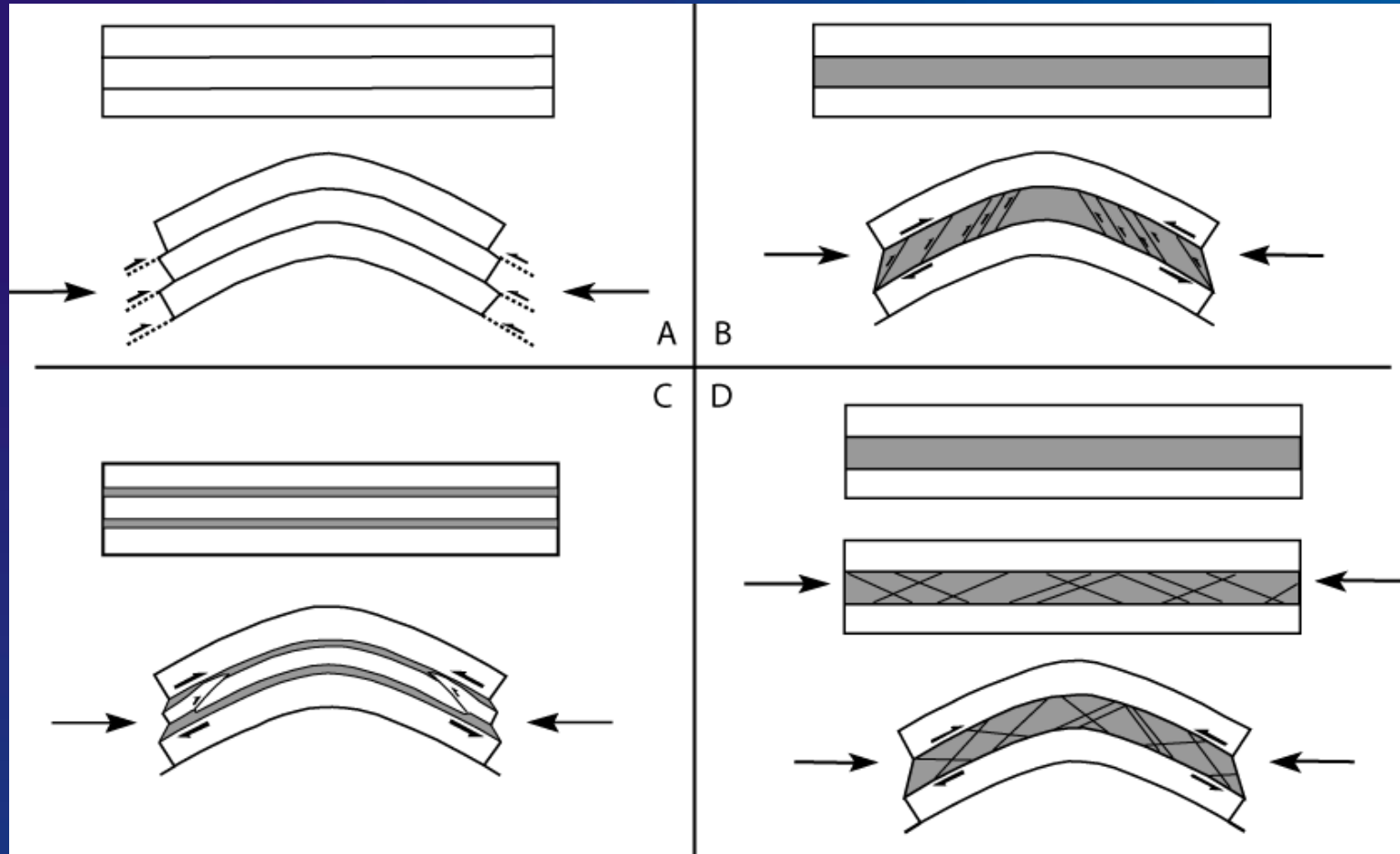


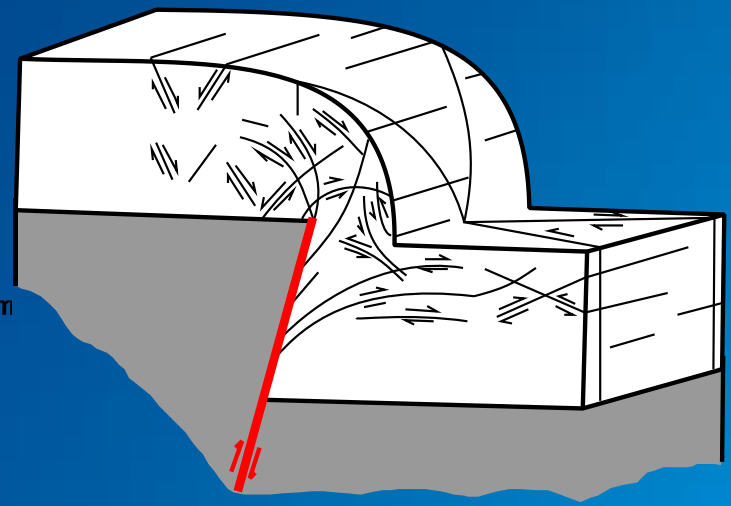
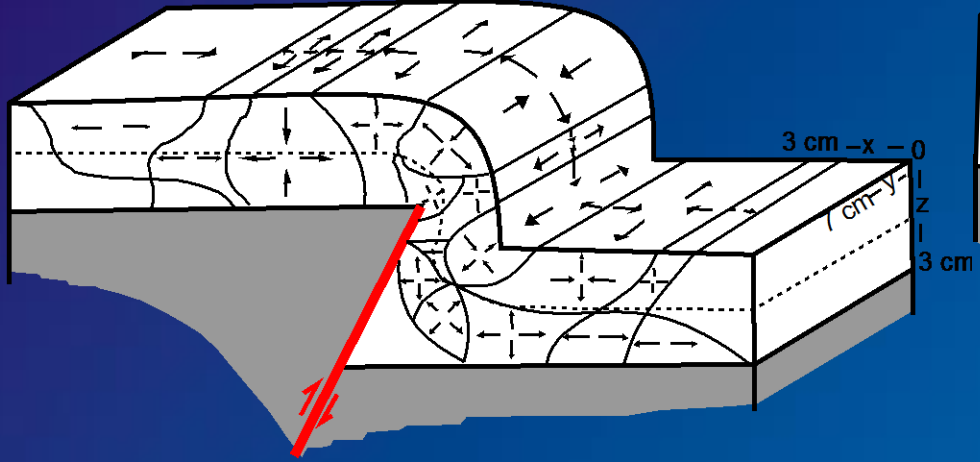
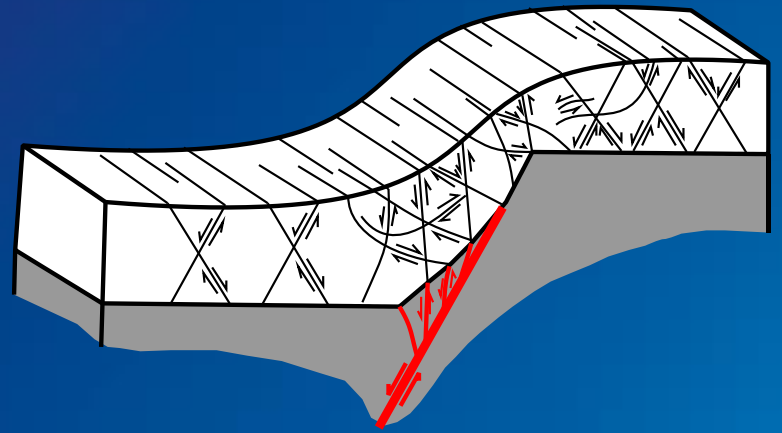
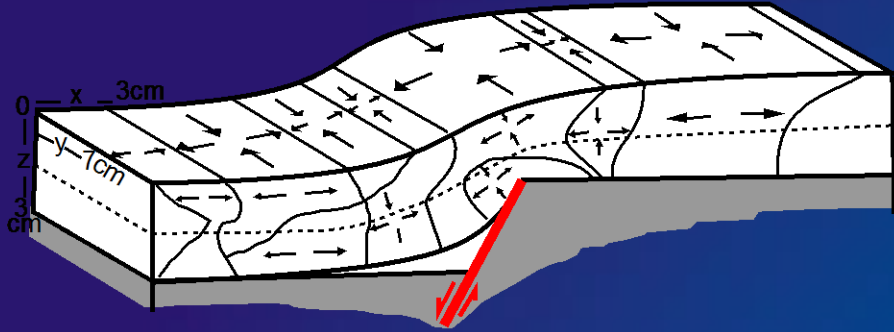
Slip direction

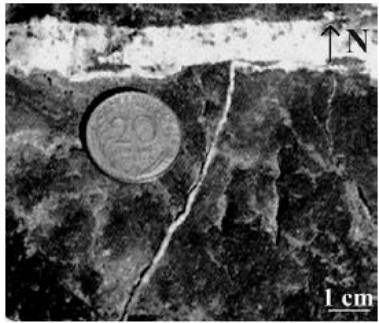




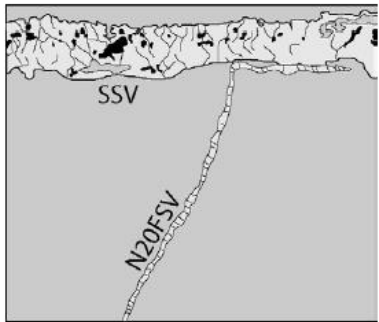
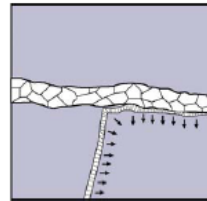
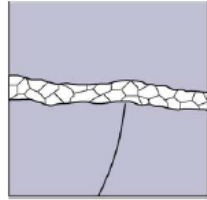
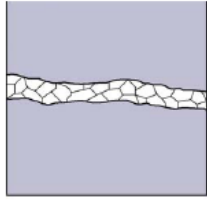








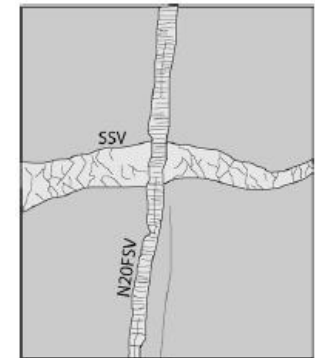
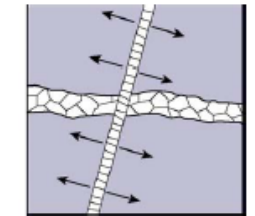
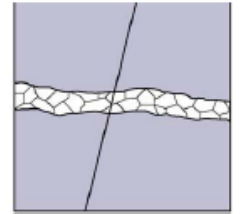
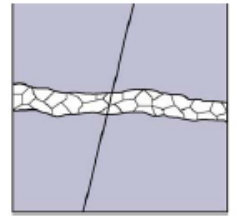
a



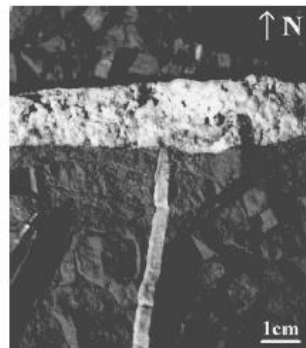
b



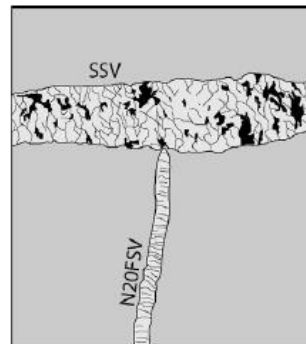
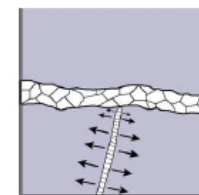
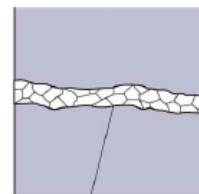
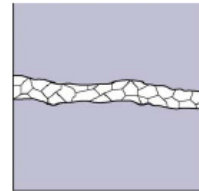
a



b



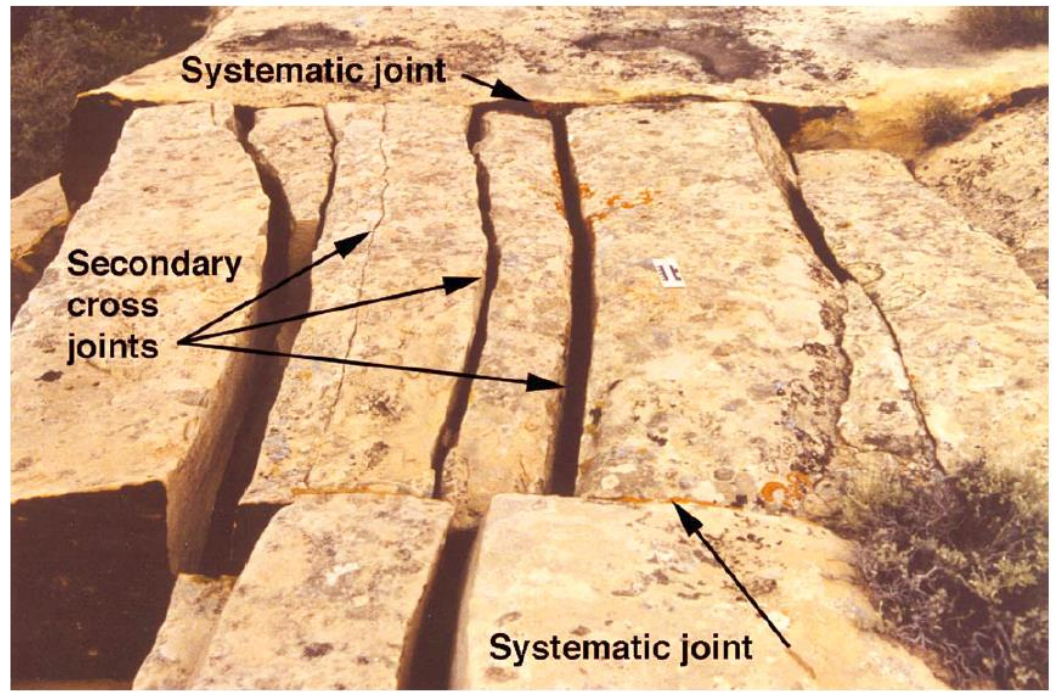
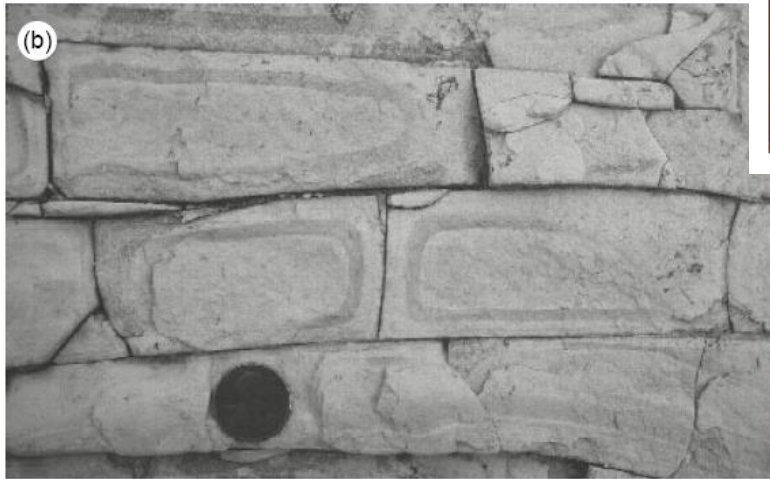
a



b







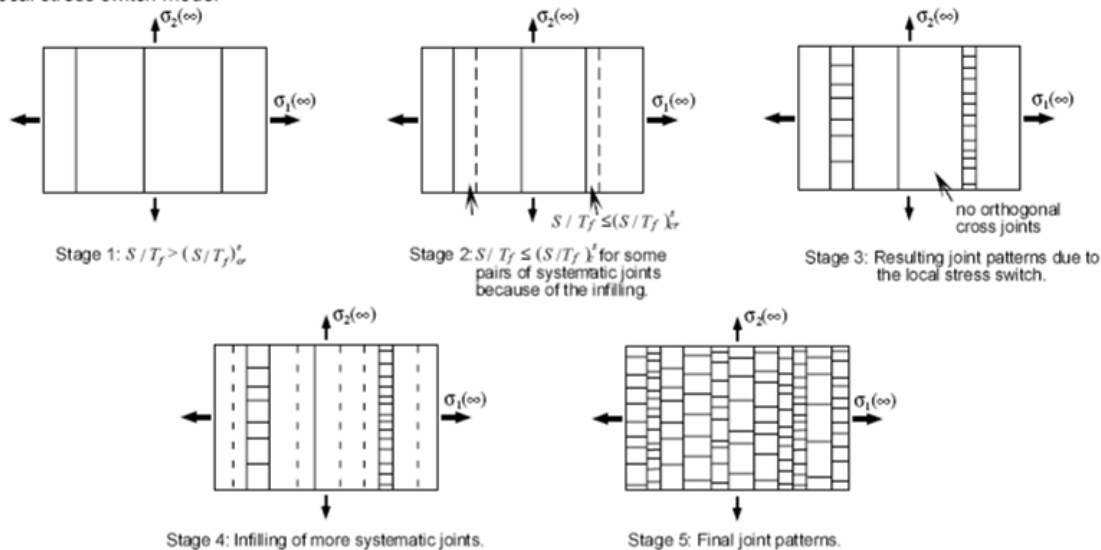
Caution with perpendicular fracture sets

# Stress perturbations/permutations :

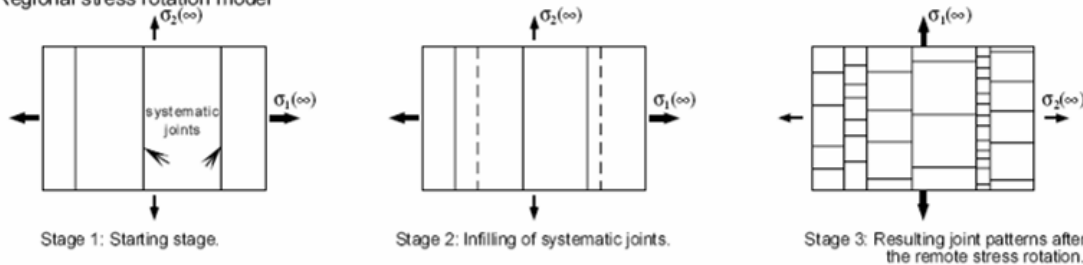
Around a fracture, there is a stress perturbation that creates a stress shadow where development of a new fracture is inhibited.

When 2 joints are close to each other, the formation of a new joint is inhibited. According to local stresses, a stress permutation may occur that may lead to formation of a perpendicular fracture set.

(a) Local stress switch model

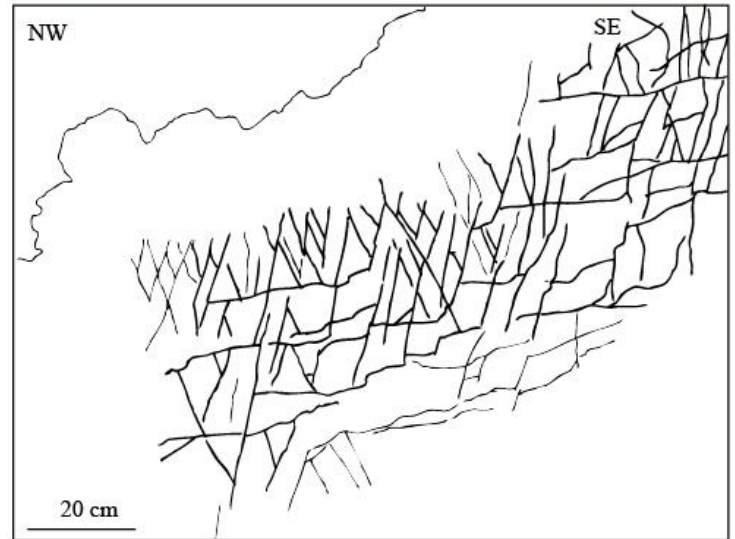
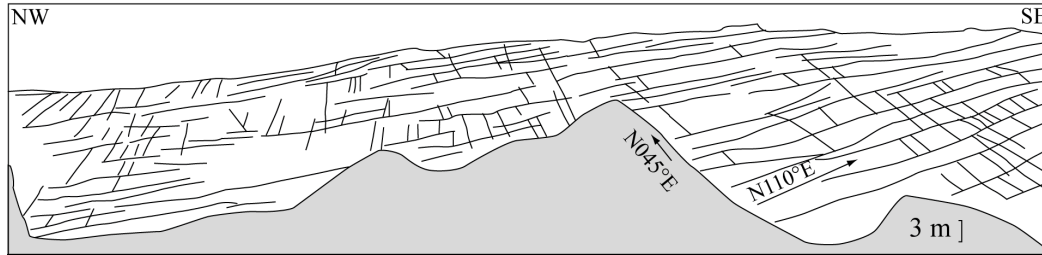


(b) Regional stress rotation model



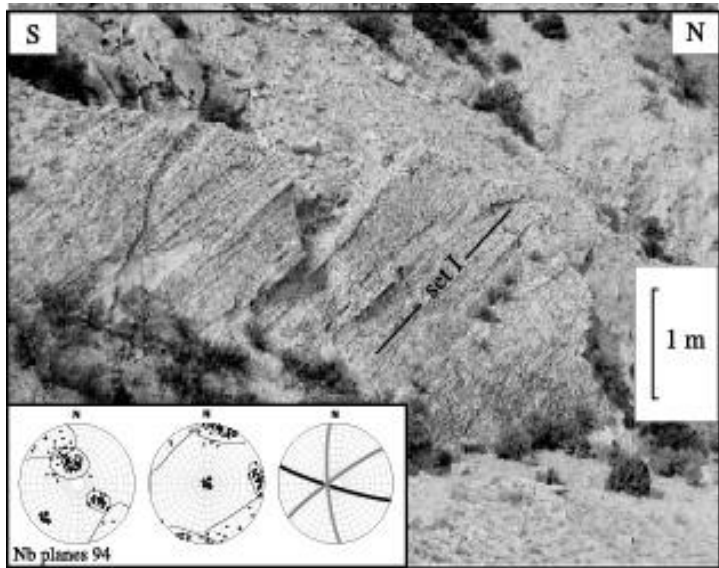
**No regional meaning**



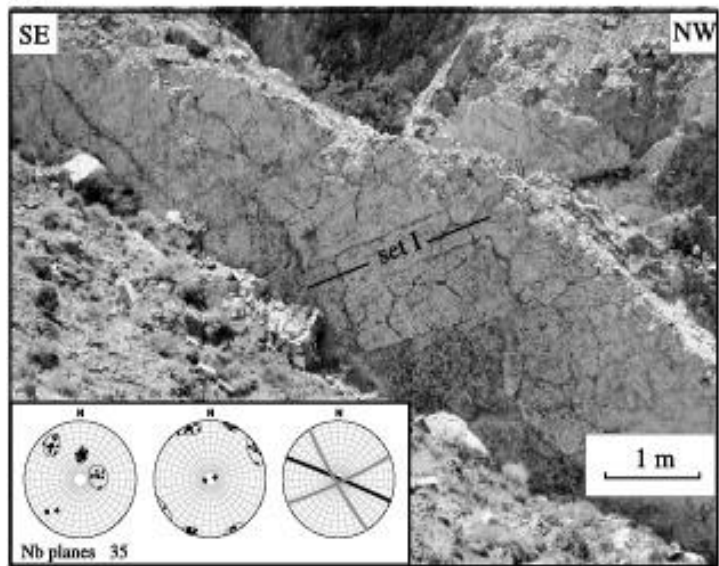


(Bellahsen et al., 2006; Amrouch et al., 2010)

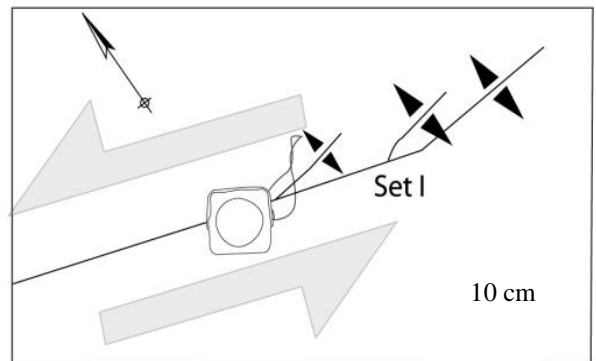




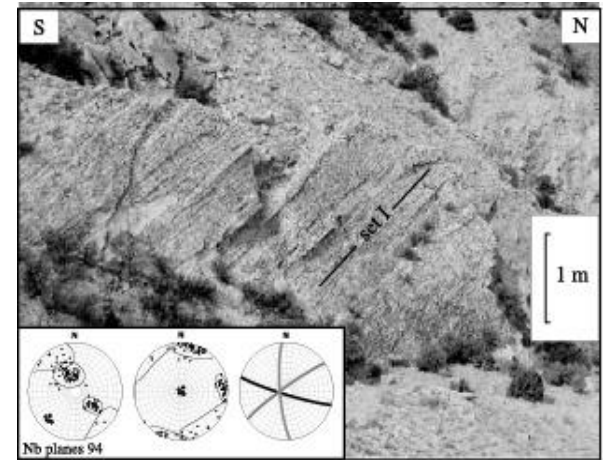
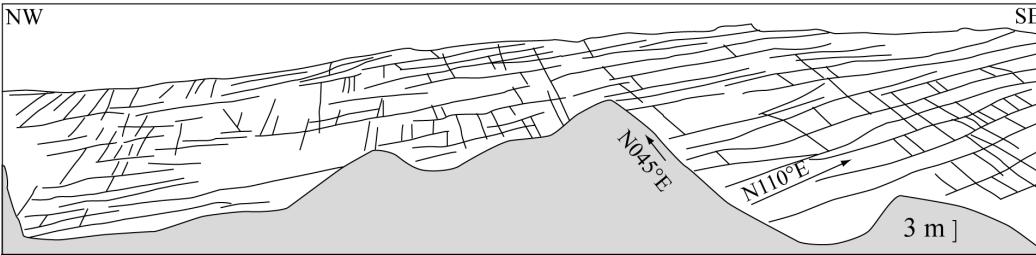
(a)



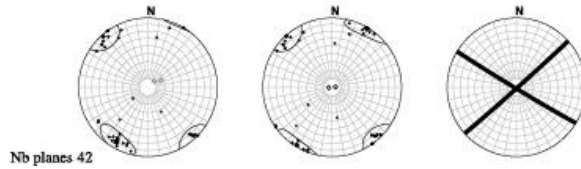
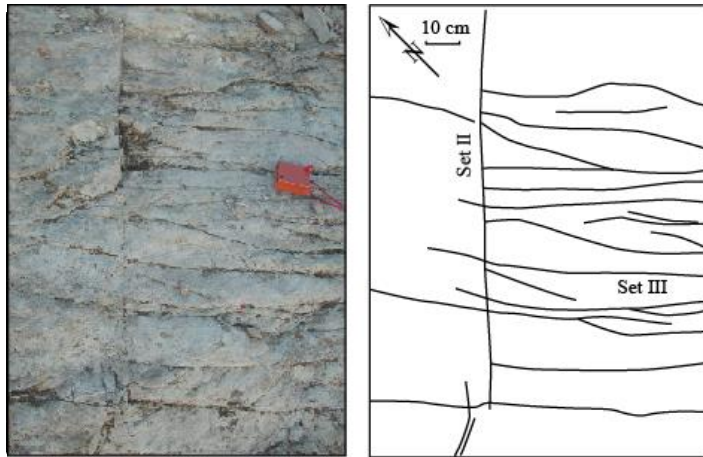
(b)



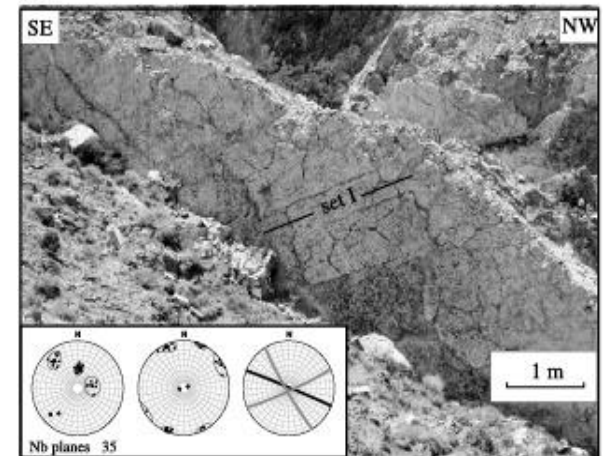




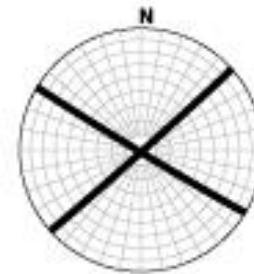
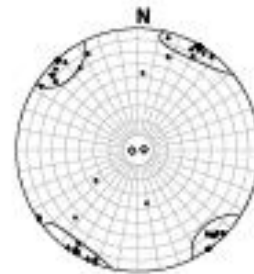
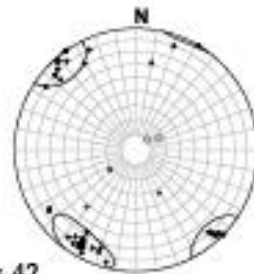
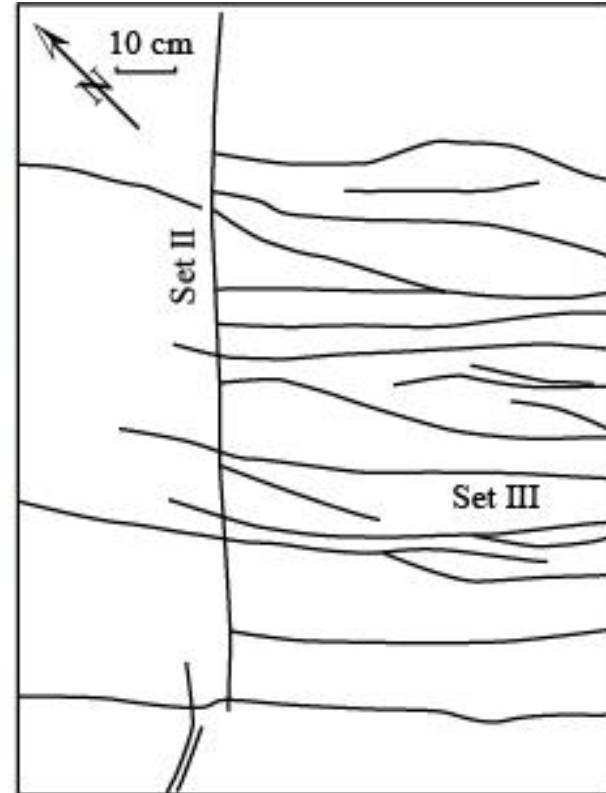
(a)



(Bellahsen et al., 2006;  
Amrouch et al., 2010)

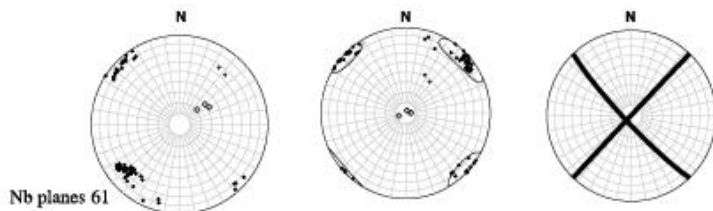
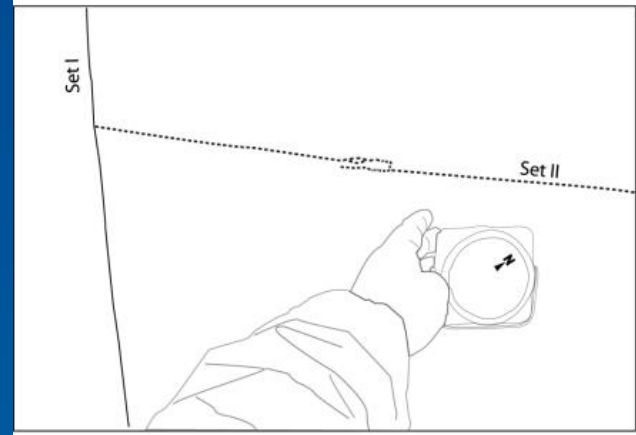
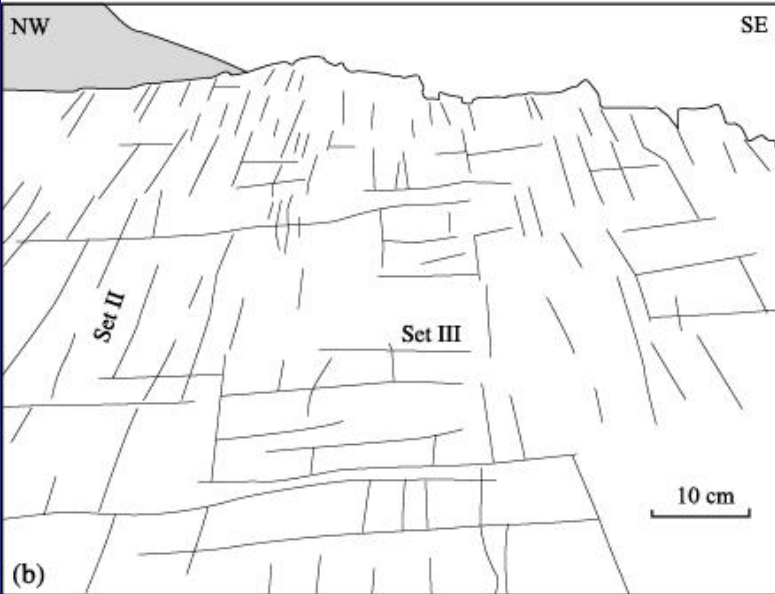


(b)



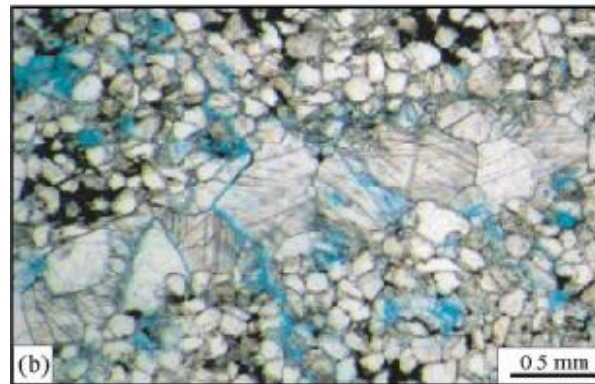
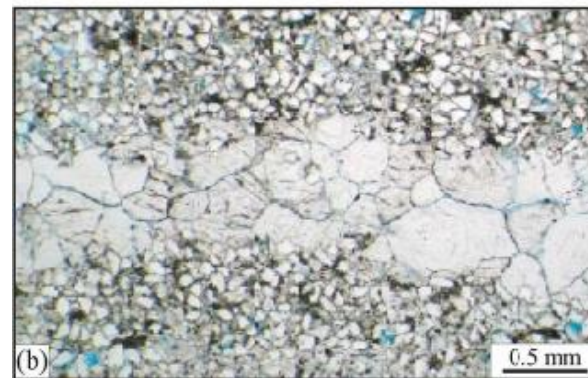
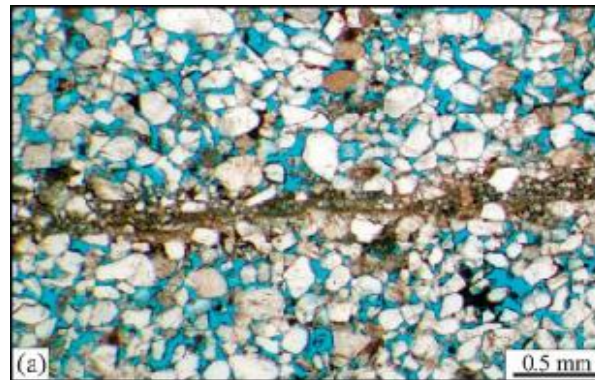
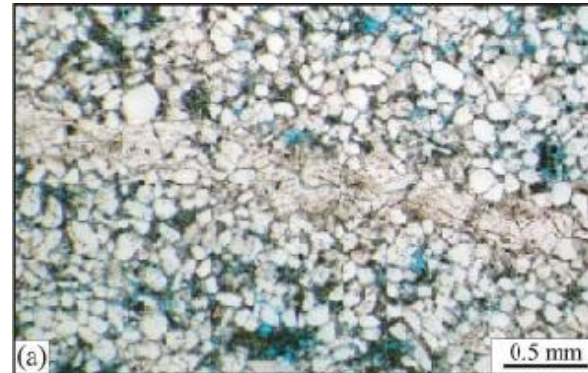
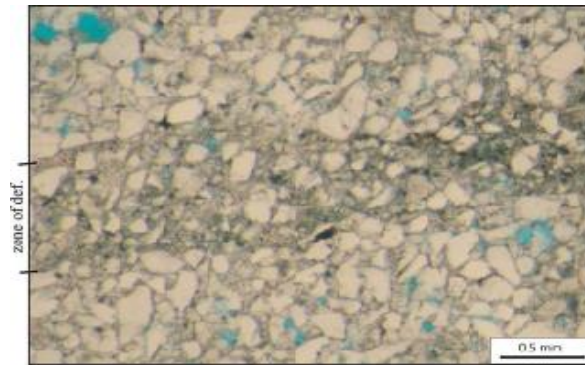
Nb planes 42



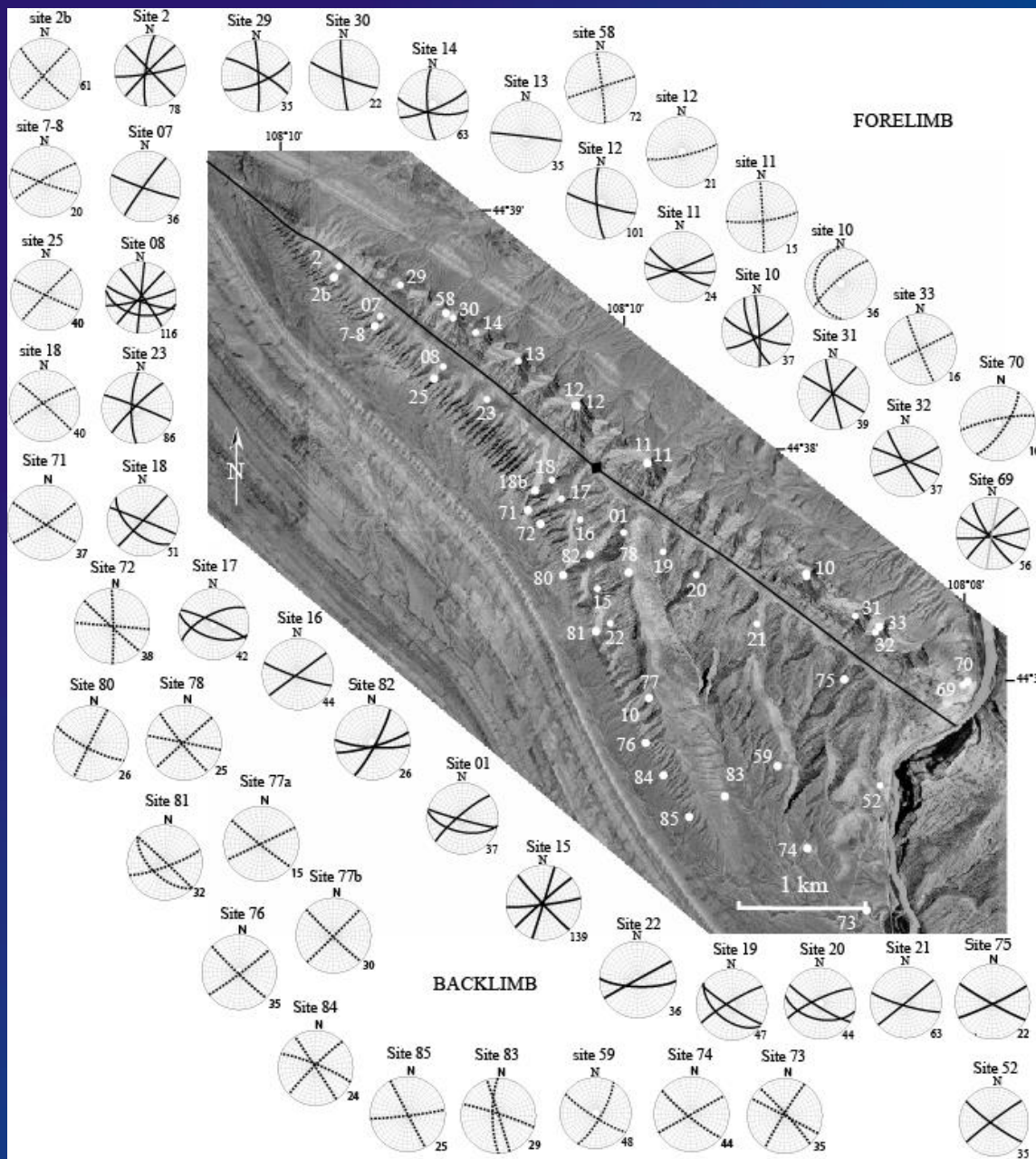


(Bellahsen et al, 2006)

# Checking opening mode of joints/veins in thin sections





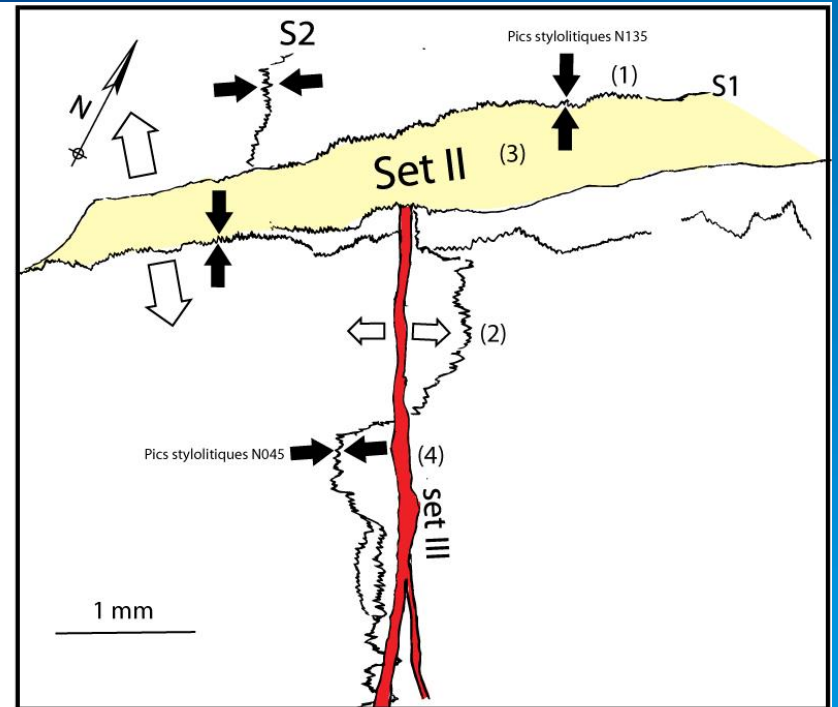
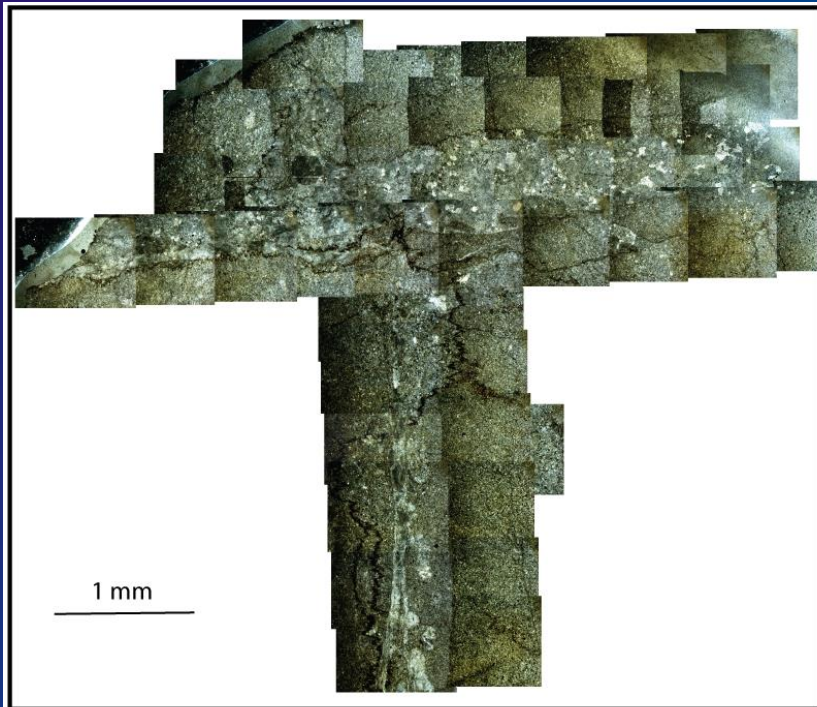
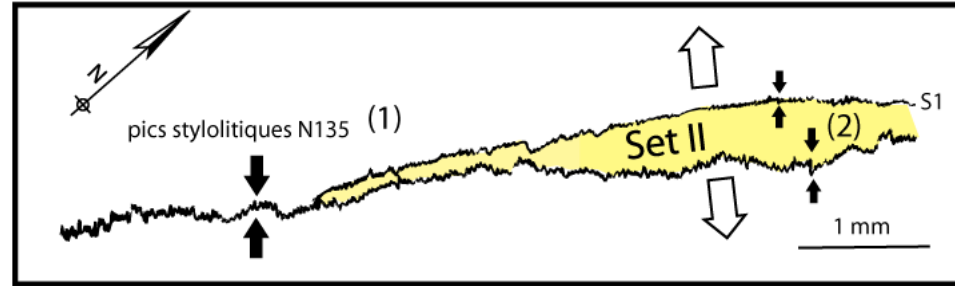


Distribution of joint/vein sets

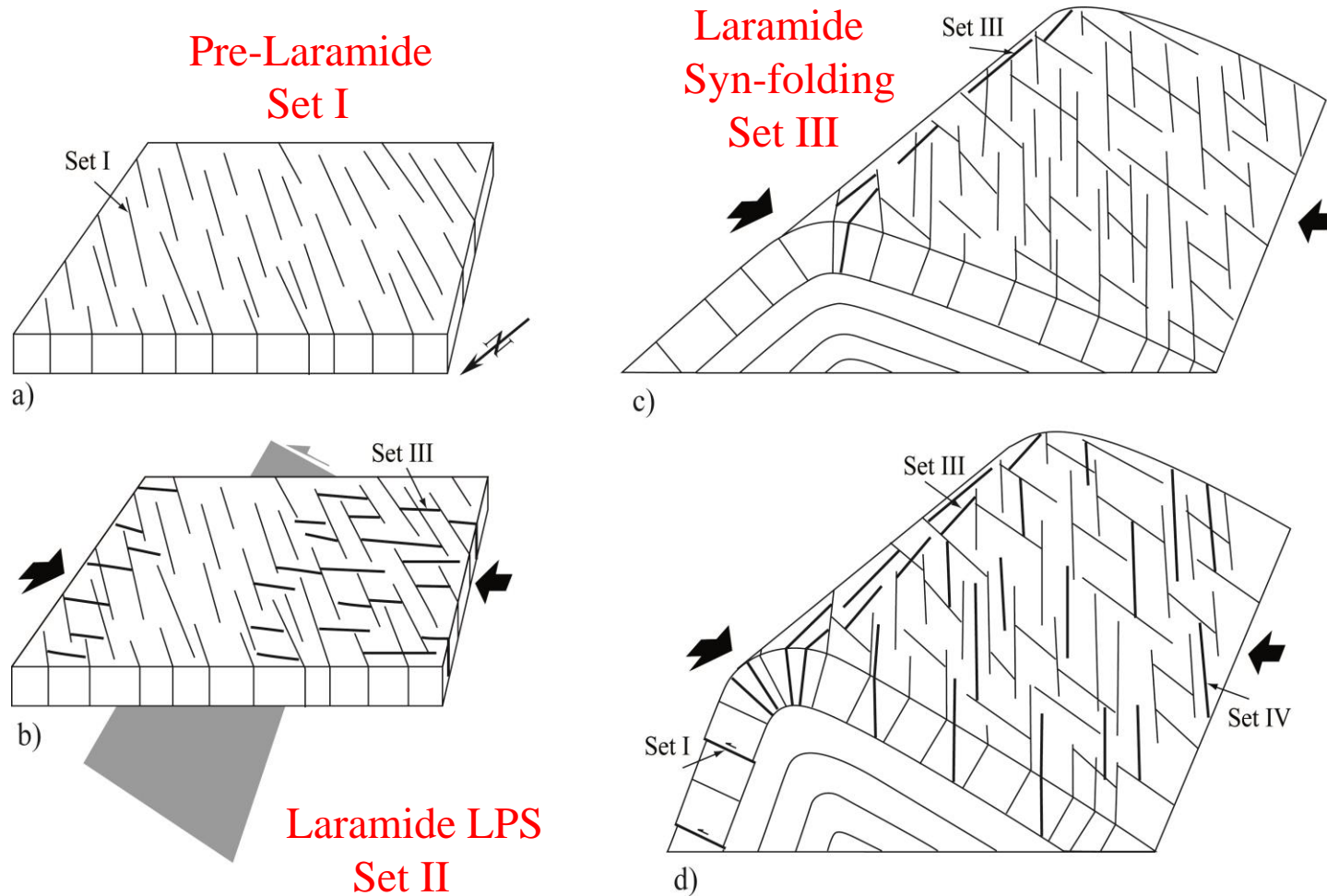
(Bellahsen et al., 2006; Fiore, 2007; Amrouch et al., 2010)

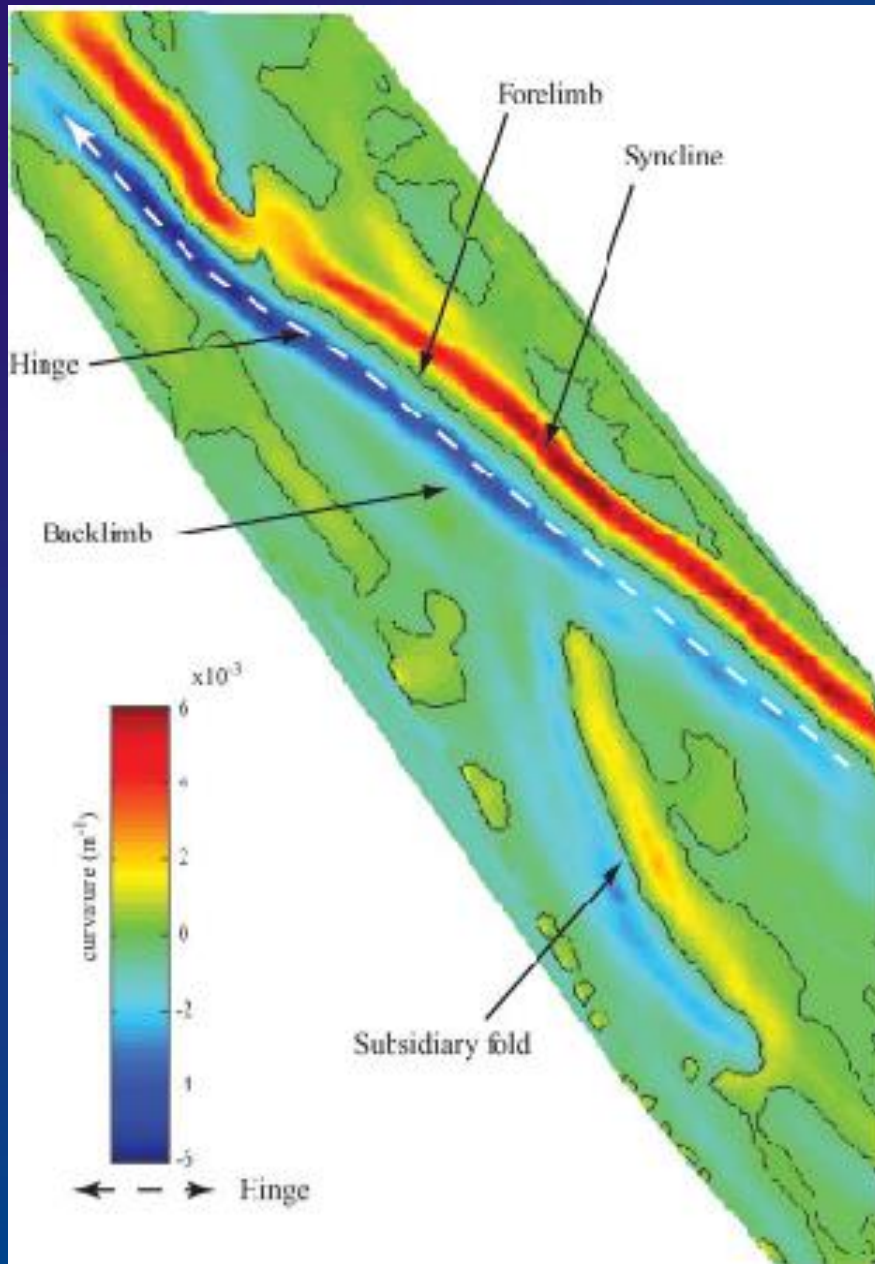


# Relationships between pressure solution seams and fractures



# First-order sequence of fracture development



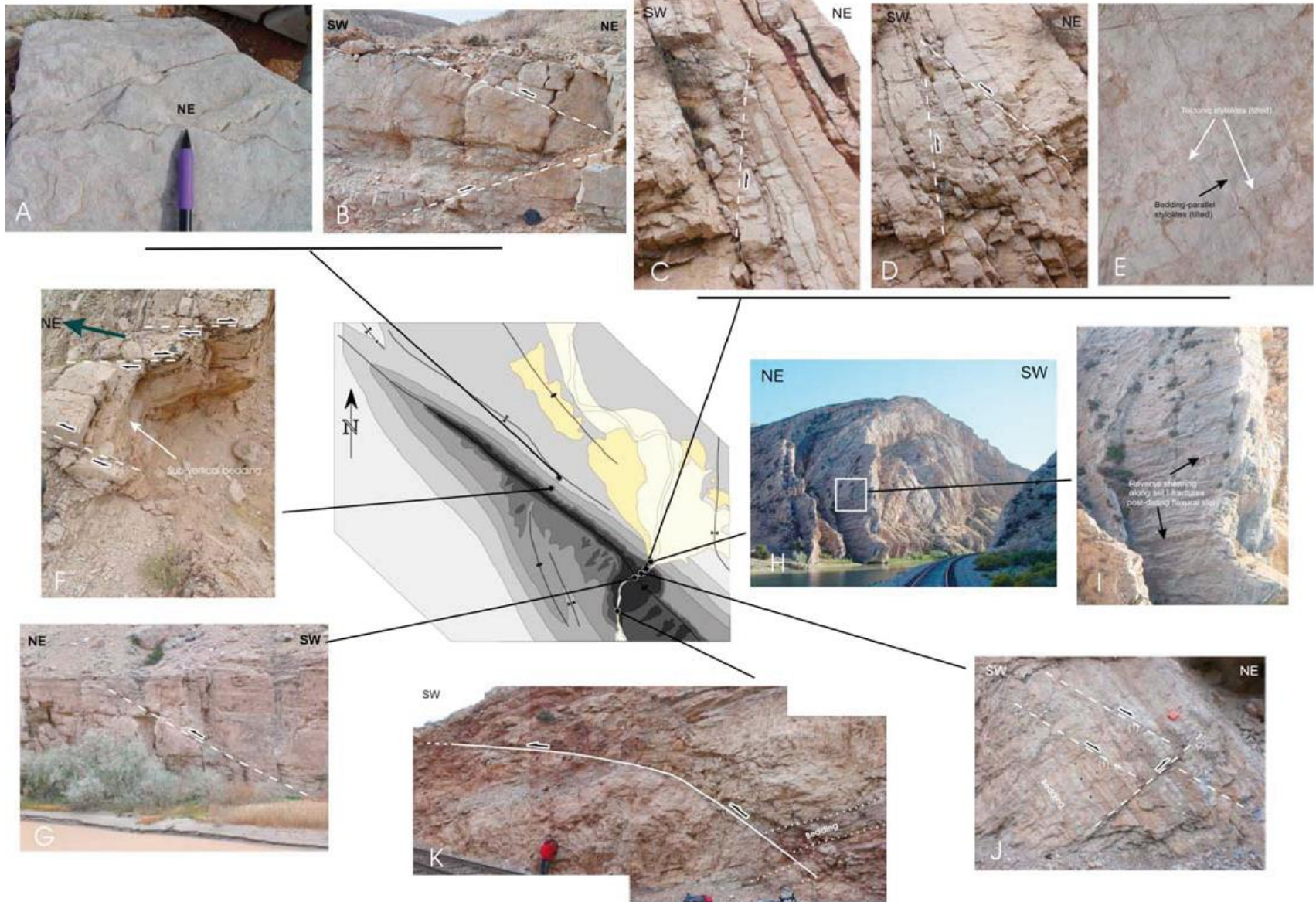


## Curvature analysis

Bellahsen et al, 2006

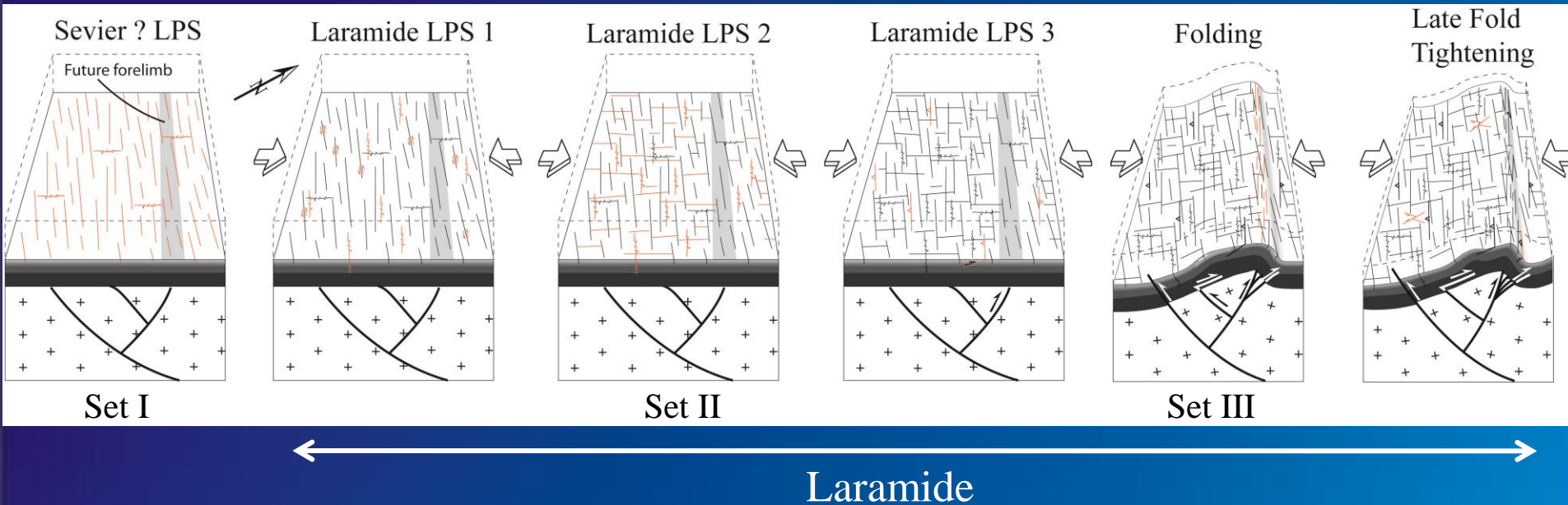


# Meso-scale faulting



# Scenario of fault-fracture development in space and time

(Amrouch et al.,2011)



- Mode I opening of pre-Laramide set I fractures
- Shear reactivation of pre-Laramide set I fractures (LPS 1).
- Laramide stylolites with NE-trending peaks and mode I opening of set II fractures (LPS2)
- Reverse faulting parallel to the fold axis (LPS3).
- Mode I opening of syn-folding, outer-rim extension-related set III fractures
- Late stage fold tightening (LSFT) marked by strike-slip faults and reactivation of tilted set I fractures as small reverse faults in the forelimb

# Insights into mechanical behaviour of folded strata :

## \* Early folding stage - LPS :

Forelimb : stress perturbations, that partly prevented development of fractures. In turn limited fracture development + weak internal deformation (AMS and APWV) → poor stress relaxation → differential stress increase.

Backlimb : no stress perturbation + stress relaxation by widespread development of fractures and by internal strata deformation (AMS) → much lower differential stresses

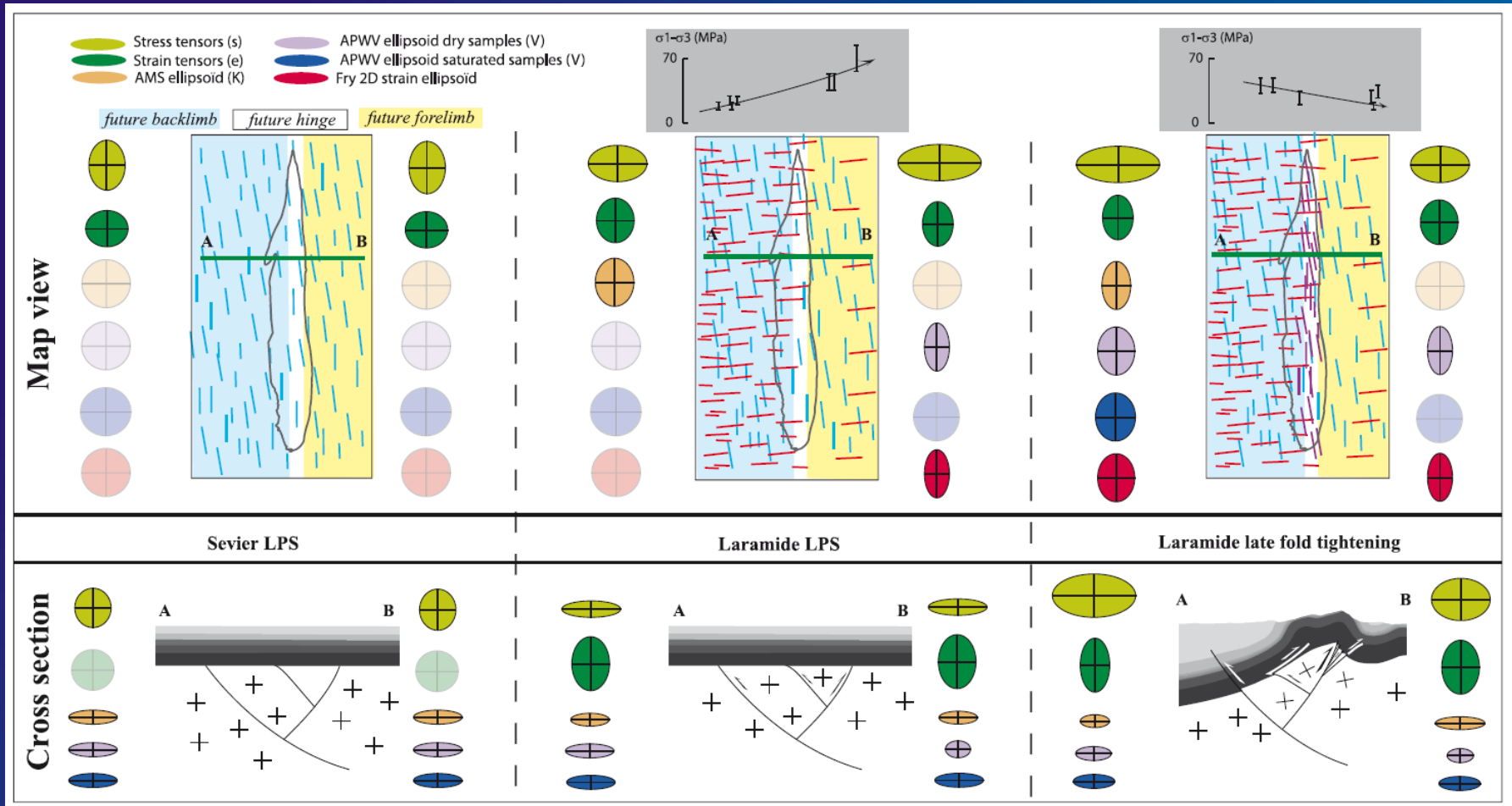
## \* Late-folding stage - LSFT :

Forelimb : drop of differential stresses while limited internal deformation (poorly evolved AMS fabrics and low anisotropy of the matrix revealed by APVW → strata were tilted during folding without any additional significant internal deformation, LSFT being mainly accommodated by newly formed microfaults and reactivation of earlier fractures → stress relaxation

Backlimb : Strata sustained most of LSFT without developing much fractures, → increase of differential stresses and development of more evolved ASM fabrics

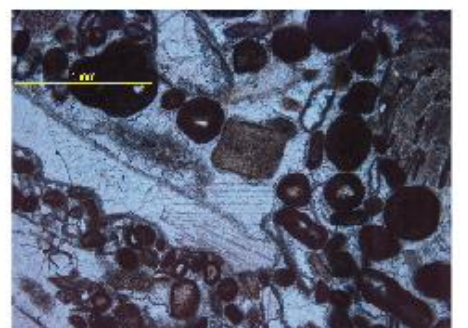
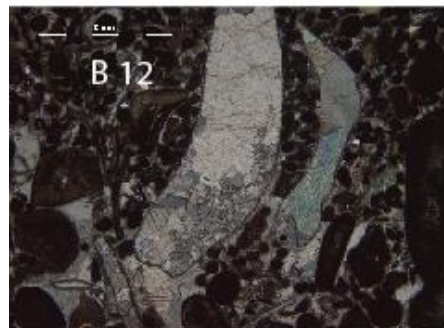
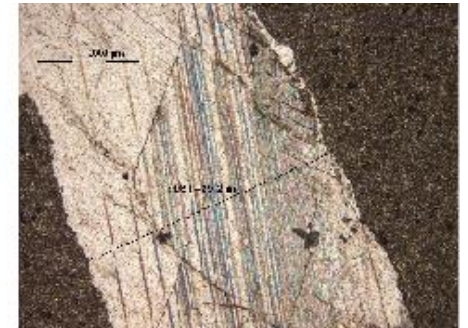
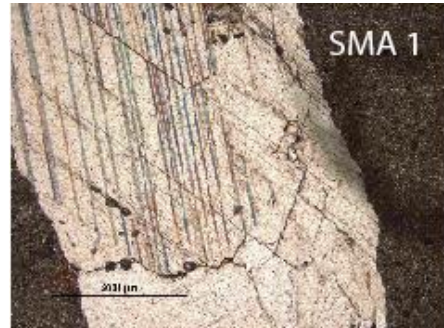
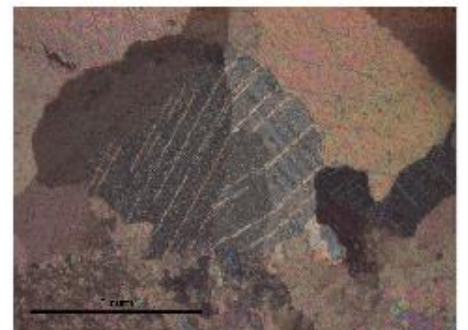
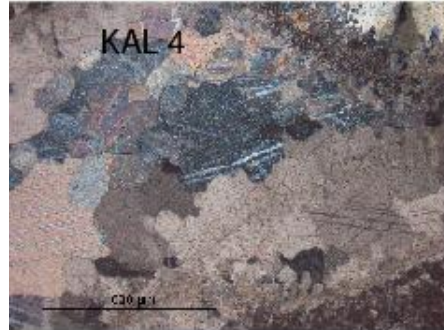
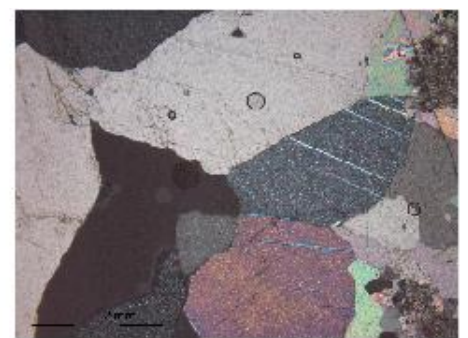
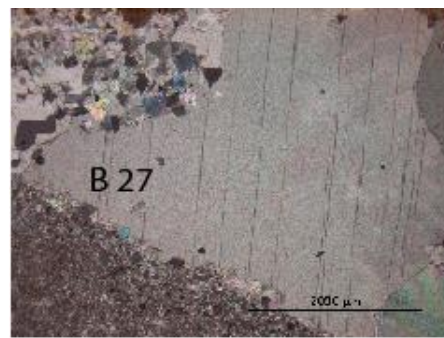
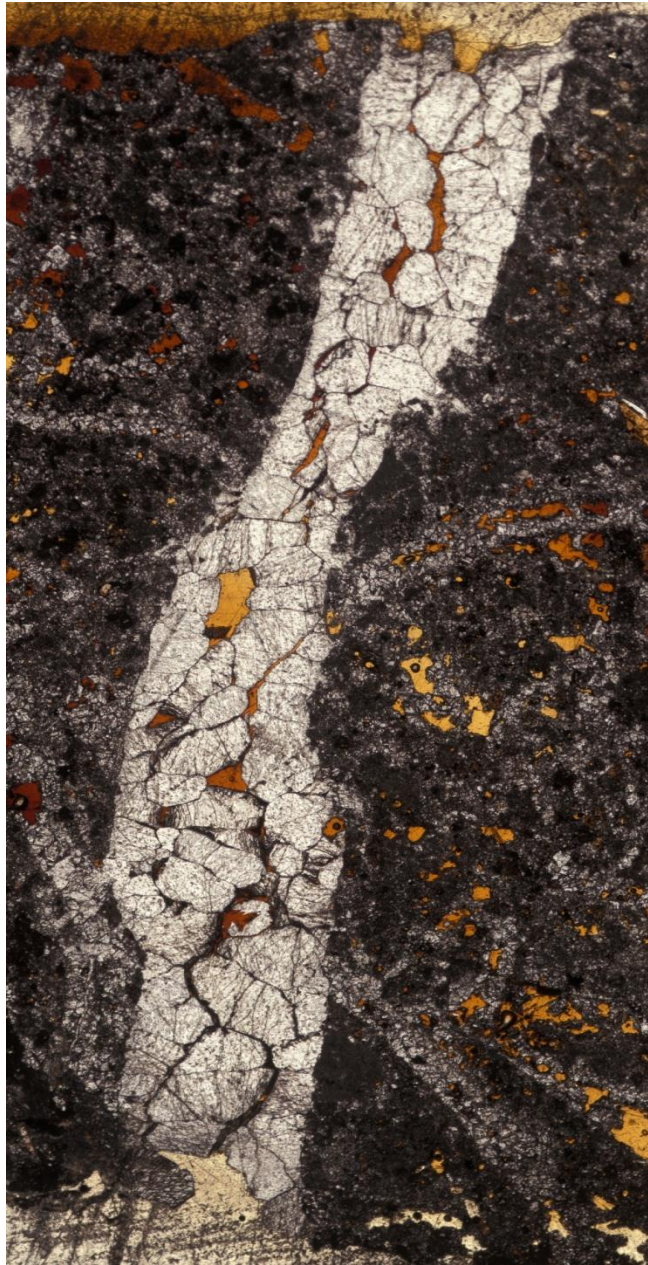


# Coaxiality of stress and strain and consistency with anisotropy of rock physical properties



Investigating fluid flow in folds (1) :  
geochemical and microthermometric analyses  
of cemented fractures in folded strata







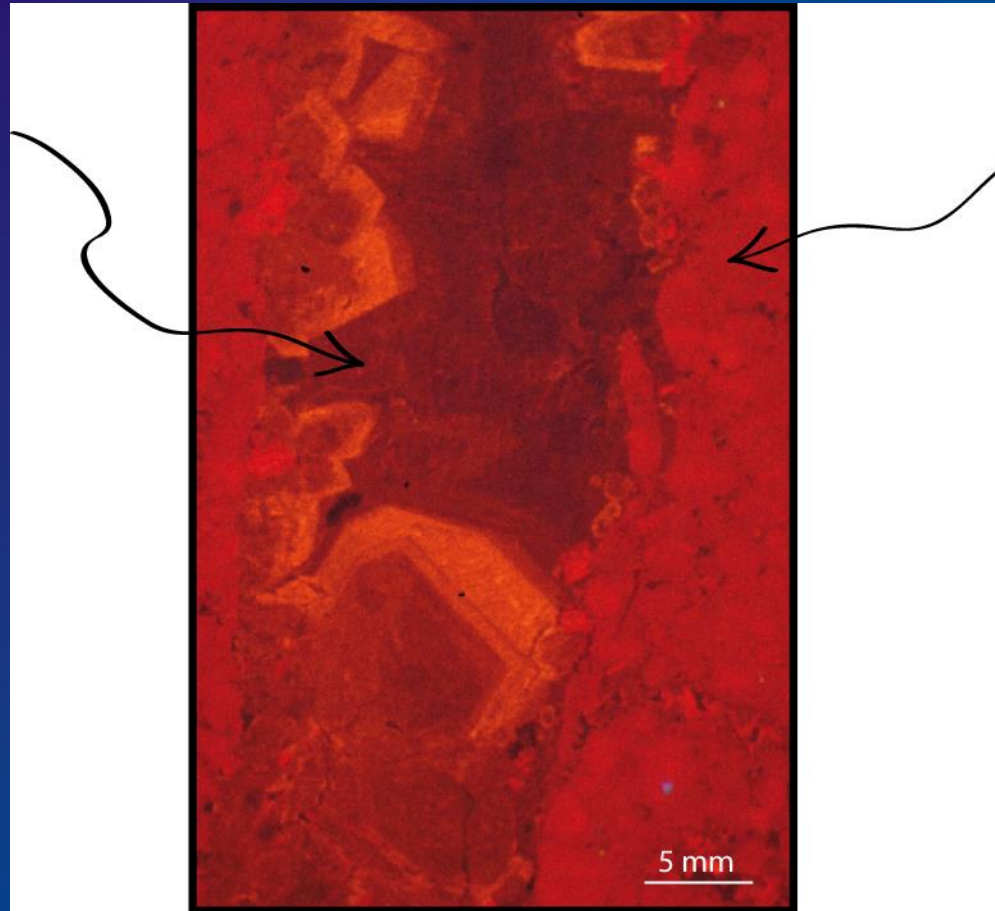
# Veins : an access to fossil fluids

**Calcite veins**

O, C stable isotopes

Microthermometry of fluid inclusions

- $^{87}/^{86}$  Sr ratios



**Limestone  
Host-Rock**

O, C stable isotopes

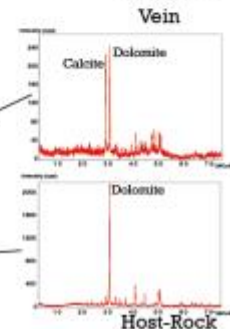
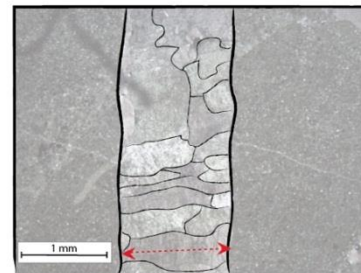
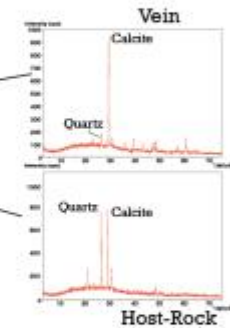
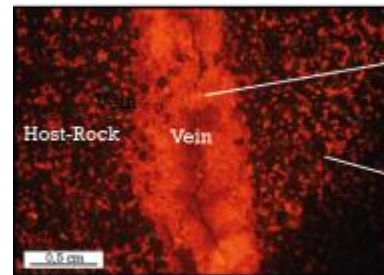
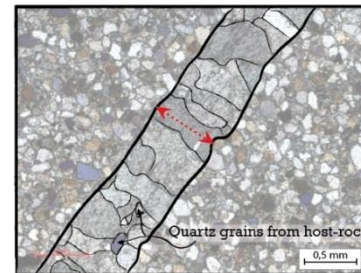
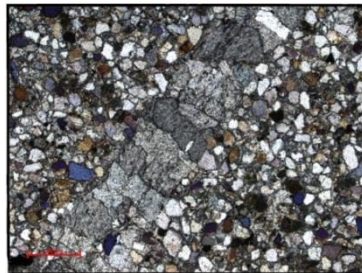
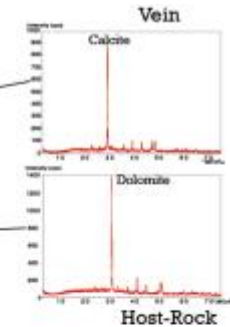
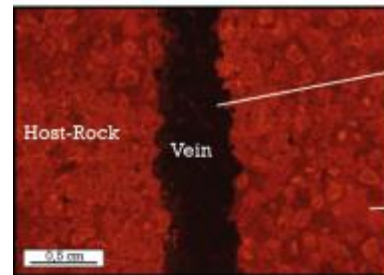
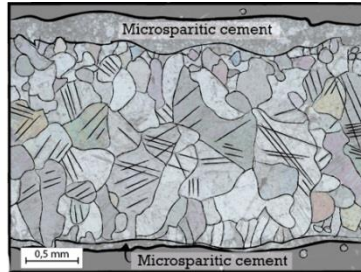
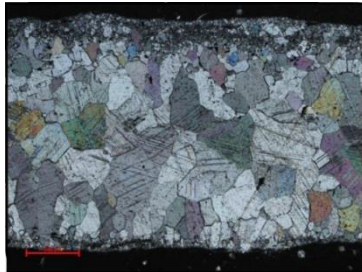
$^{87}/^{86}$  Sr ratios

**Fluid temperature**

**Fluid origin and  
pathways**

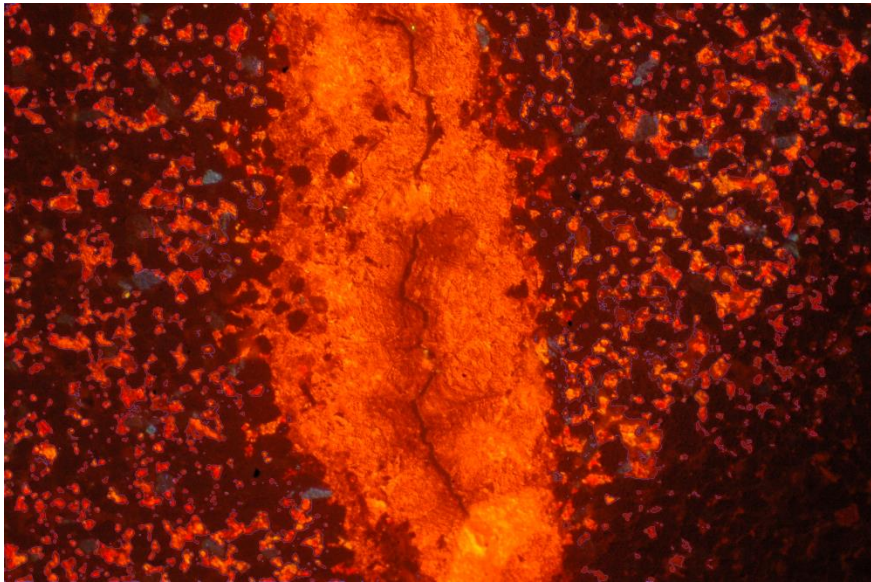
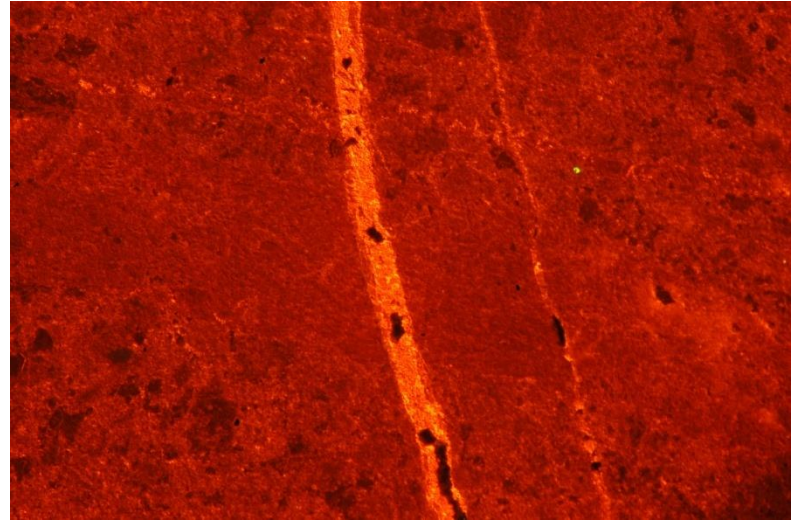
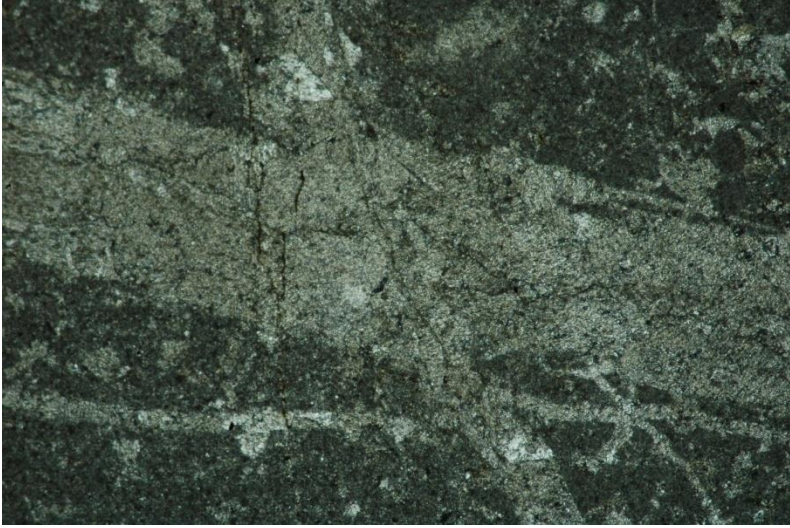
**Fluid-Rock  
Interactions**

# Textures and vein fillings



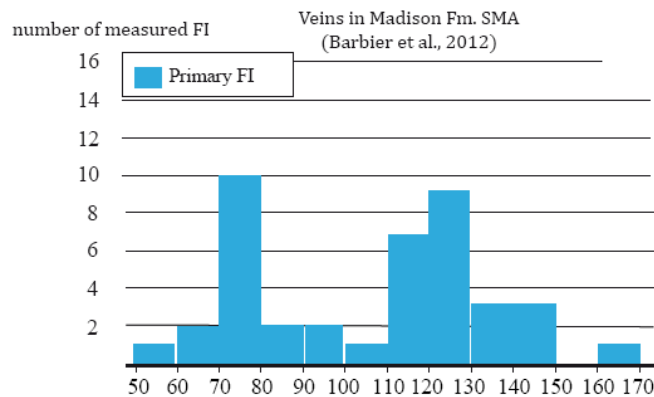
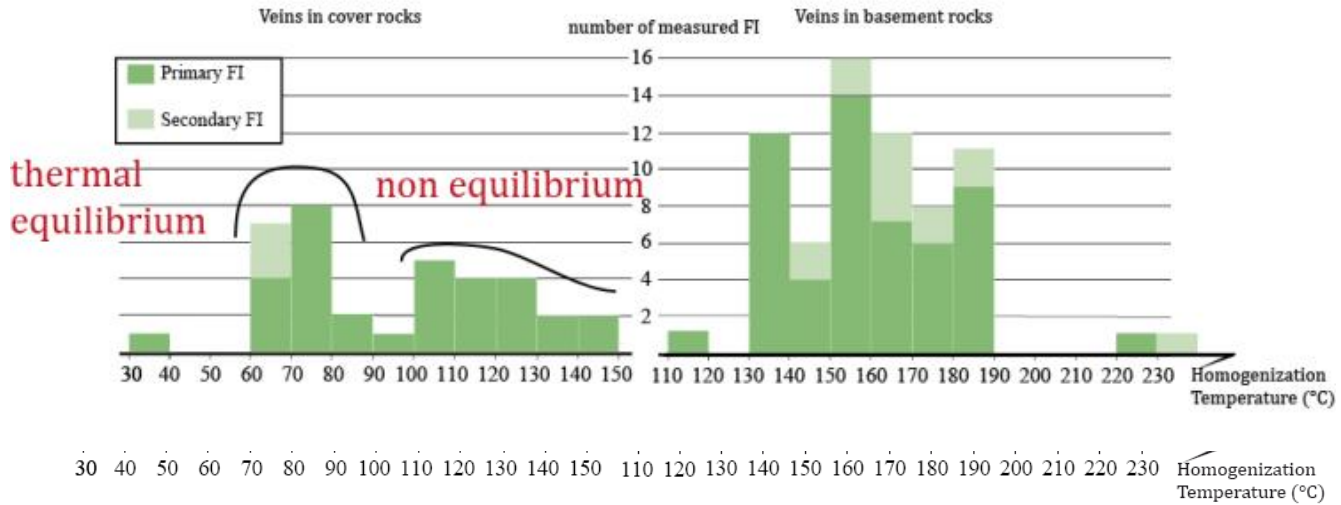
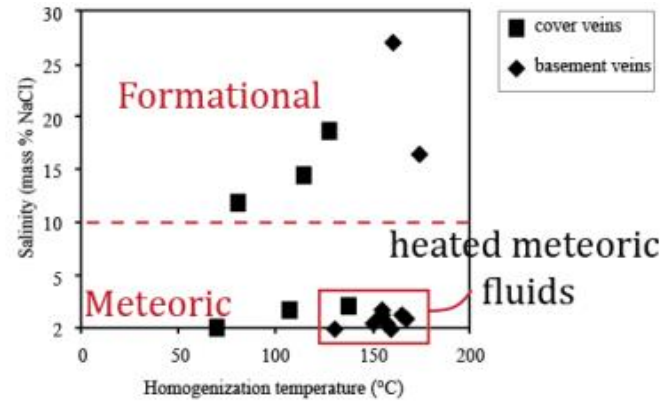
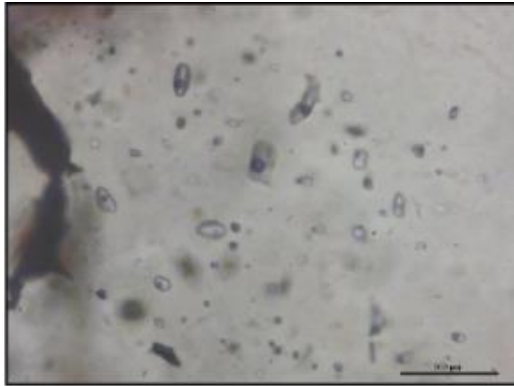


# Cathodoluminescence



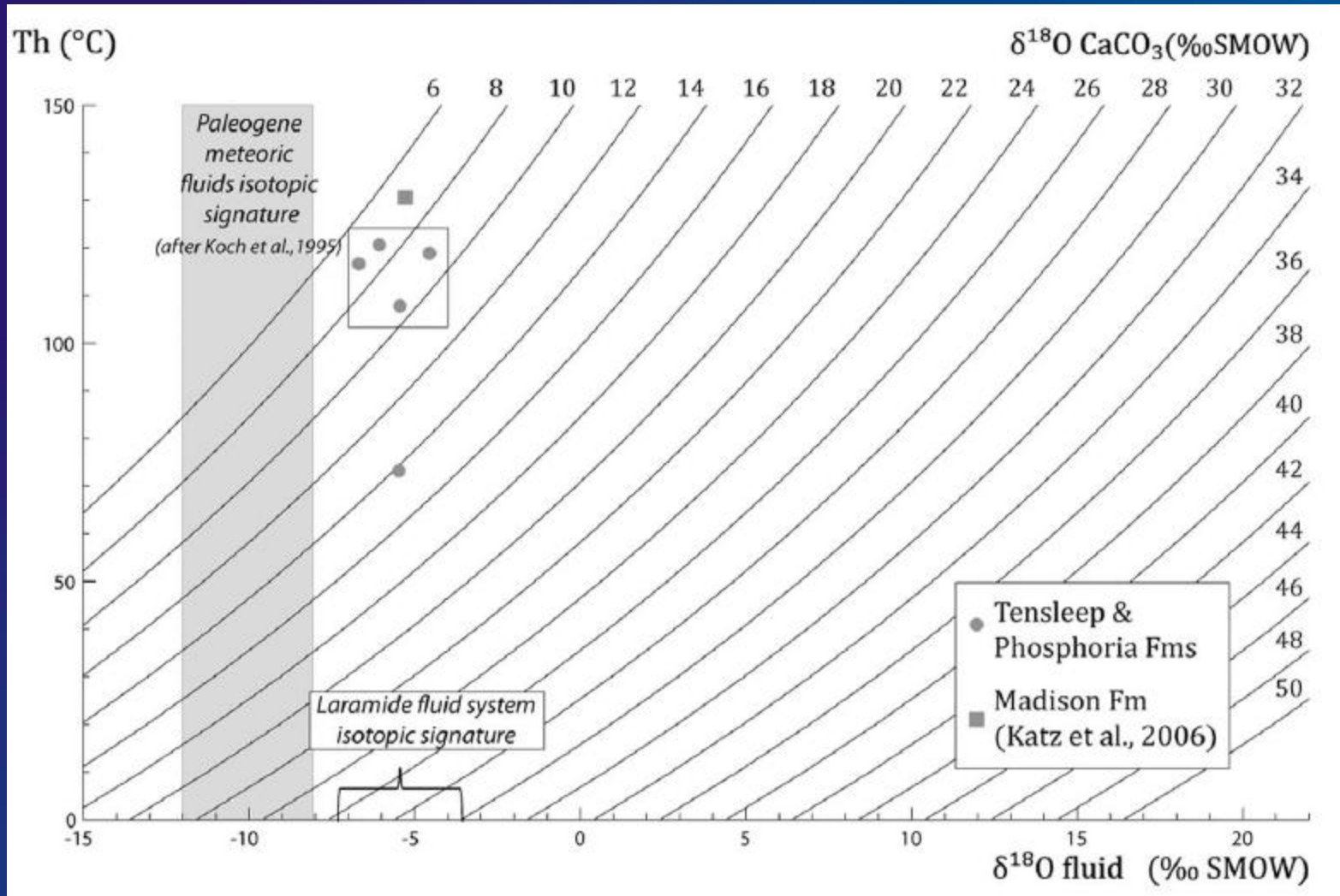
Identifying successive filling phases and parageneses





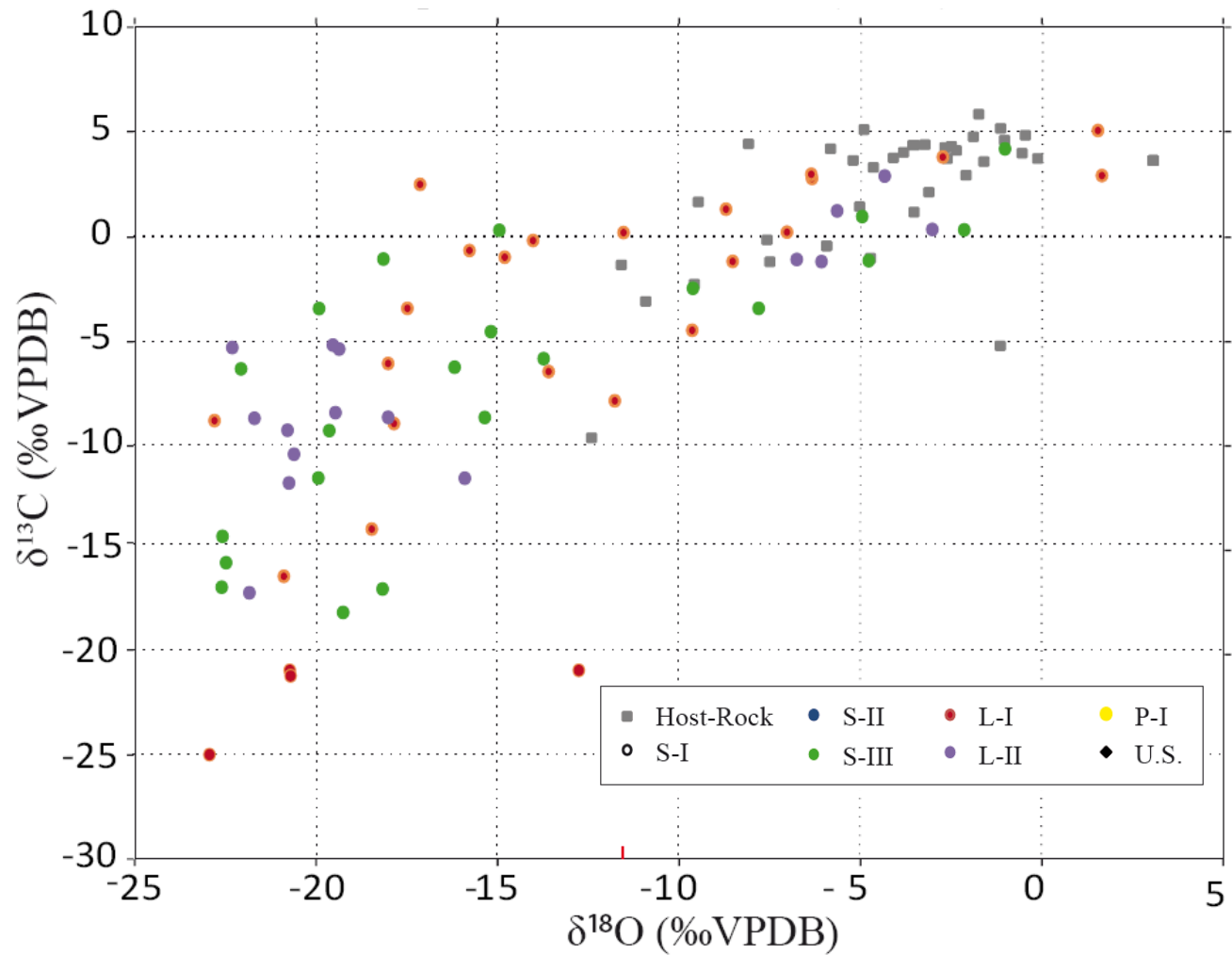
Microthermometry  
and Raman  
spectrometry  
of fluid inclusions

# Homogenization temperatures vs $\delta^{18}\text{O}$

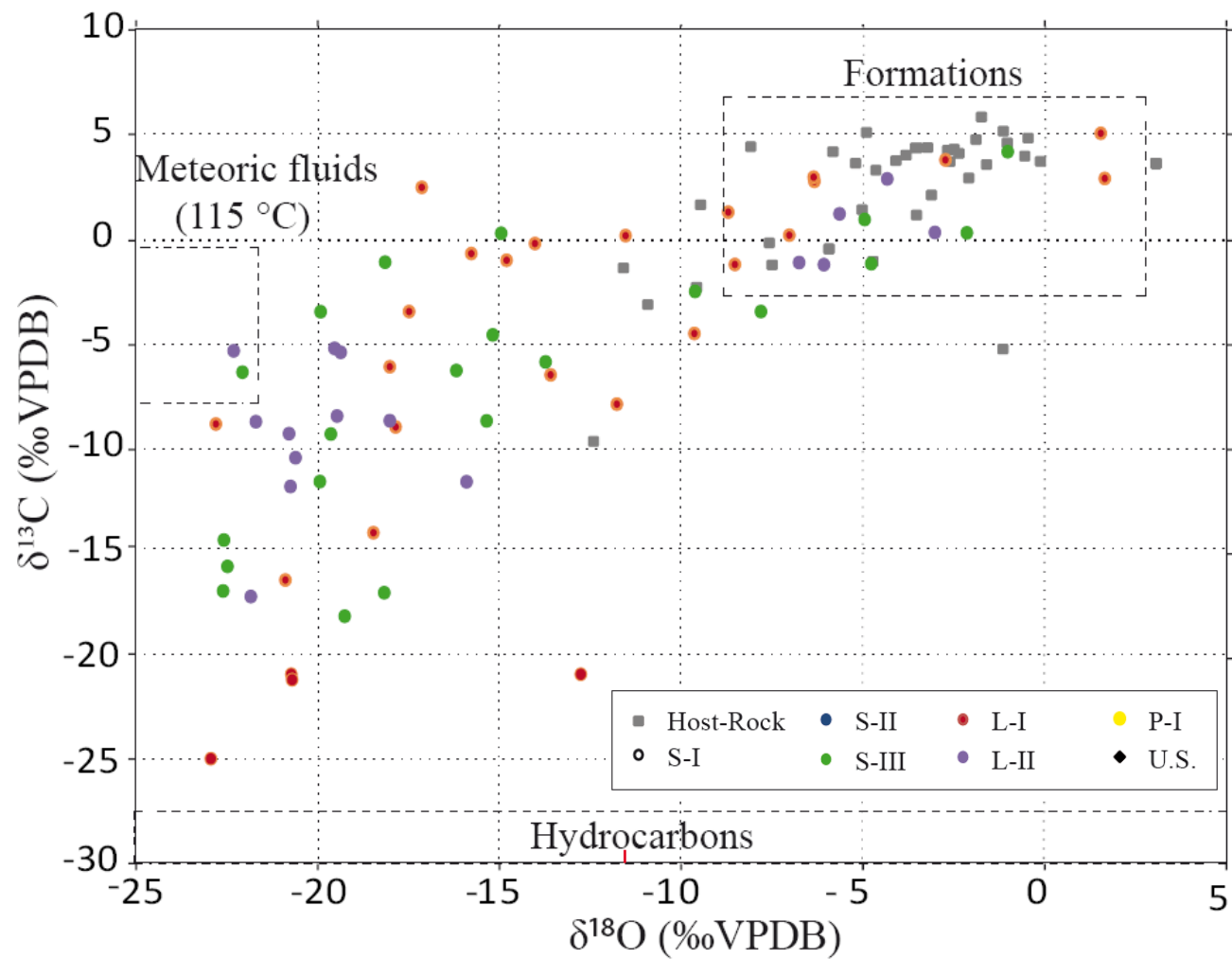


(Beaudoin et al, 2011)

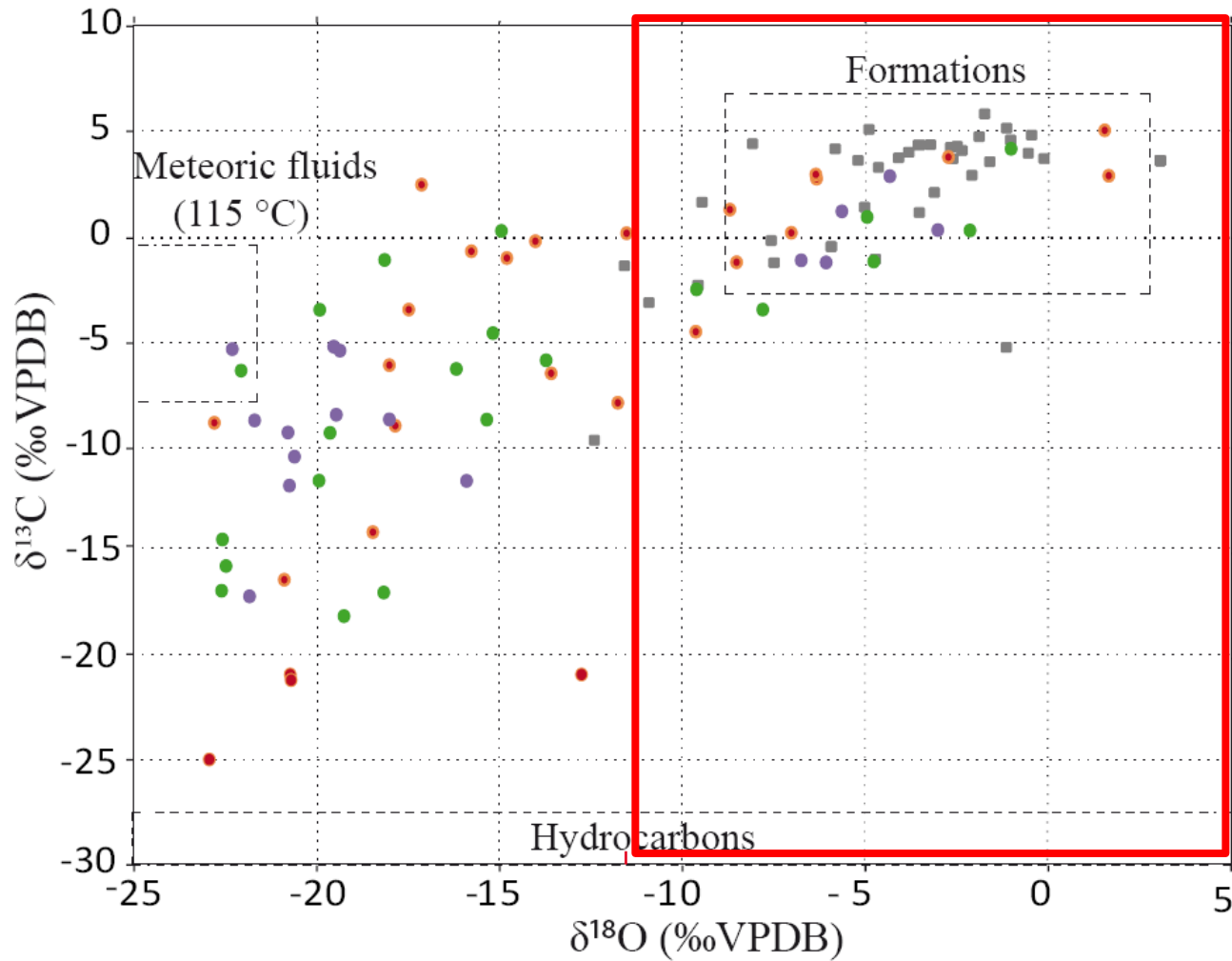
# O, C stable isotope geochemistry



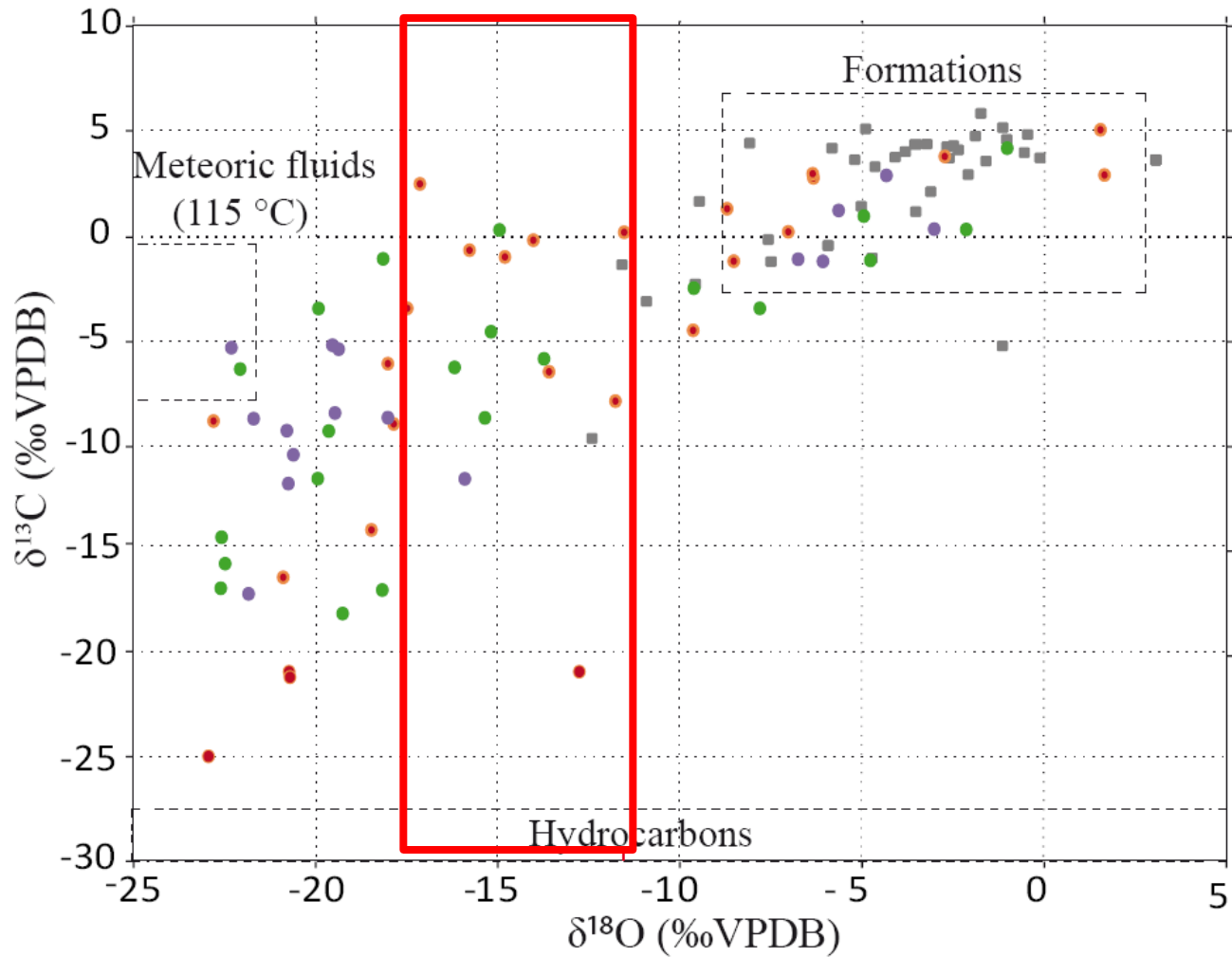




# Total isotopic and thermal equilibrium with host-rock

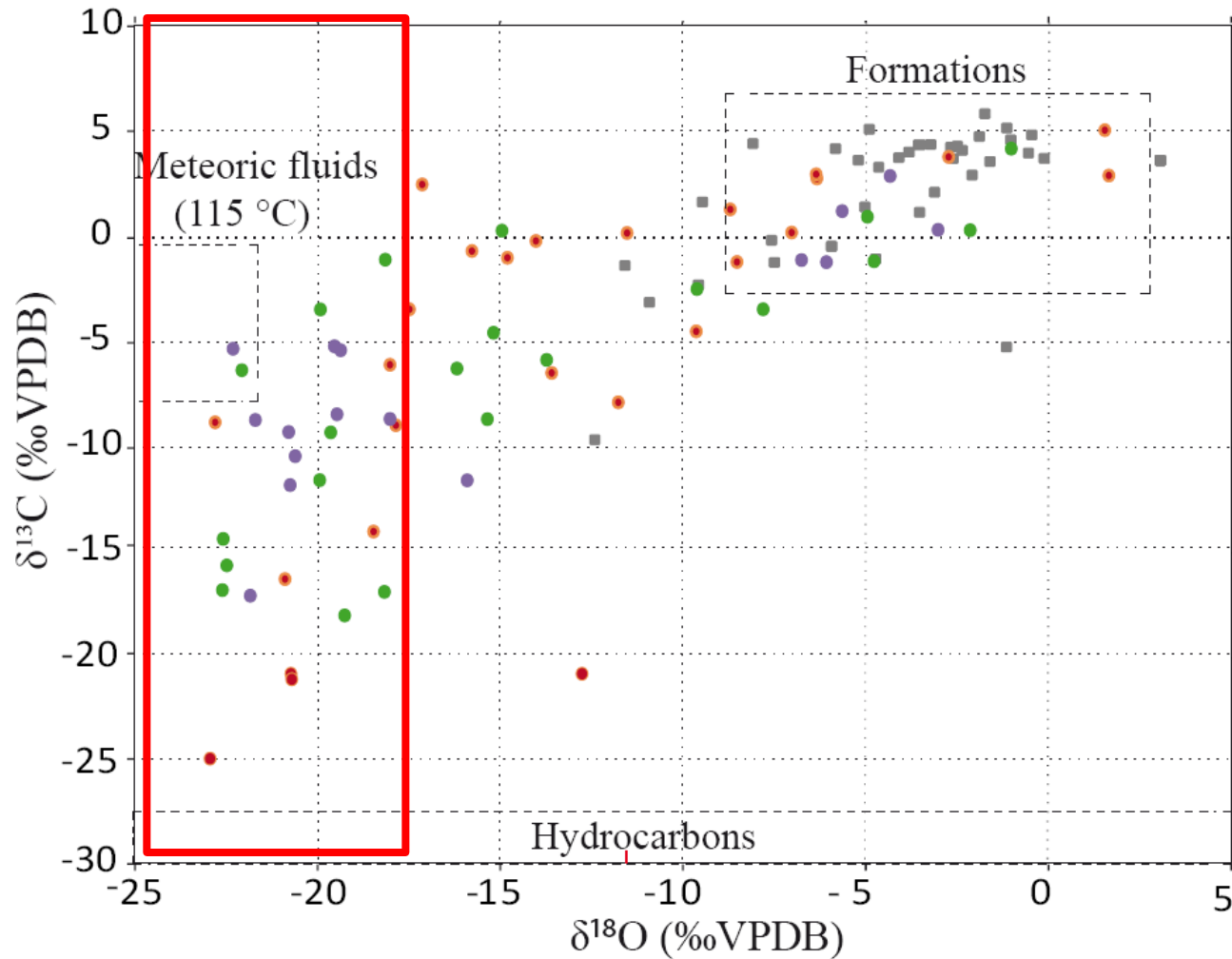


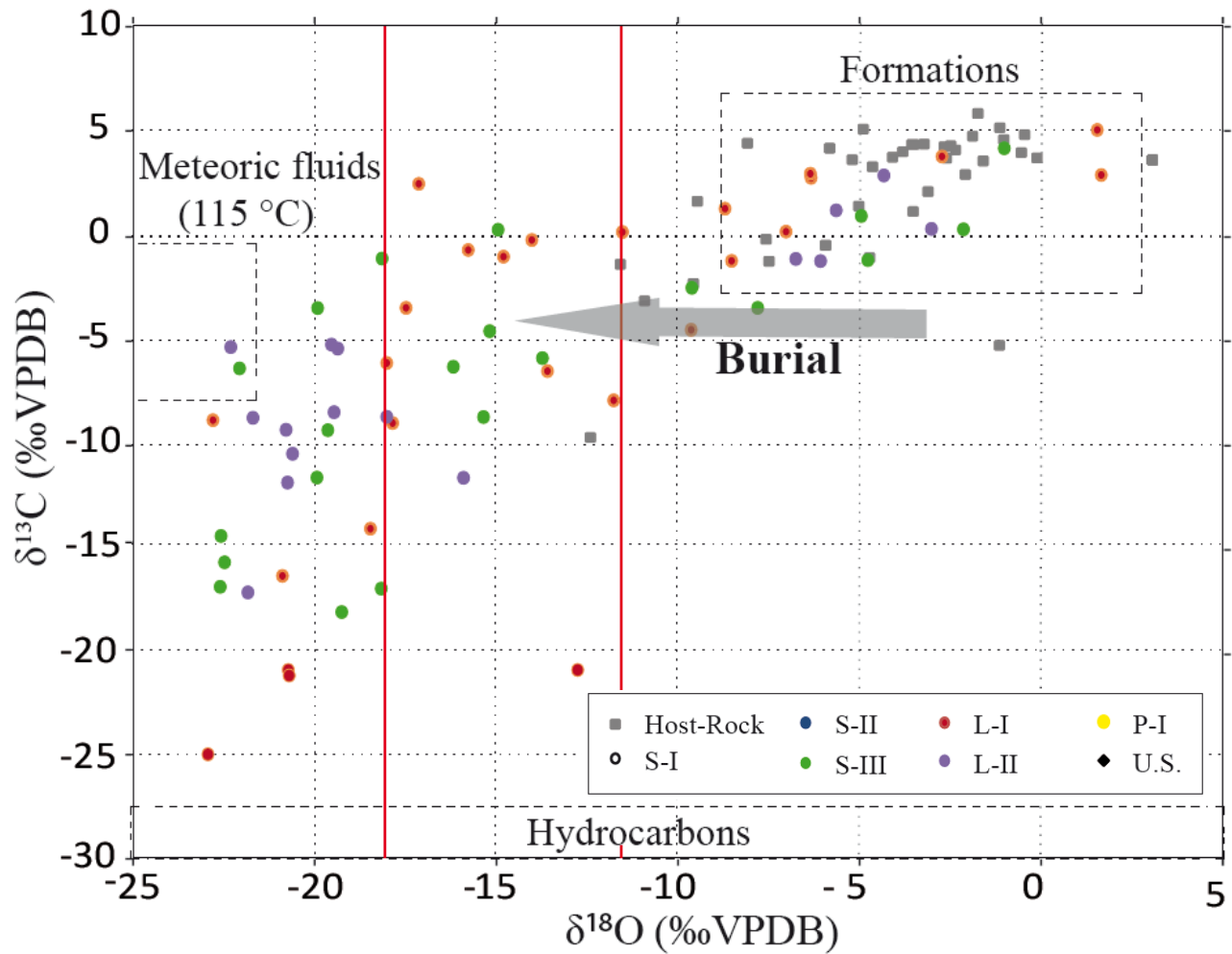
# $\delta^{18}\text{O}$ depletion but thermal equilibrium with host-rock

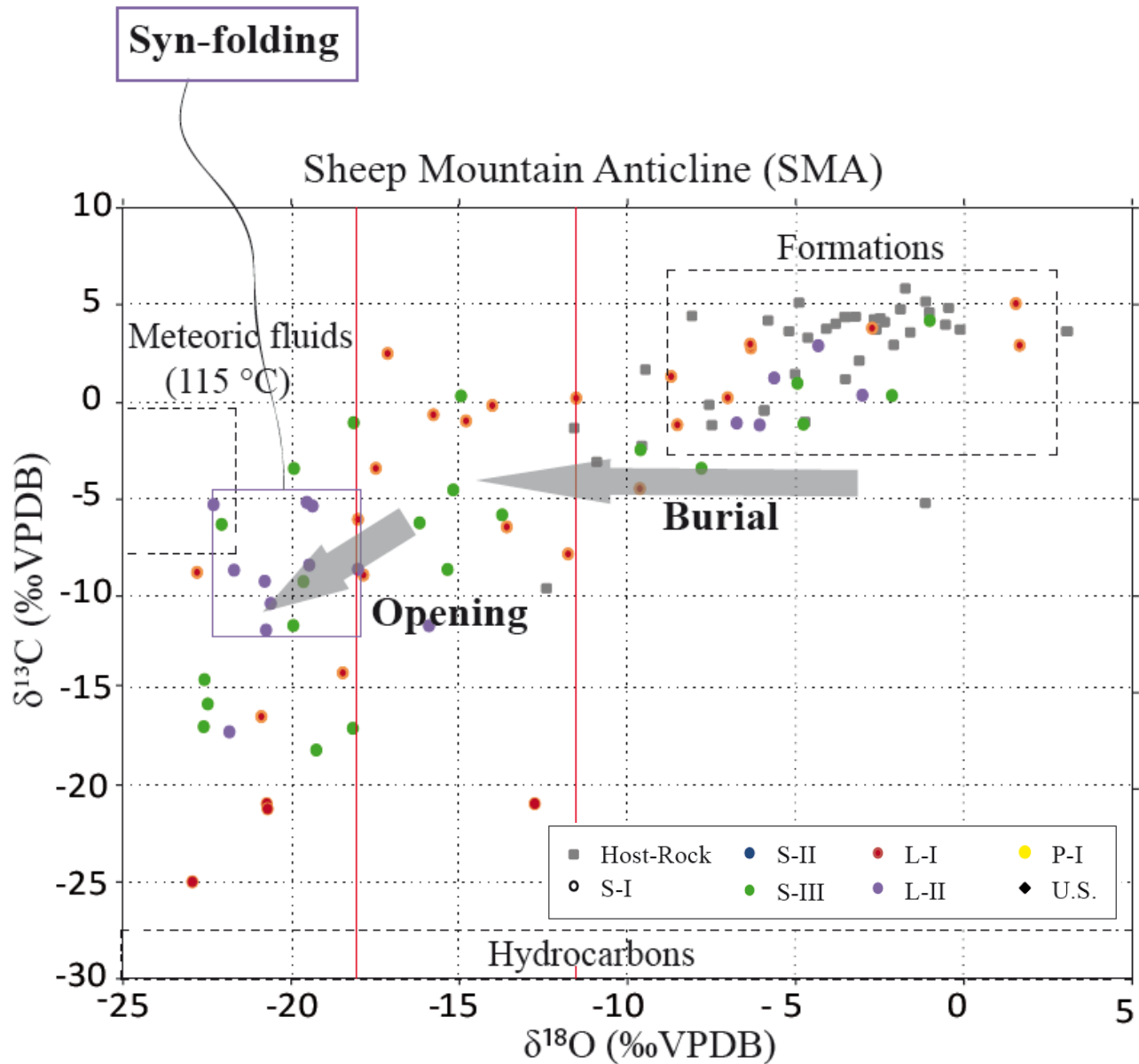




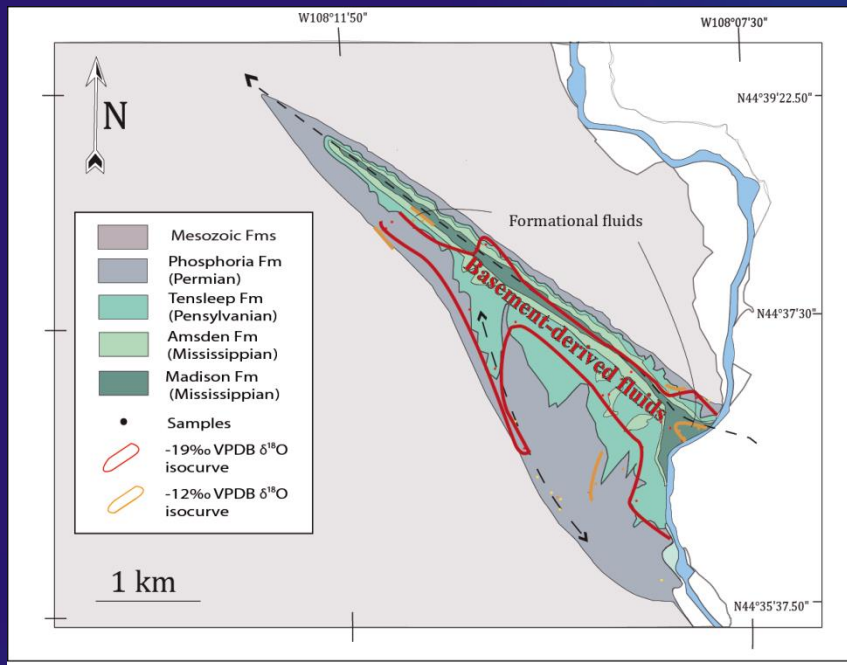
# High $\delta^{18}\text{O}$ depletion and thermal disequilibrium with host-rock





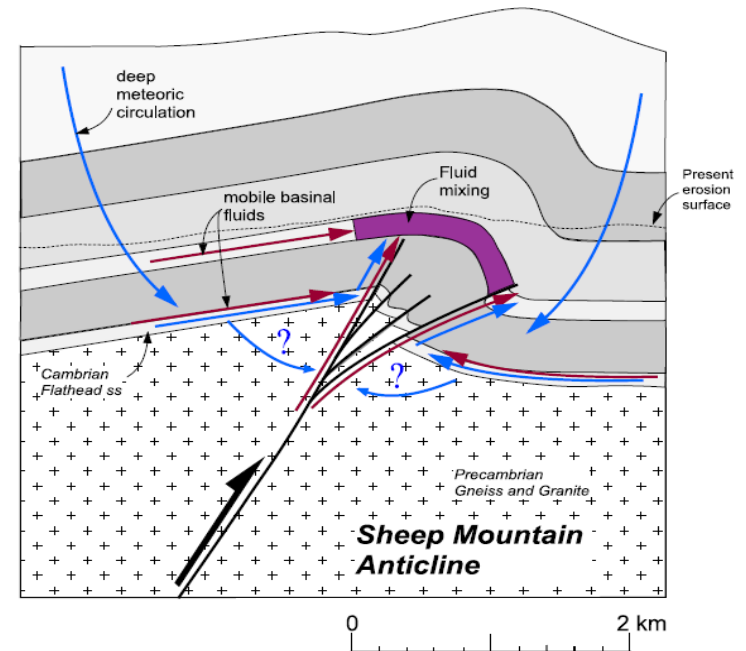
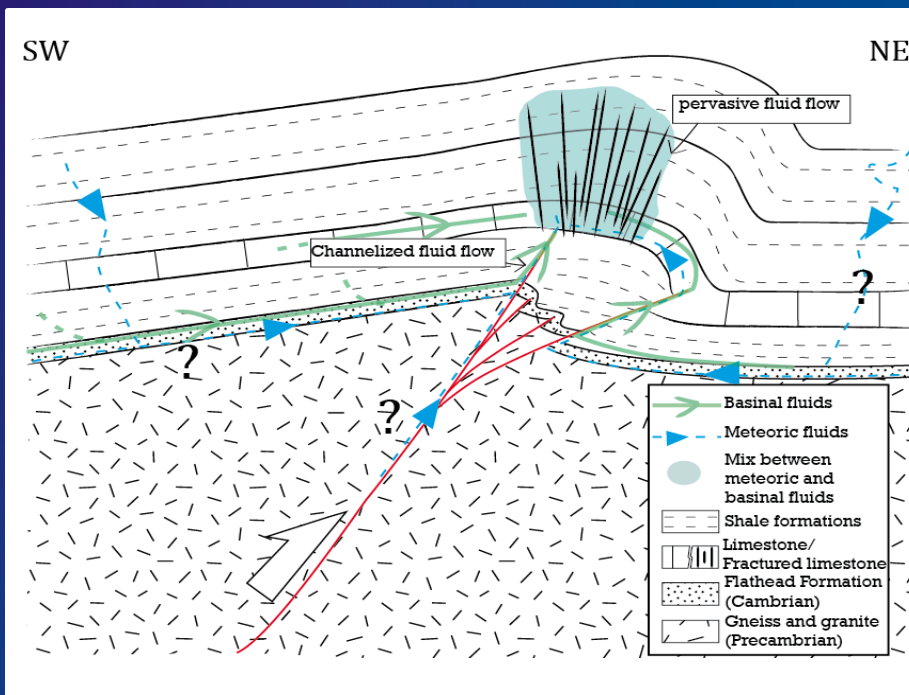






# Localization of basement-derived hydrothermal fluid pulse at SMA

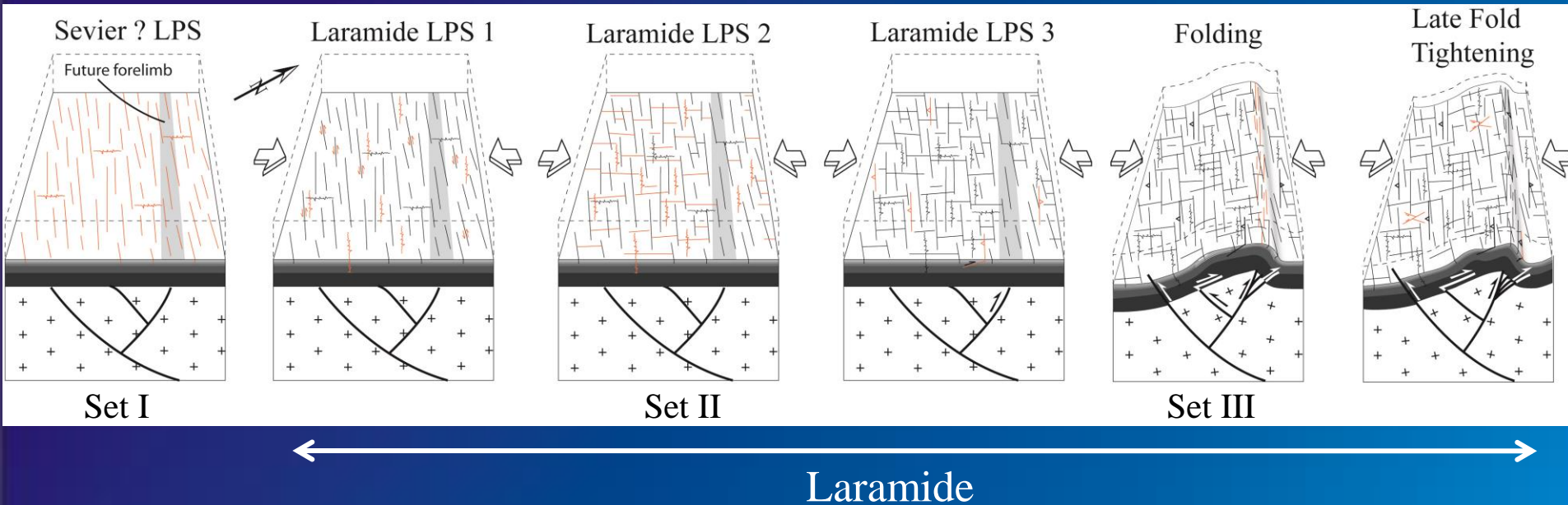
(Beaudoin et al, 2011; later redrawn by Evans and Fischer, 2012)



Investigating fluid flow in folds (2) :  
constraining fluid (over) pressure

# Scenario of fault-fracture development in space and time

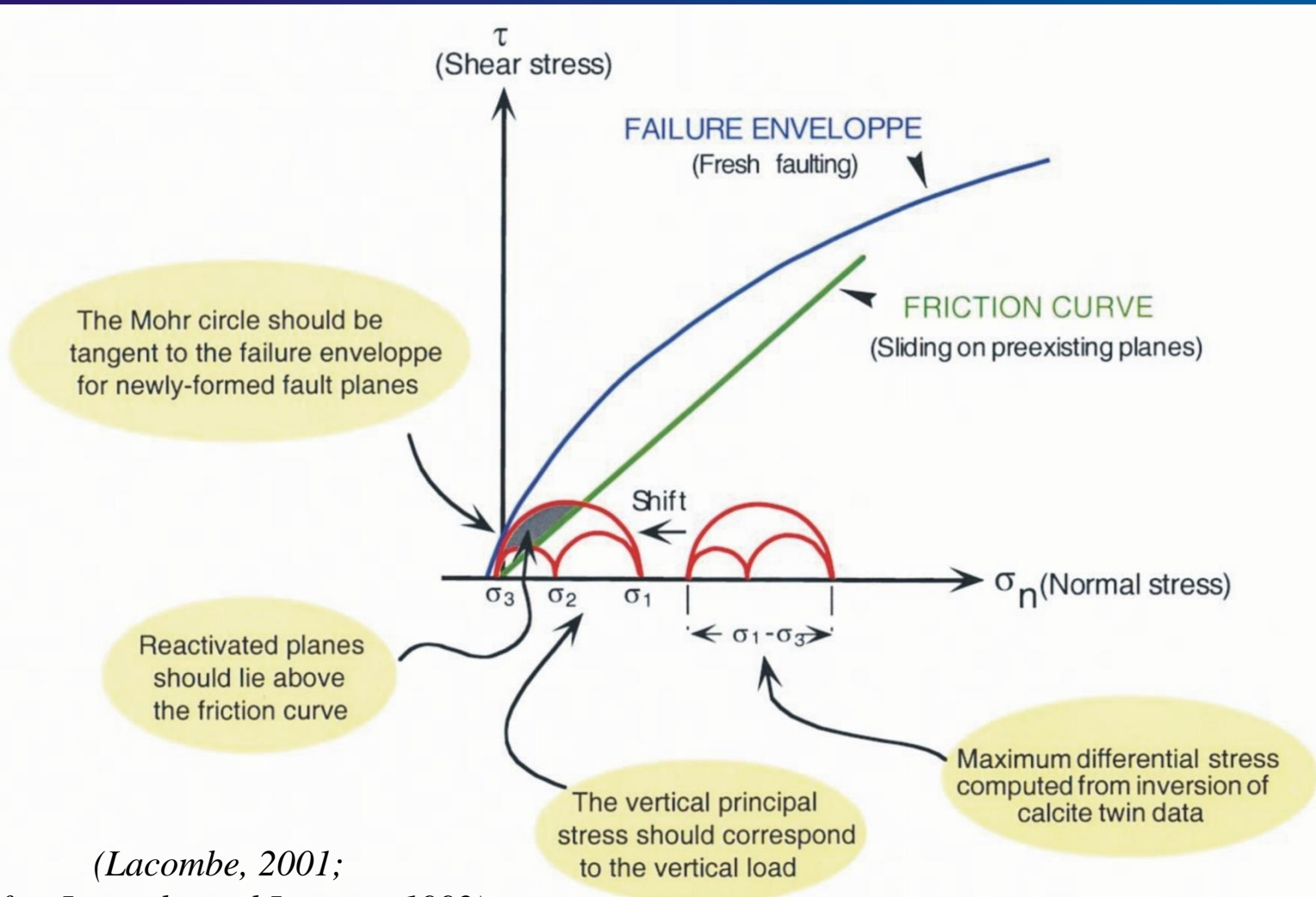
(Amrouch et al., 2011)



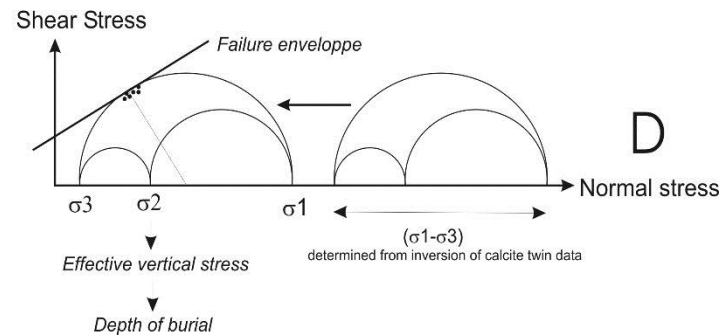
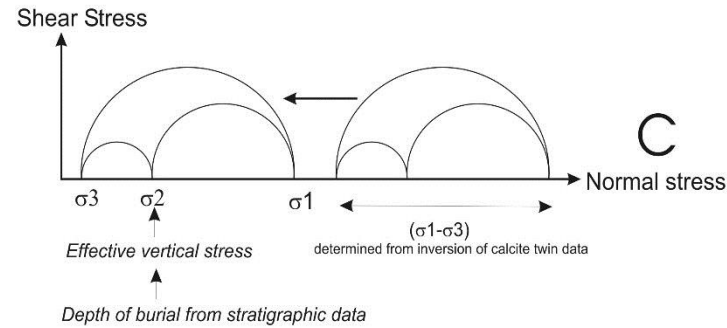
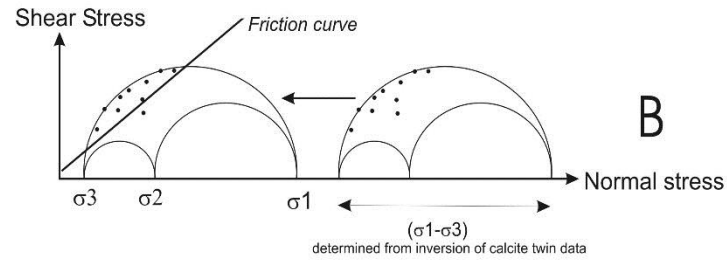
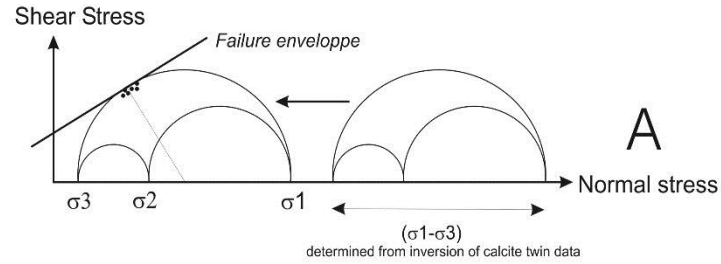
- Mode I opening of pre-Laramide set I fractures
- Shear reactivation of pre-Laramide set I fractures (LPS 1).
- Laramide stylolites with NE-trending peaks and mode I opening of set II fractures (LPS2)
- Reverse faulting parallel to the fold axis (LPS3).
- Mode I opening of syn-folding, outer-rim extension-related set III fractures
- Late stage fold tightening (LSFT) marked by strike-slip faults and reactivation of tilted set I fractures as small reverse faults in the forelimb



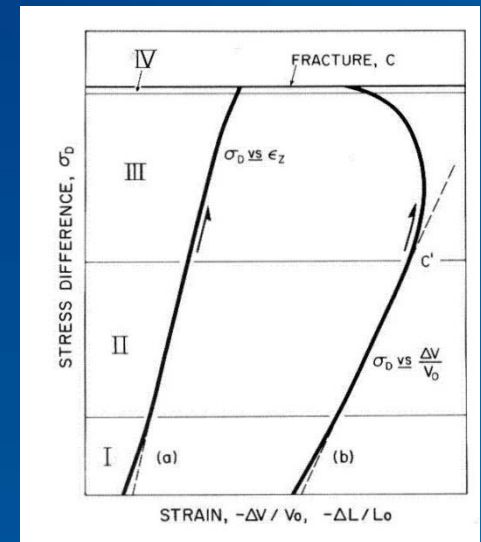
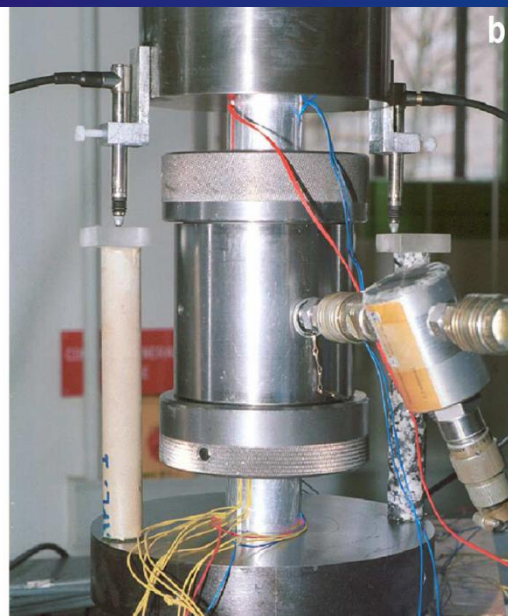
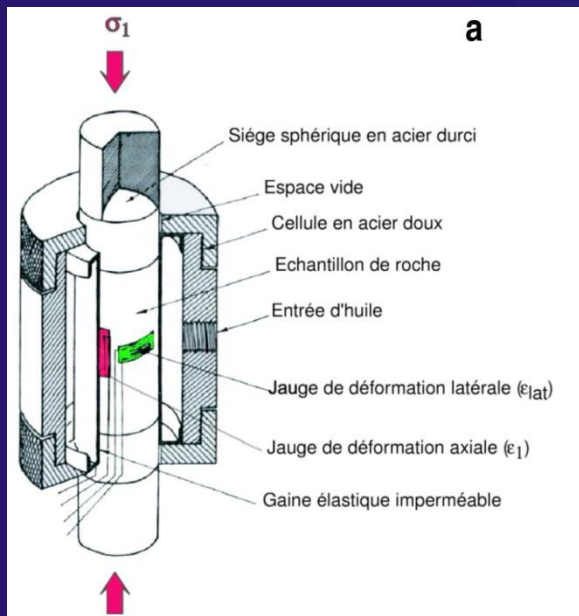
The method : finding for each deformation step the values of  $\sigma_1$ ,  $\sigma_2$  and  $\sigma_3$  required for consistency between differential stresses estimated from calcite twinning, frictional sliding along preexisting planes (i.e., Byerlee's law) and newly formed faulting/fracturing.



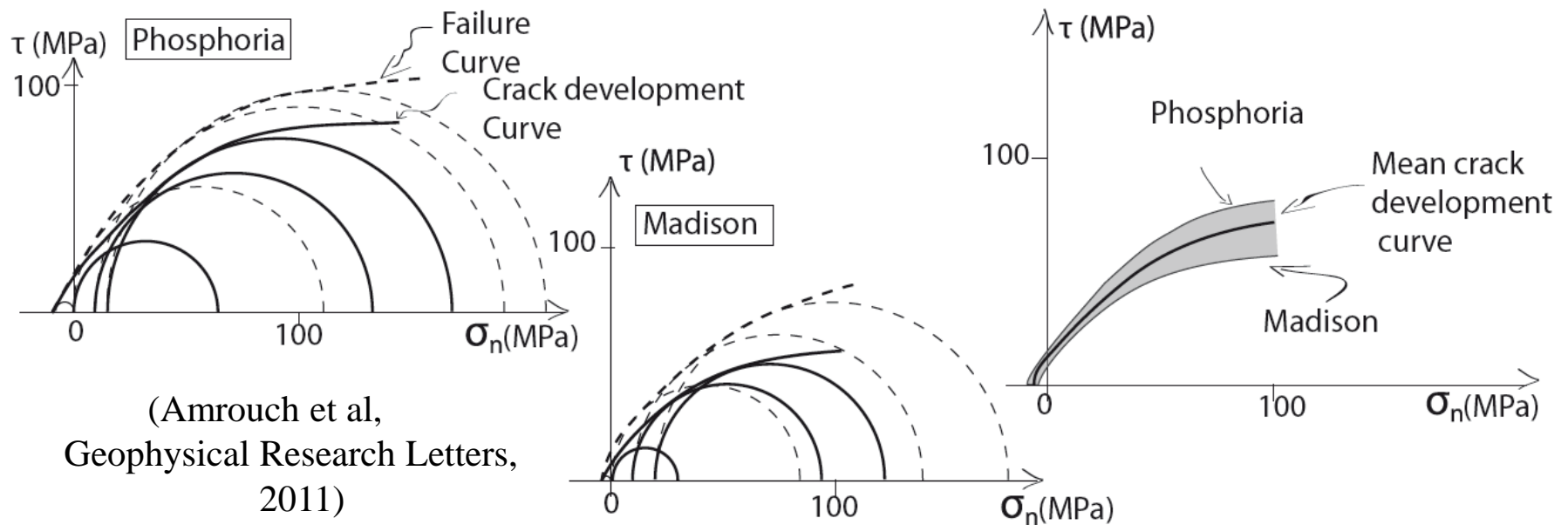
(Lacombe, 2001;  
after Lacombe and Laurent, 1992)



(Lacombe, 2007;  
Modified after  
Lacombe et al., 1996)

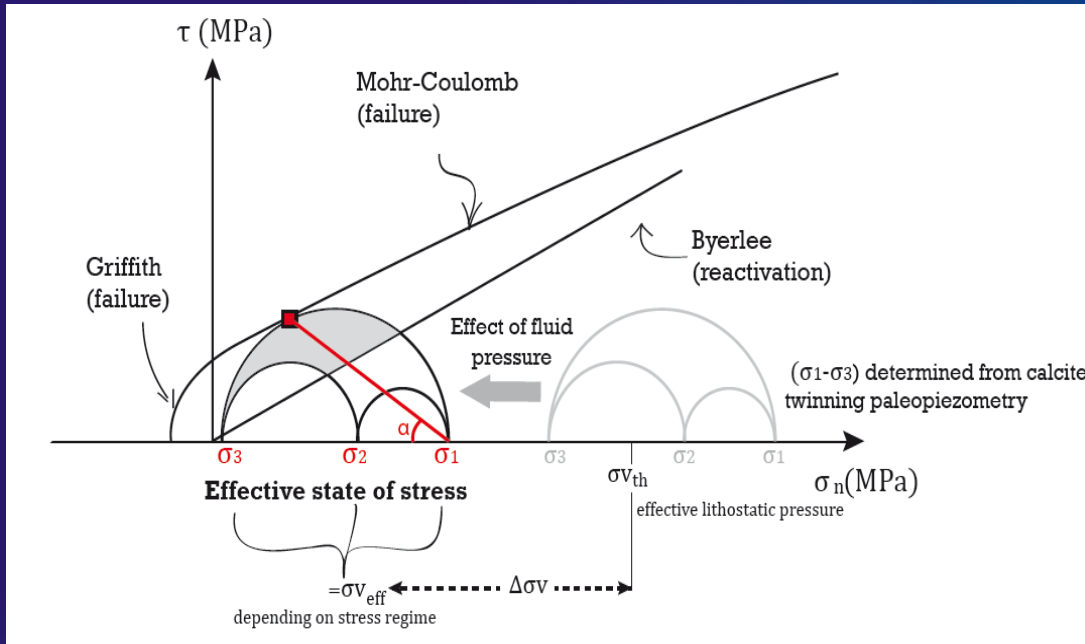


## Experimental determination of the intrinsic failure envelopes of the Phosphoria and Madison formations





# Calculation of the $\Delta\sigma_v$ to infer fluid overpressure



Theoretical effective vertical principal stress calculated considering lithostatic pressure corrected from hydrostatic fluid pressure:

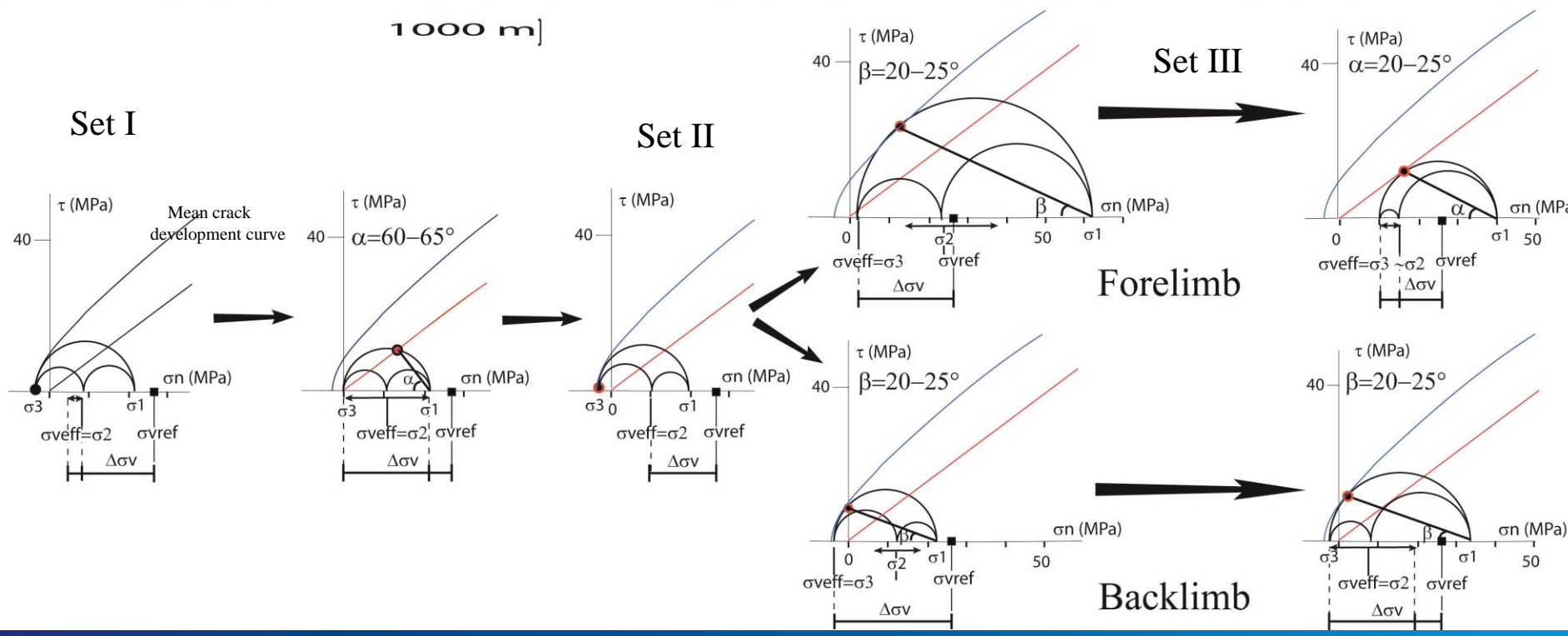
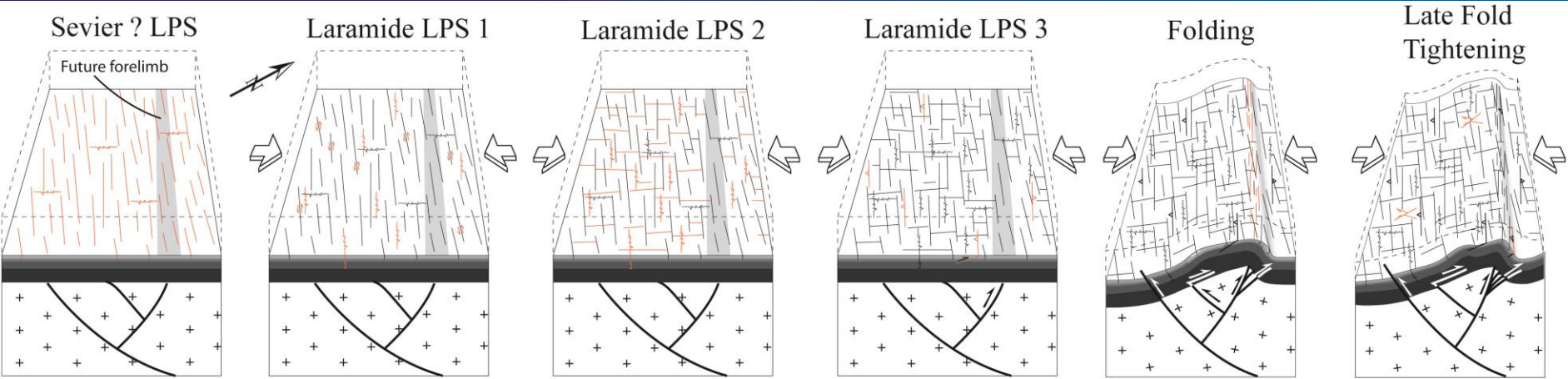
$$\sigma_{vref} = (\rho - \rho_w) \cdot g \cdot h$$

Comparison between the theoretical effective vertical principal stress  $\sigma_{veff}$  and the reconstructed effective vertical principal stress  $\sigma_{vref}$ :

$$\Delta\sigma_v = \sigma_{vref} - \sigma_{veff}$$

No erosion or increase of burial before folding

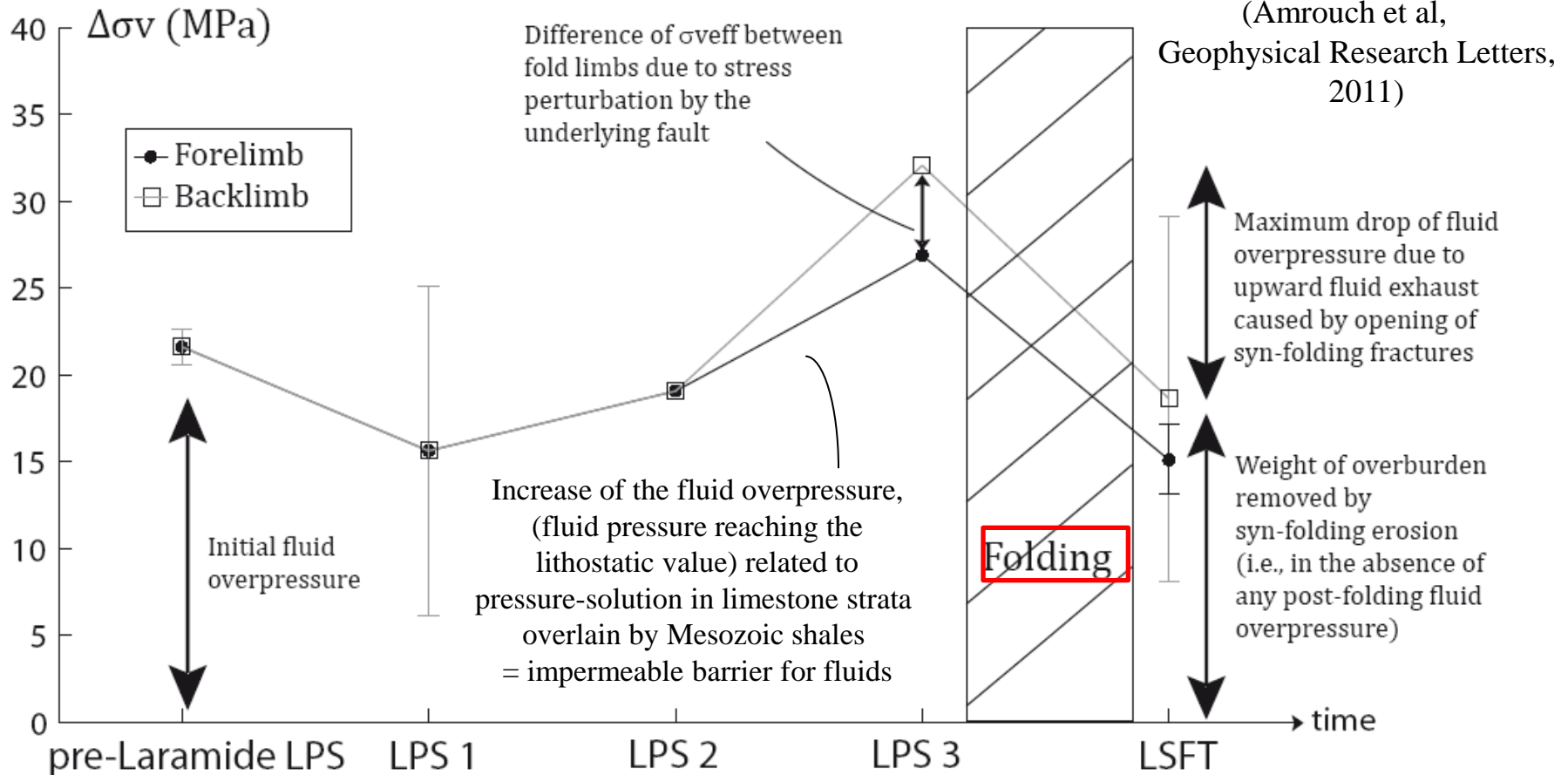
→  $\Delta\sigma_v$  primarily provides an estimate of the fluid overpressure.



Determination of principal stress magnitudes using simple Mohr constructions

(Amrouch et al, 2011)

# Inference of fluid (over)pressures



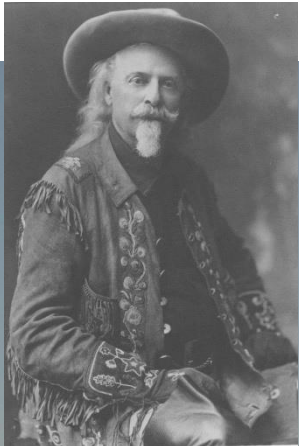
If the entire fluid overpressure was released during folding, it is possible to also derive the maximum value of syn-folding erosion (~1000m)



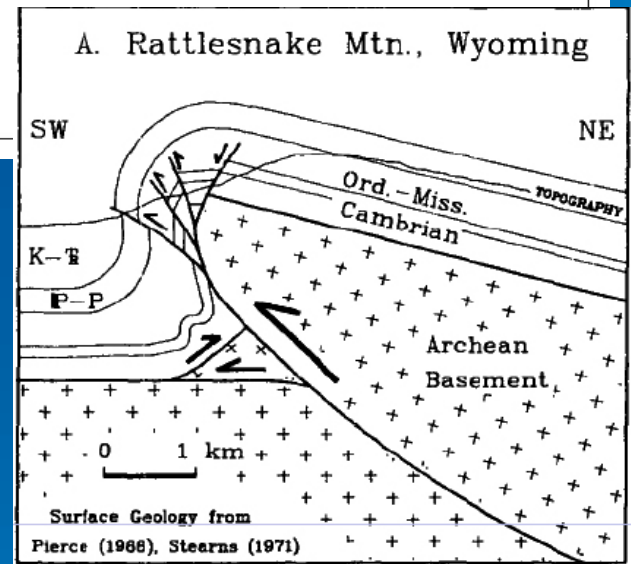
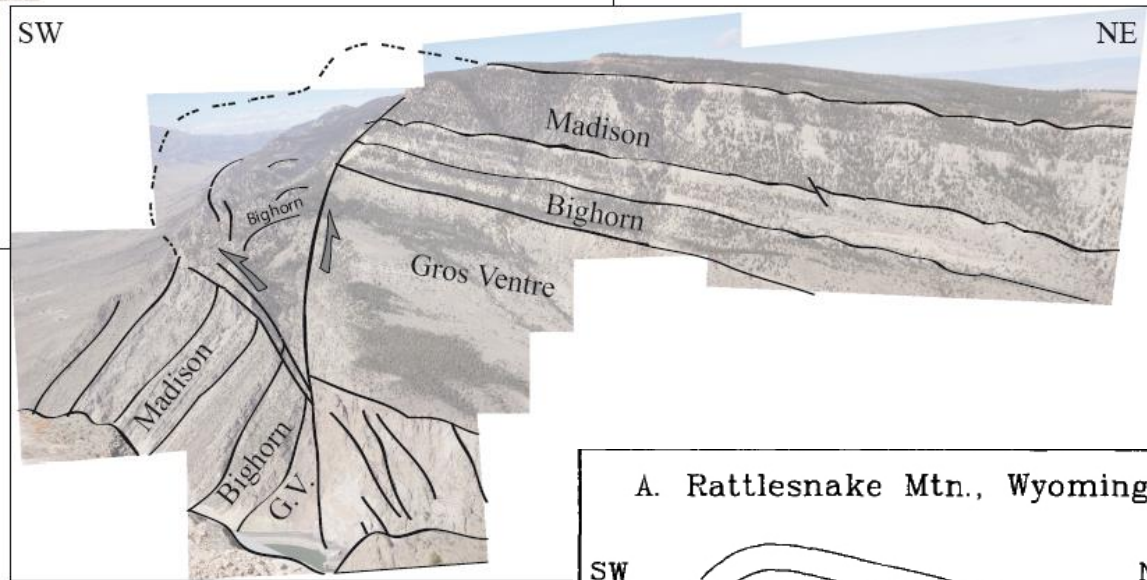
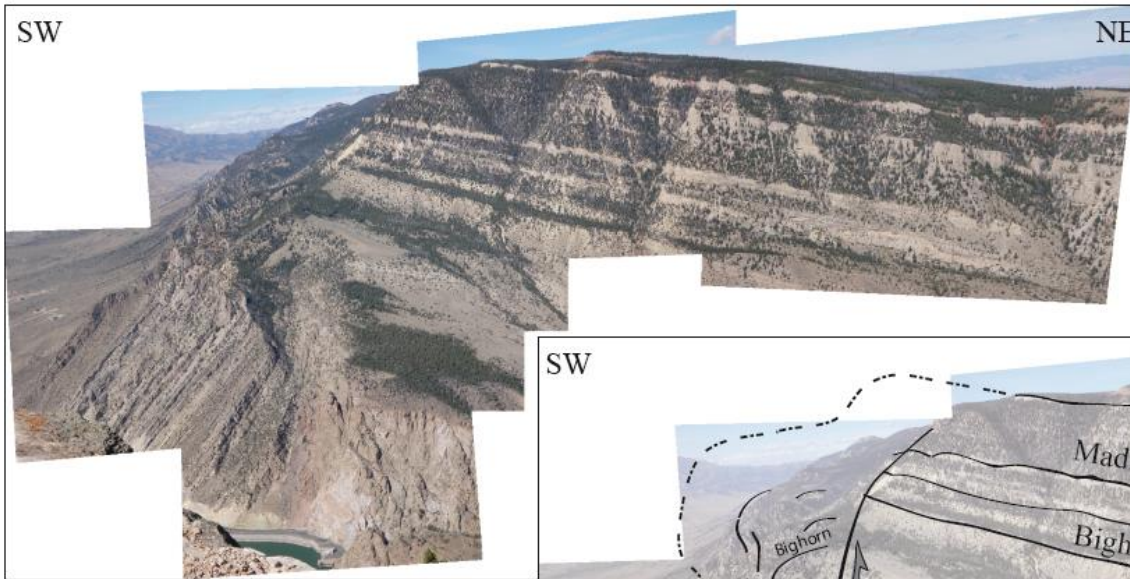
## **Comparison with Rattlesnake Mountain Anticline**

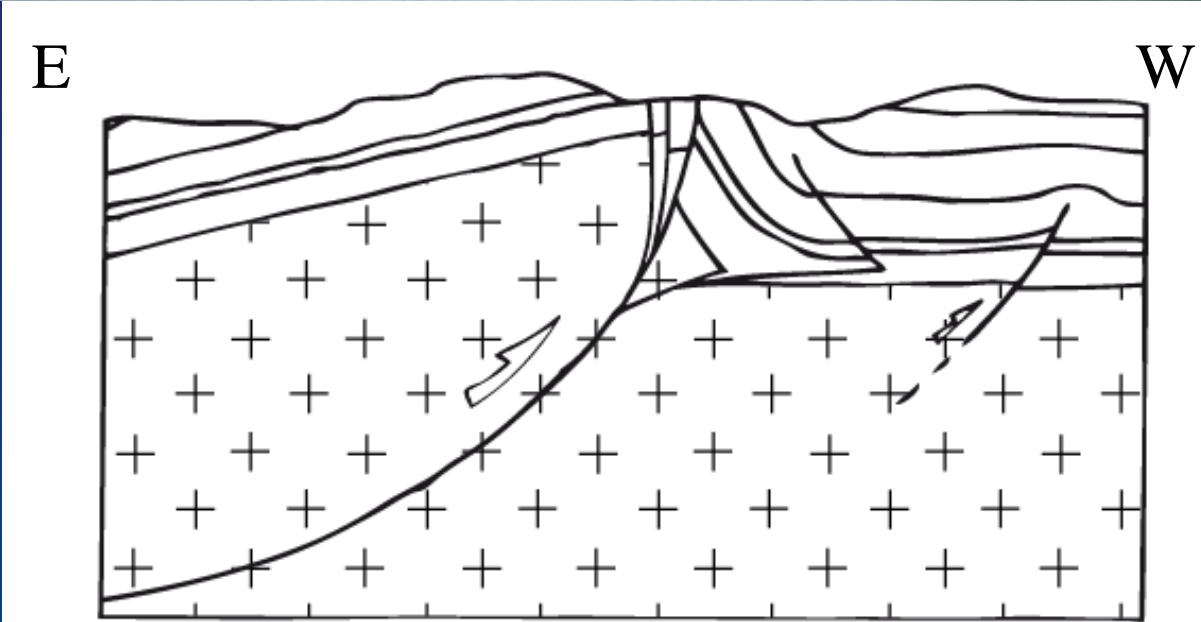
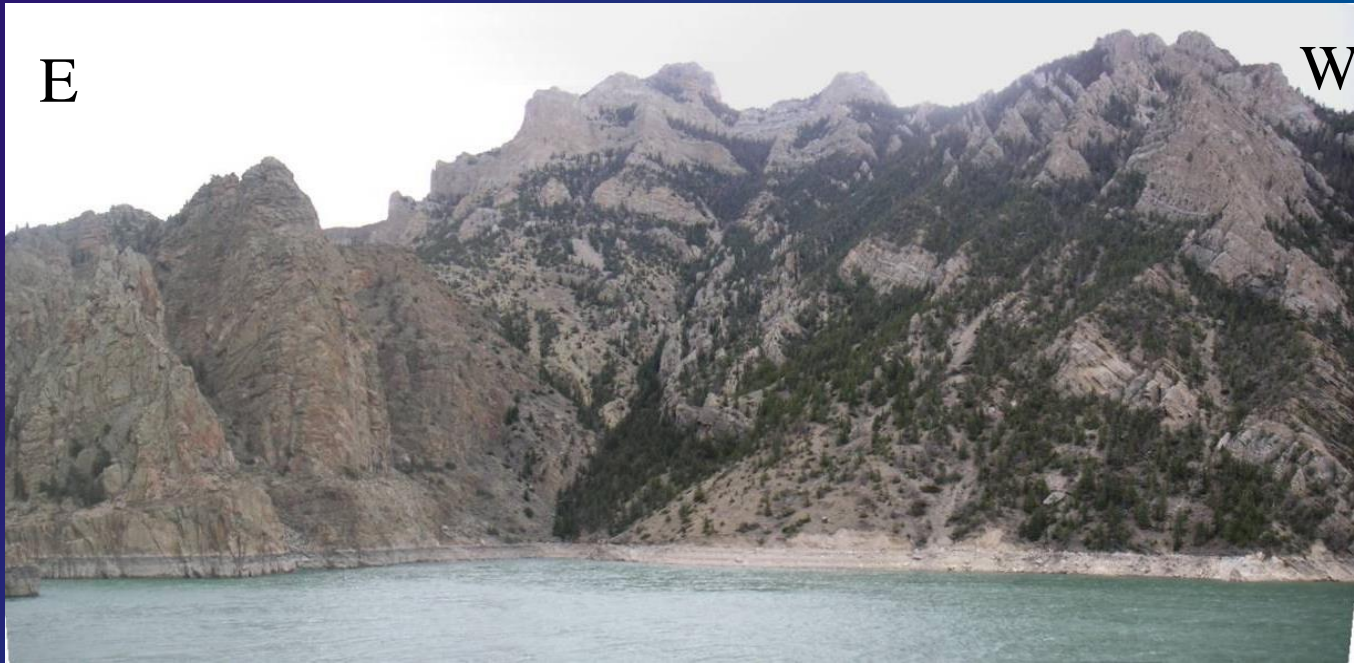


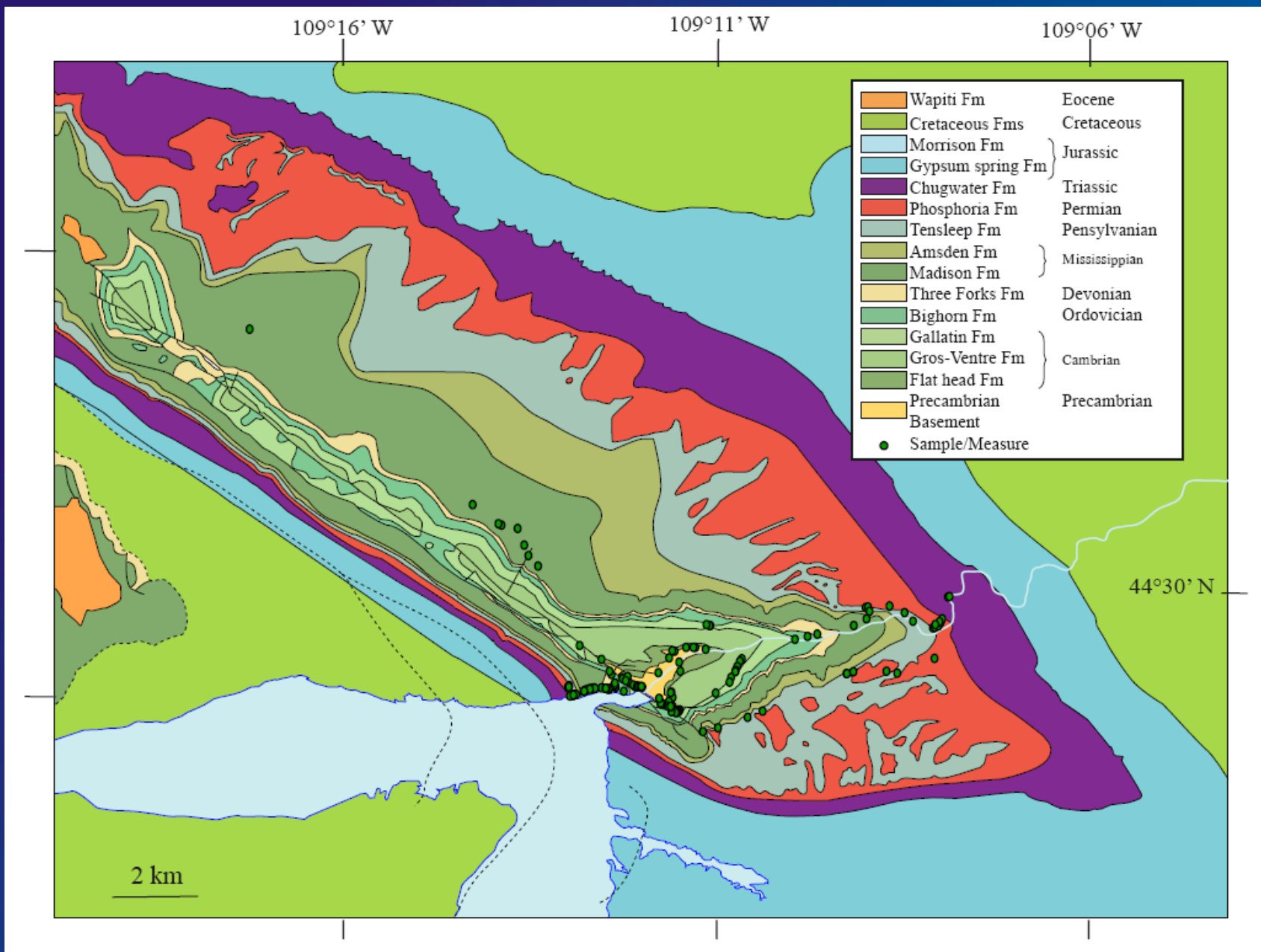




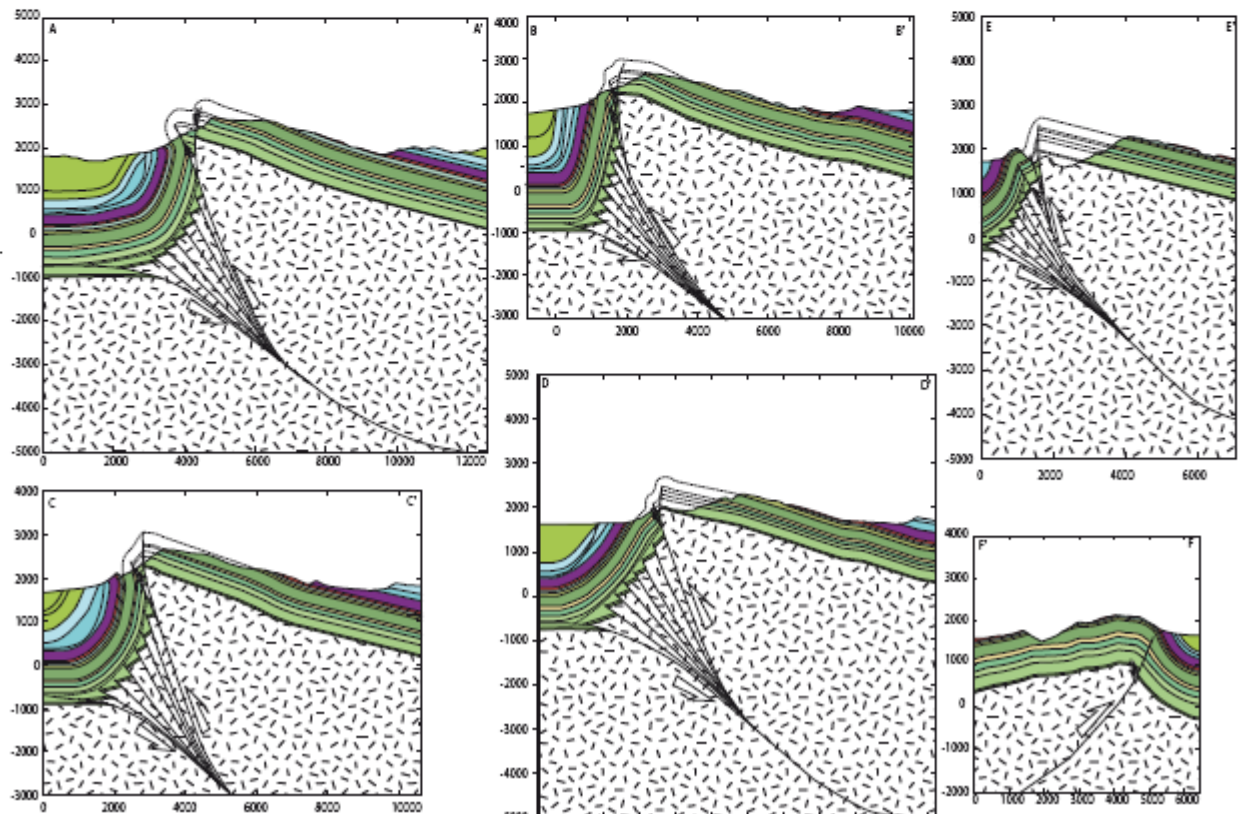
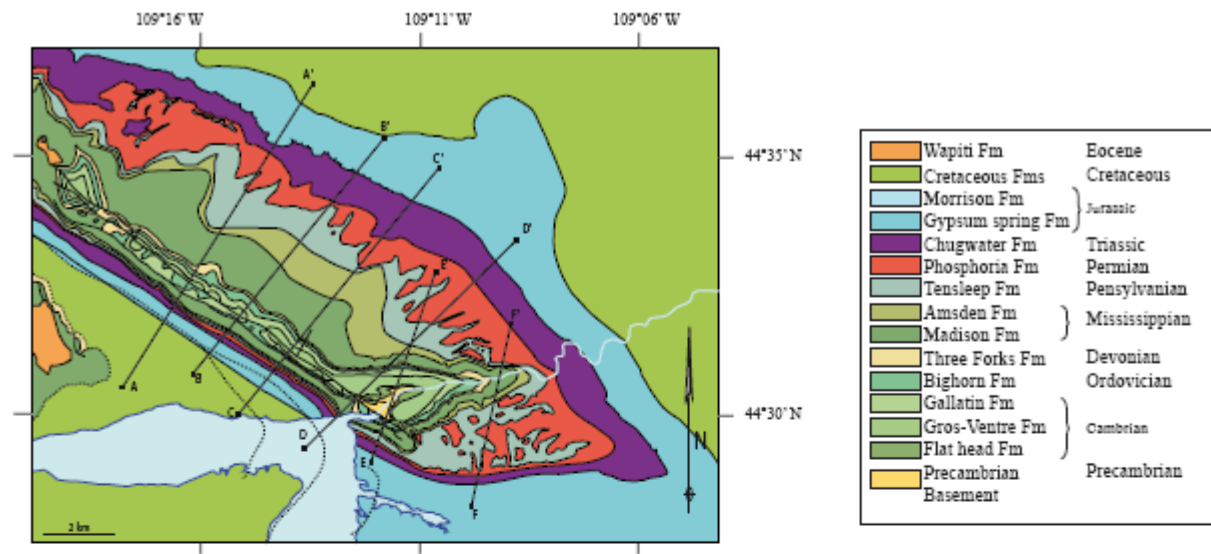










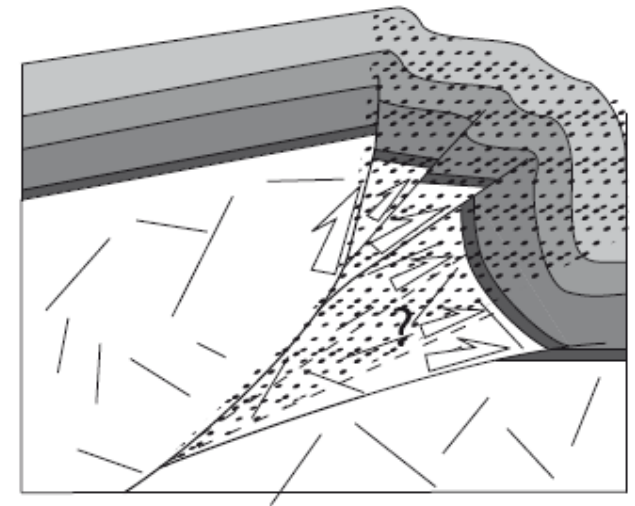
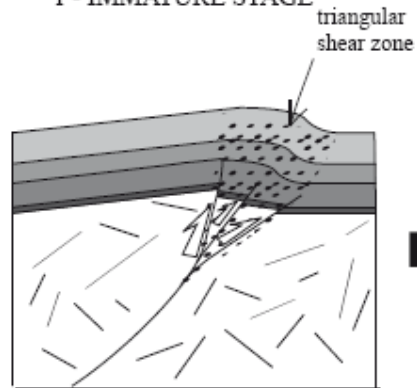
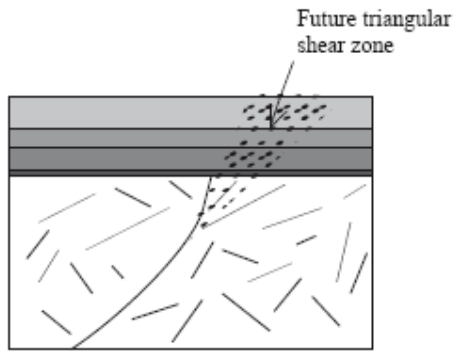


Beaudoin et al, 2012

a

0 - INITIAL STAGE

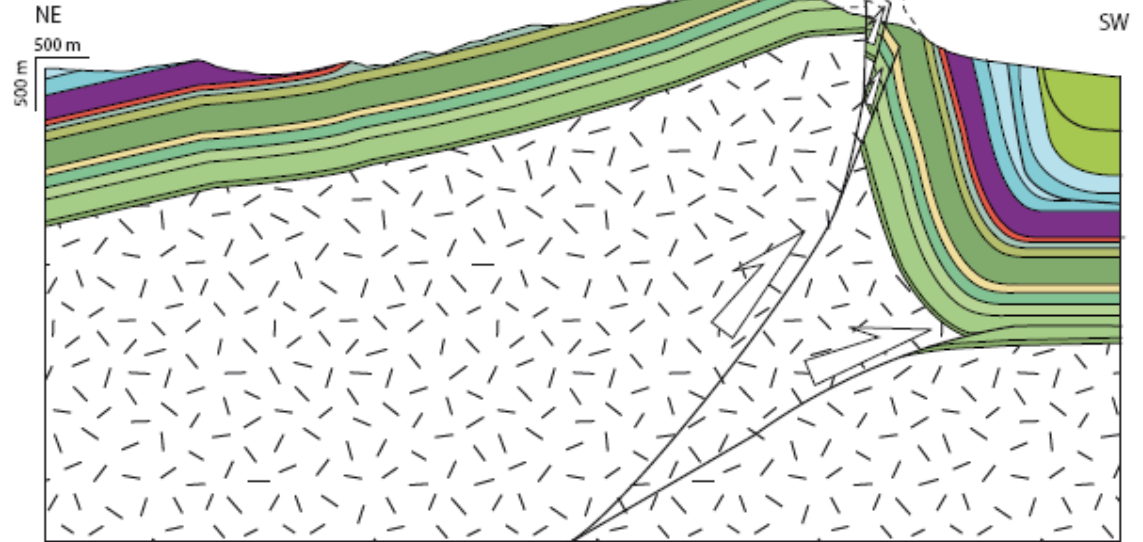
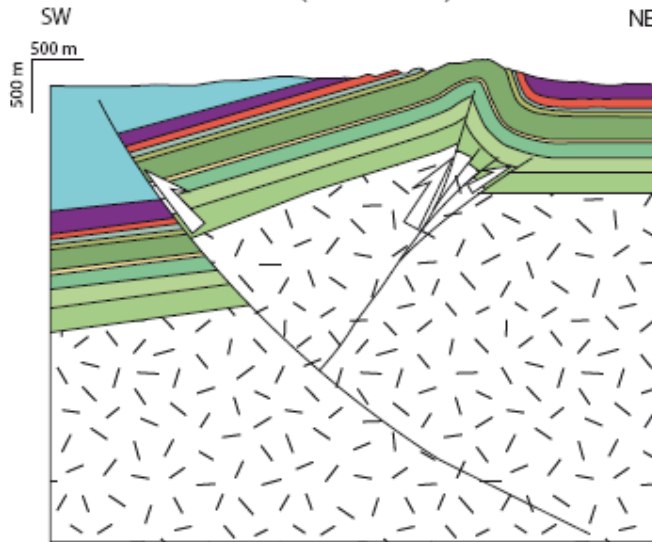
1 - IMMATURE STAGE



b

SMA  
(IMMATURE)

RMA  
(MATURE)



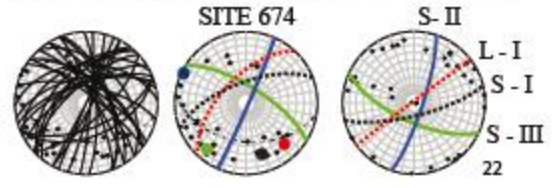
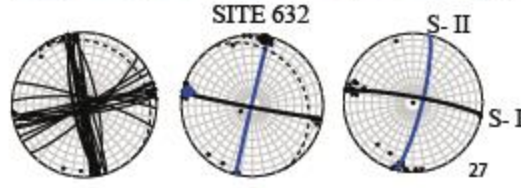
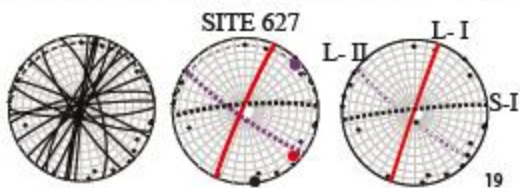
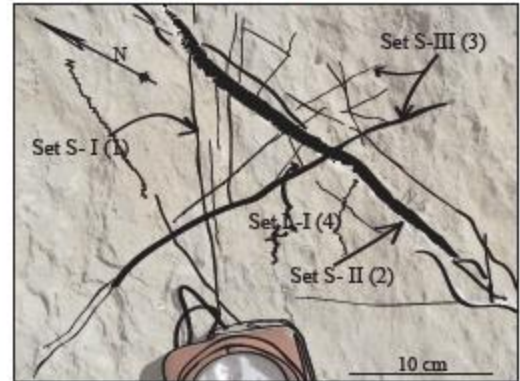
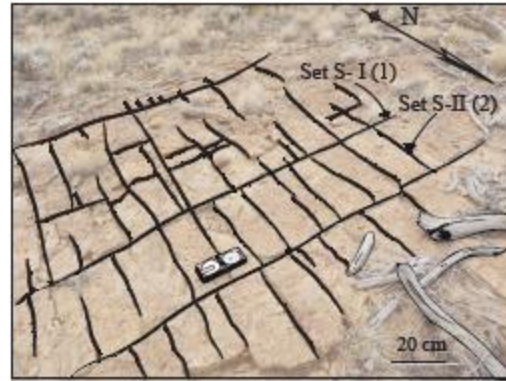
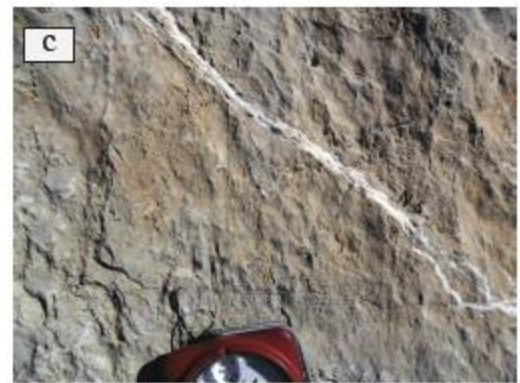




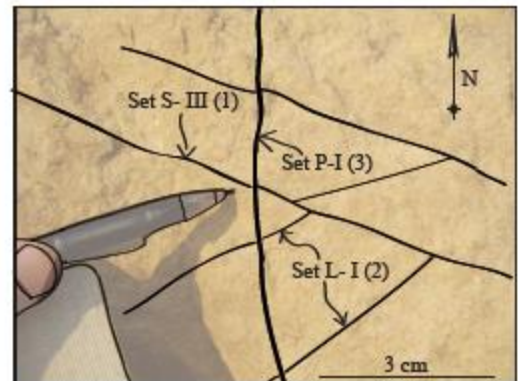
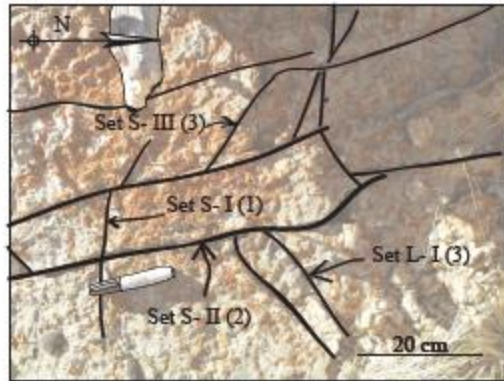
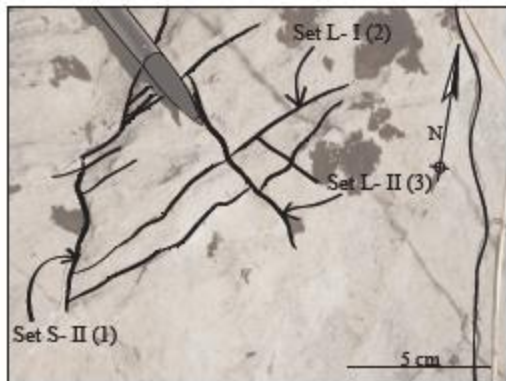
## ATTENTION

YOU ARE ENTERING GRIZZLY BEAR COUNTRY!  
PLEASE TAKE THE NECESSARY PRECAUTIONS.  
IF YOU WOULD LIKE TO LEARN MORE ABOUT  
THE GRIZZLY BEAR AND YOUR SAFETY, PLEASE  
CONTACT THE CODY OFFICES OF THE BLM, U.S.  
FOREST SERVICE OR WYOMING GAME AND FISH.





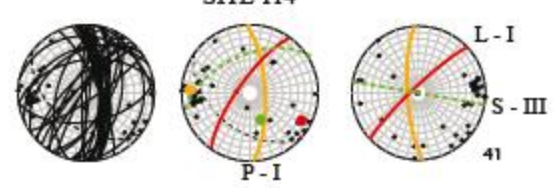
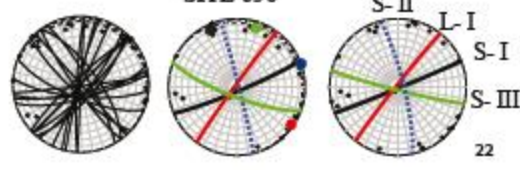
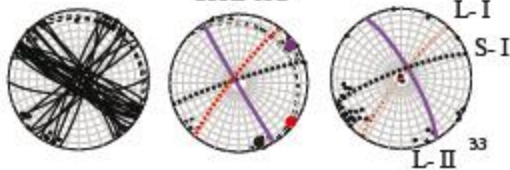


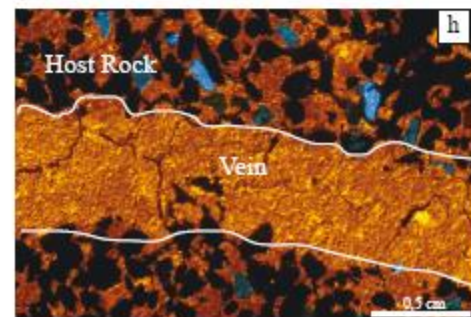
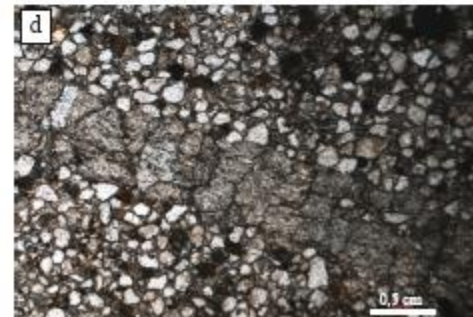
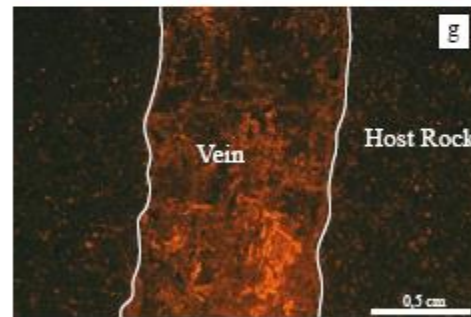
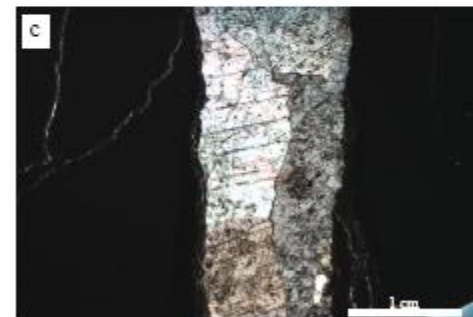
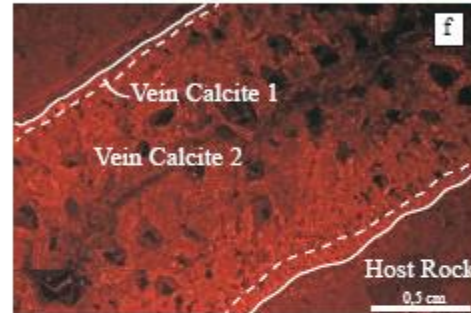
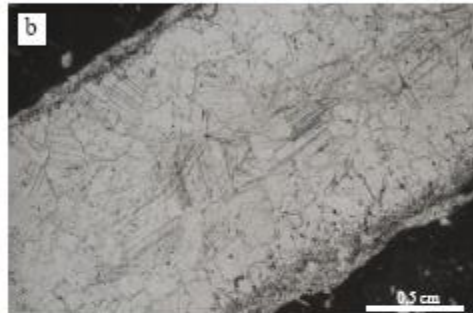
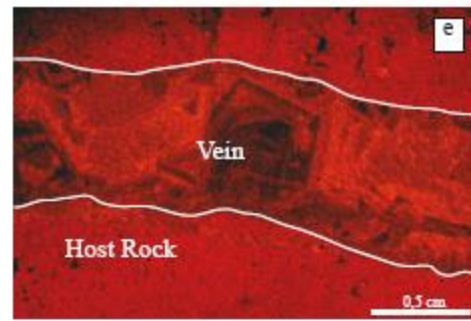
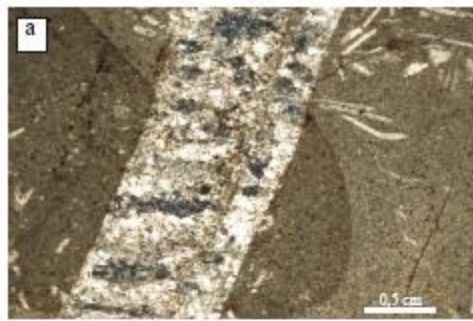


SITE 652

SITE 656

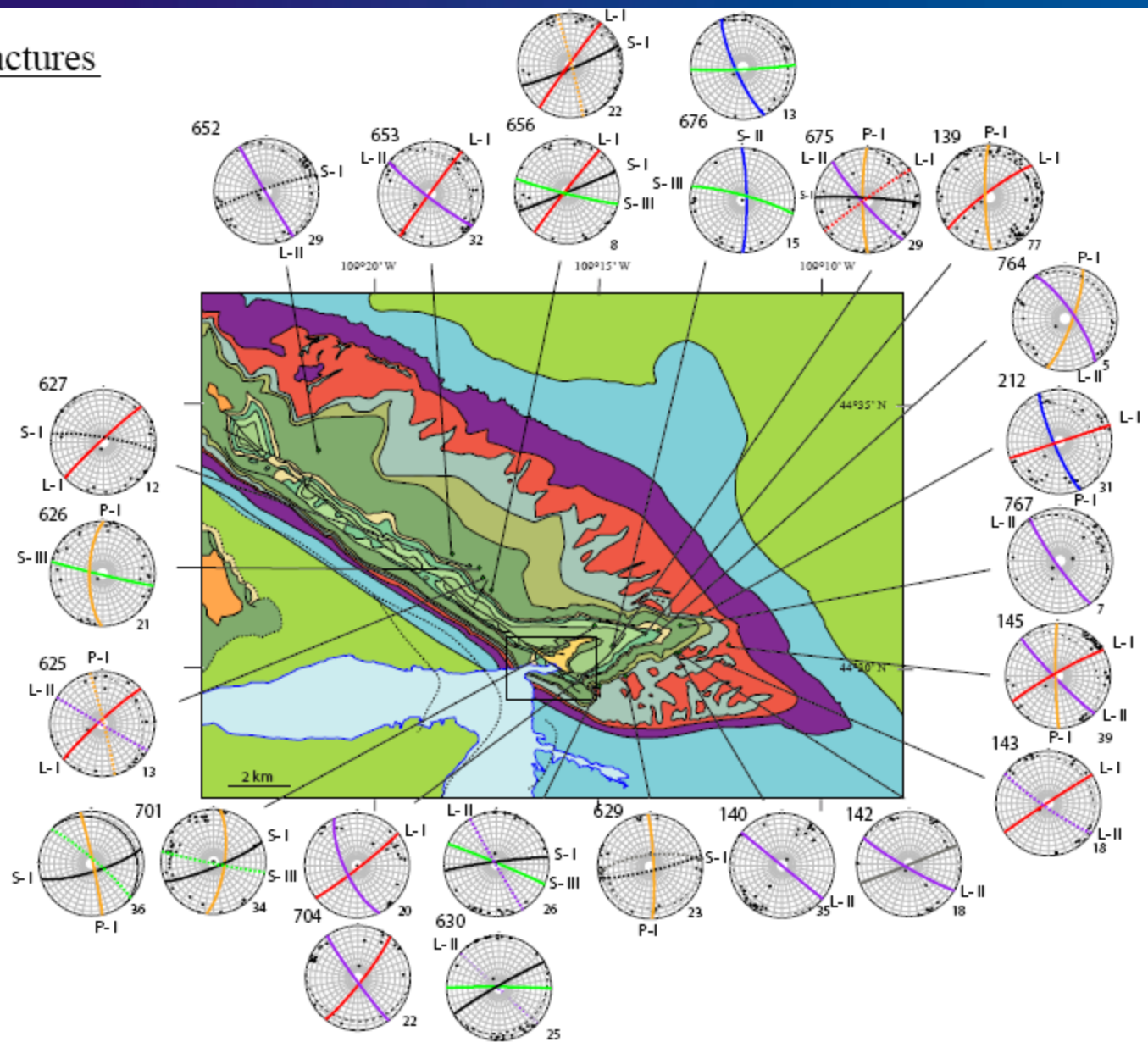
SITE 114

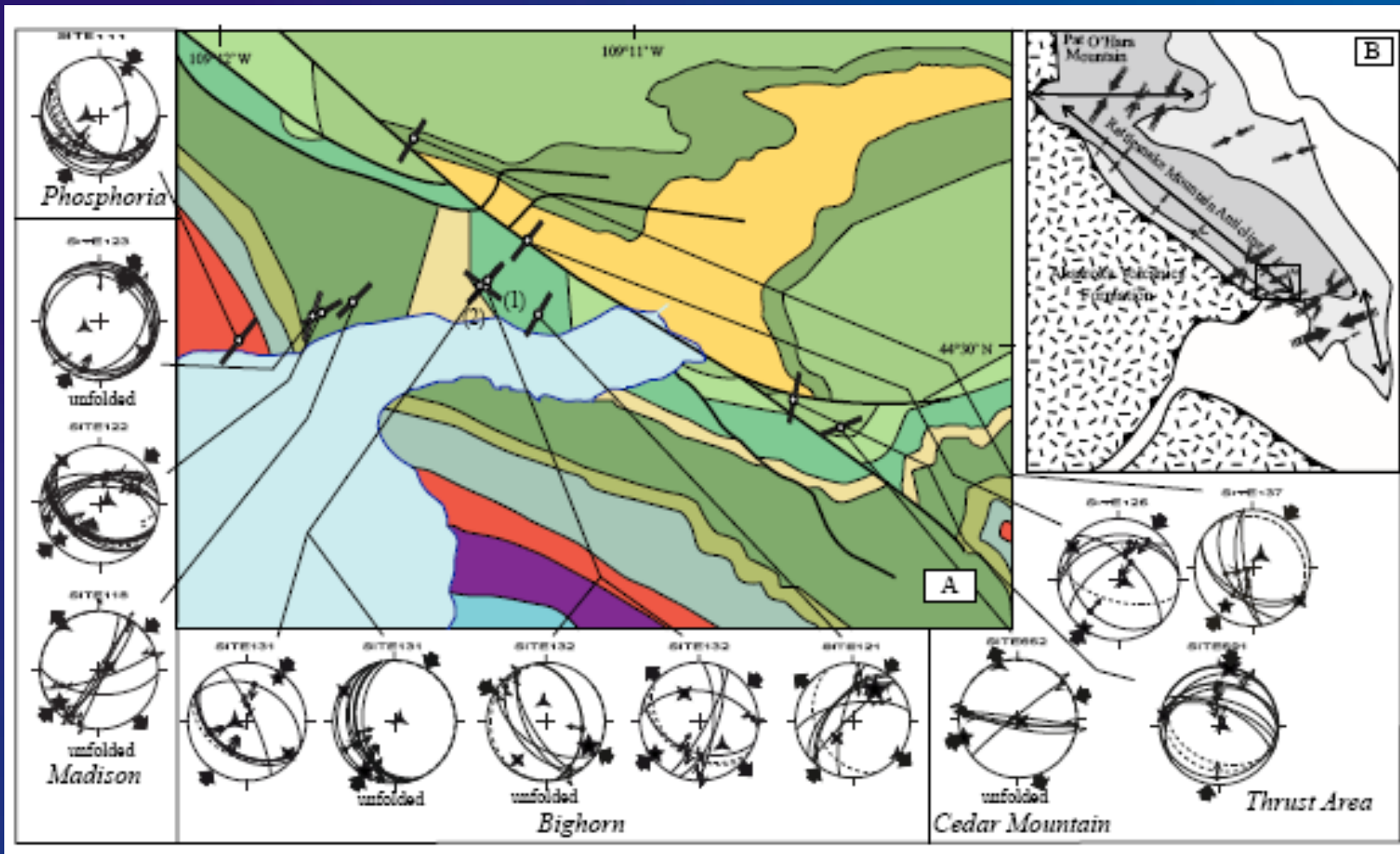


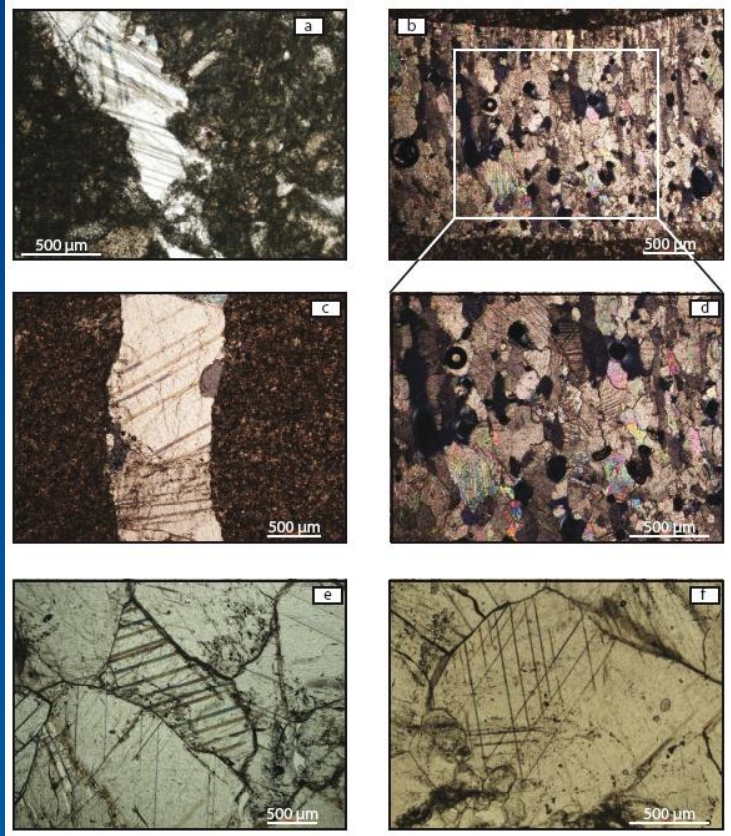
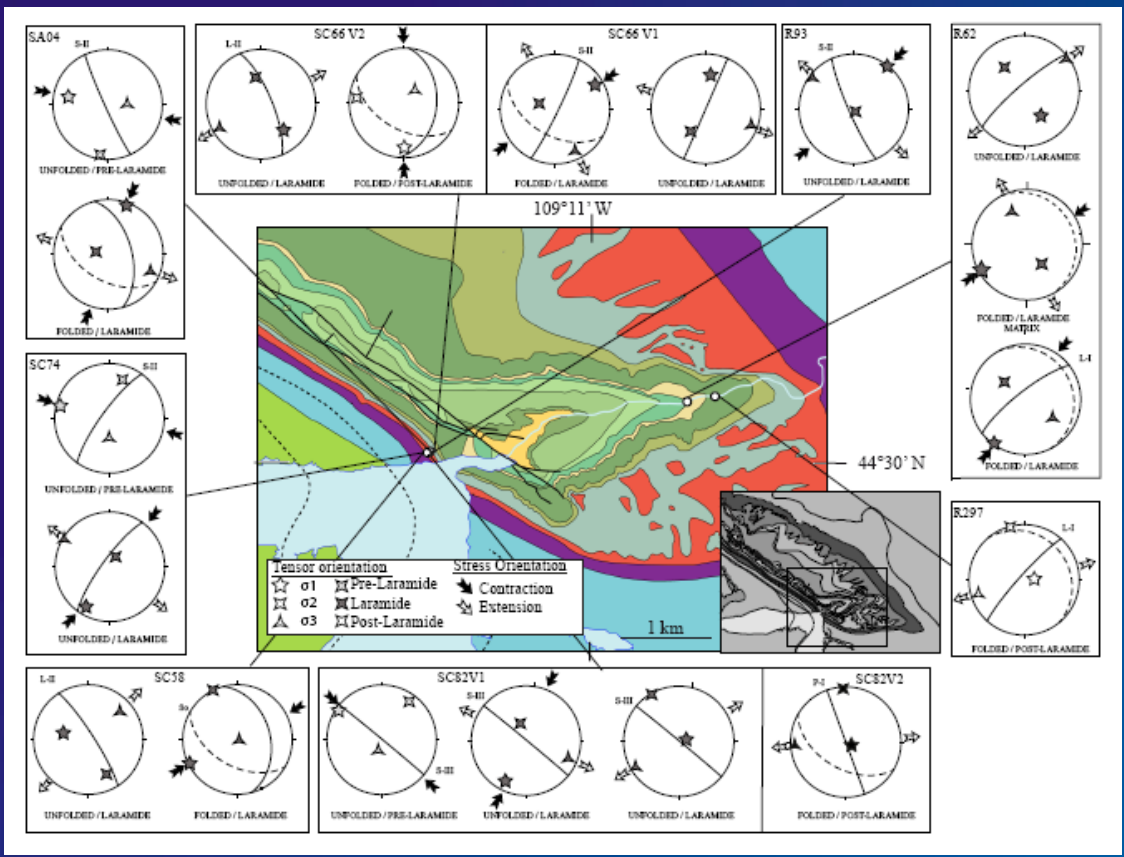















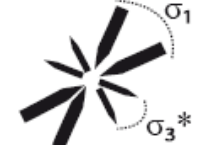


# Fold-scale fractures







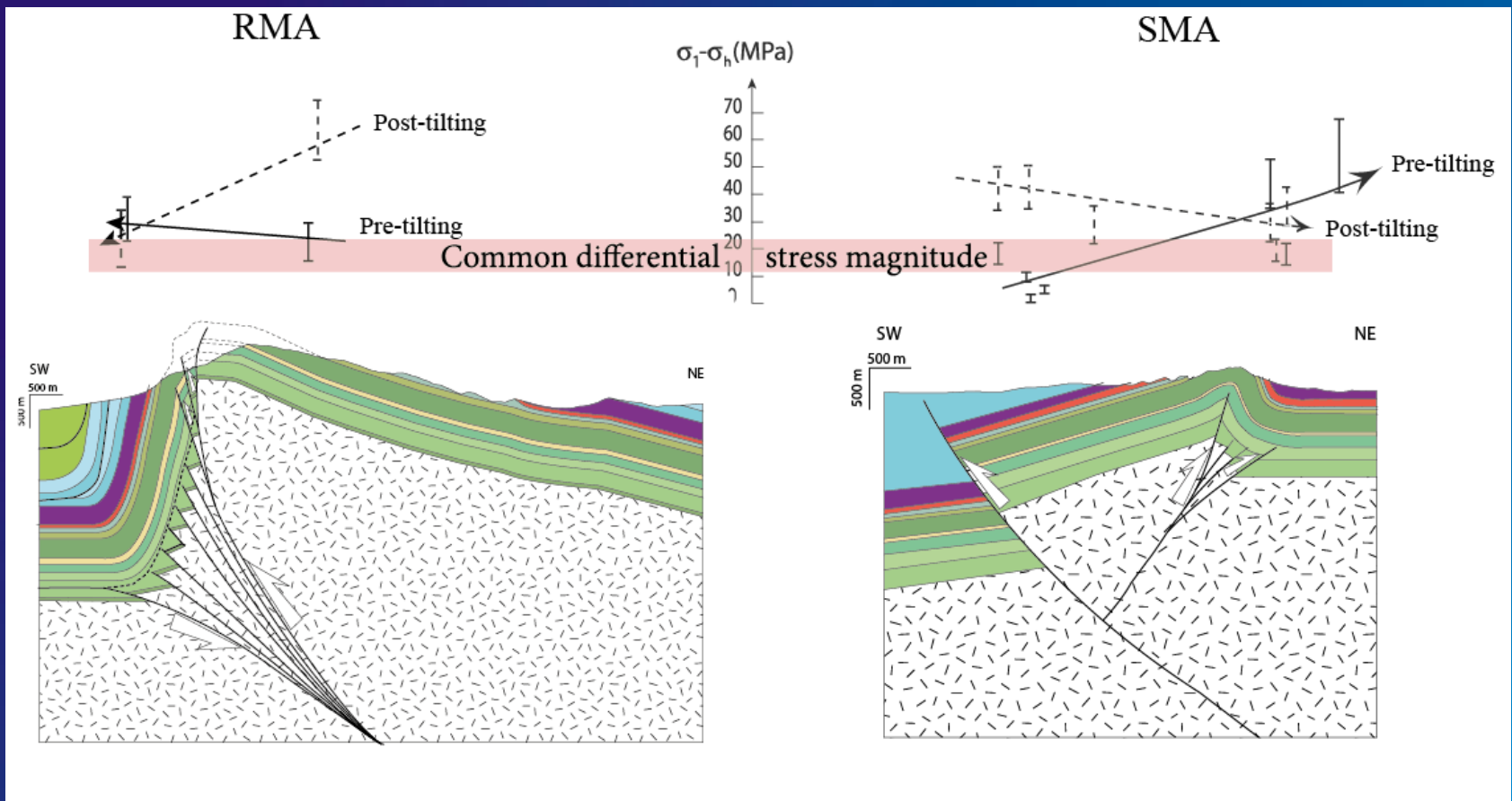


Fracture set	Mean strike of fractures	Paleostress from fractures	Paleostress from striated microfaults	Paleostress from calcite twins	Related Tectonic events
Set S-I	090°E to 060°E				Sevier layer-parallel shortening
Set S-II	180°E to 020°E				Formation of the flexural foreland basin
Set S-III	110°E				Sevier layer-parallel shortening
Set L-I	045°E				Laramide layer-parallel shortening
Set L-II	135°E				Local curvature-related extension
Set L-III	045°E				Late stage of fold tightening
Set P-I	180°E to 160°E				Basin and Range extension

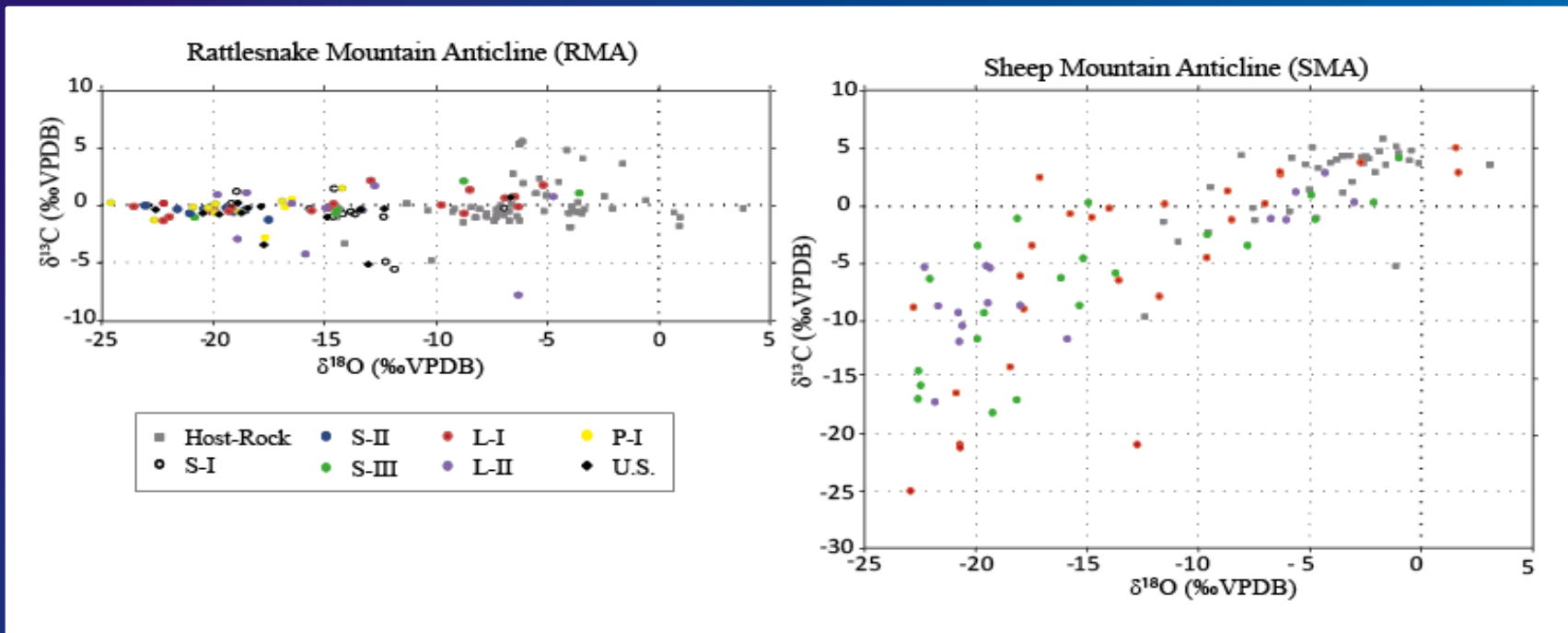
Pre-Laramide

Laramide

Post-Laramide

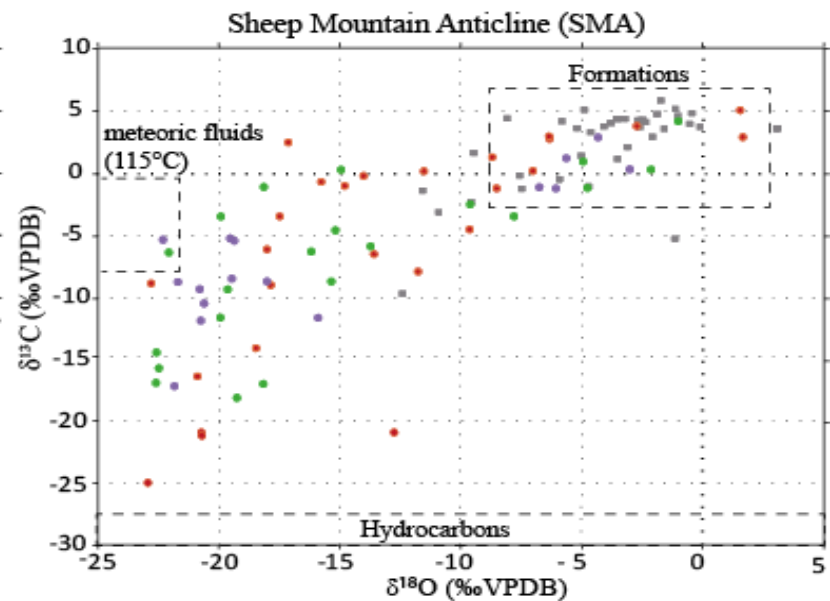
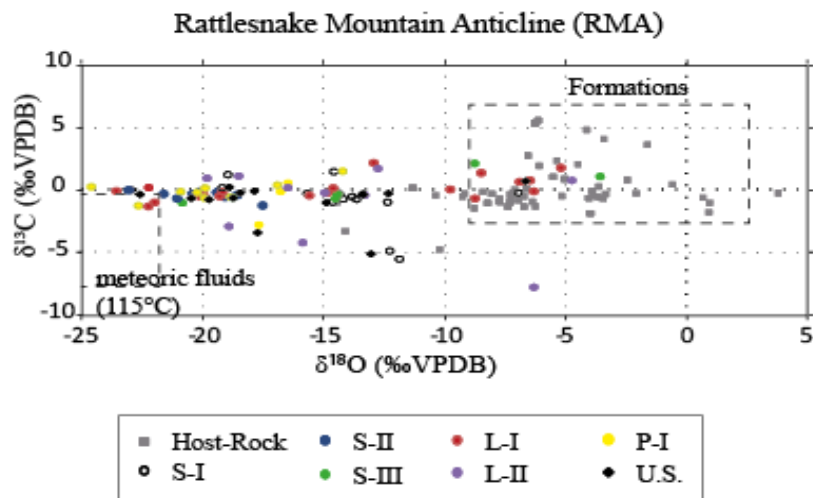


# O, C stable isotopic signatures of fluids





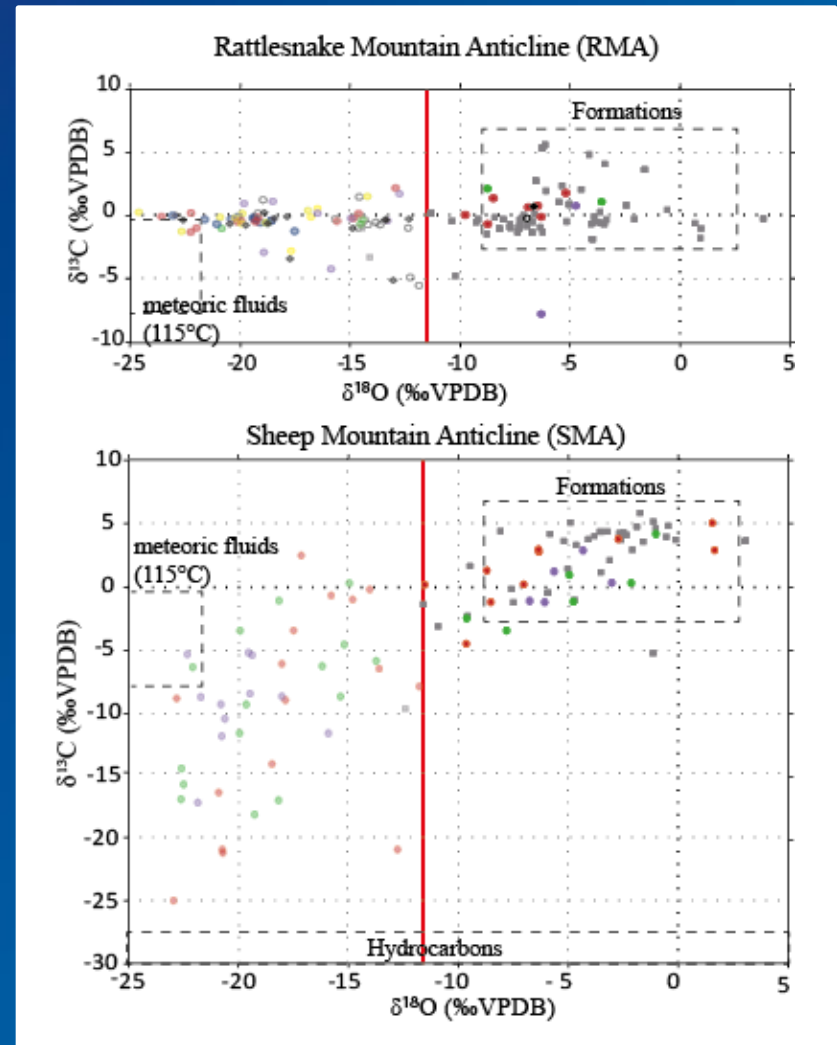
# O, C stable isotopic signatures of fluids



# Defining the fluid system

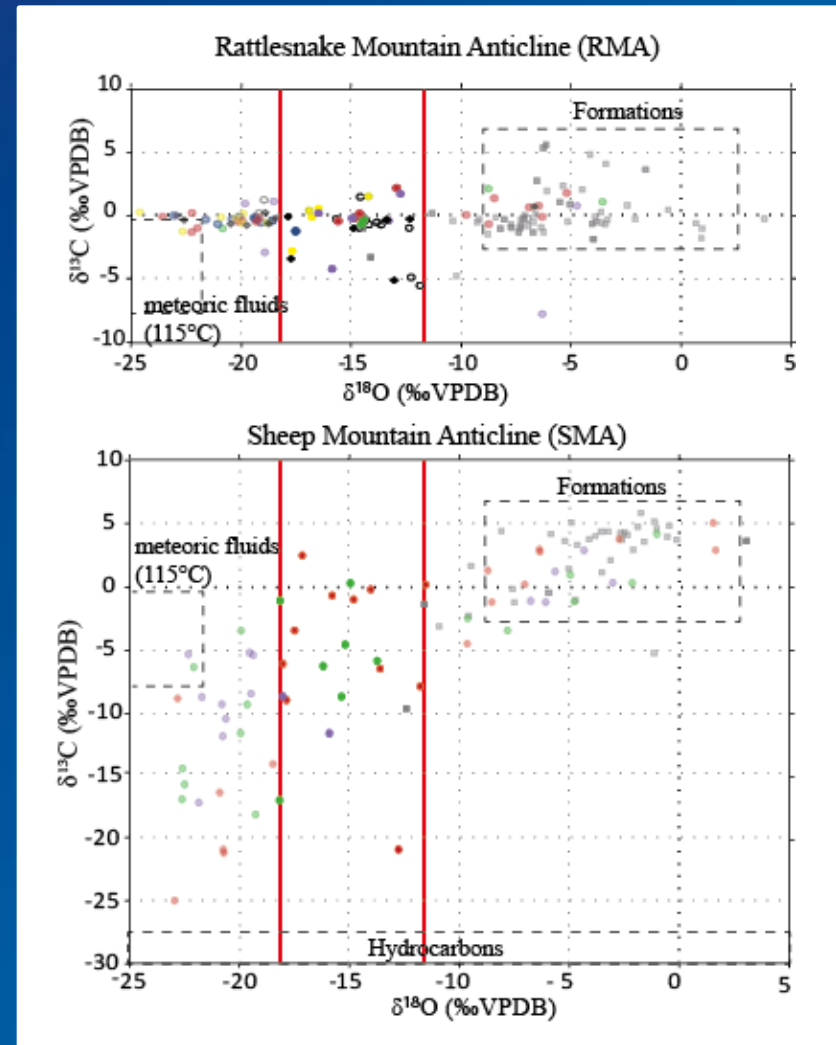
Three types of precipitating fluids:

- Total isotopic and thermal equilibrium with host-rock



# Defining the fluid system

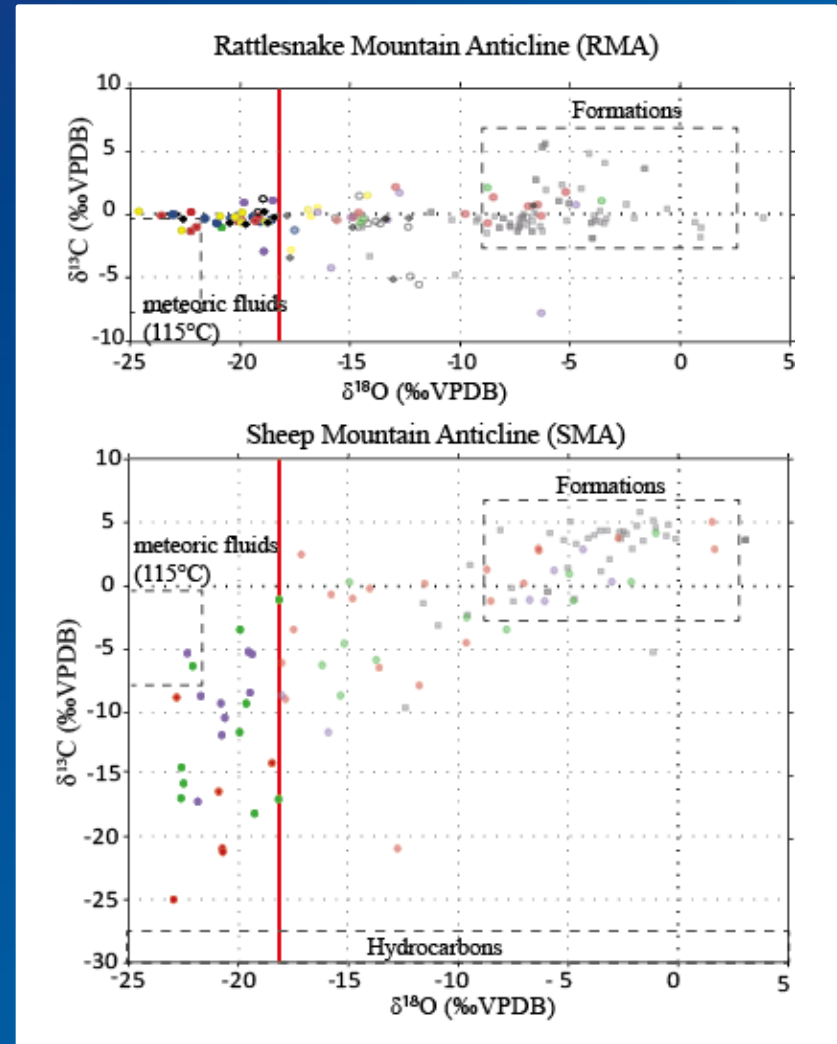
- \* Total isotopic and thermal equilibrium with host-rock
- \*  $\delta^{18}\text{O}$  depletion but thermal equilibrium with host-rock

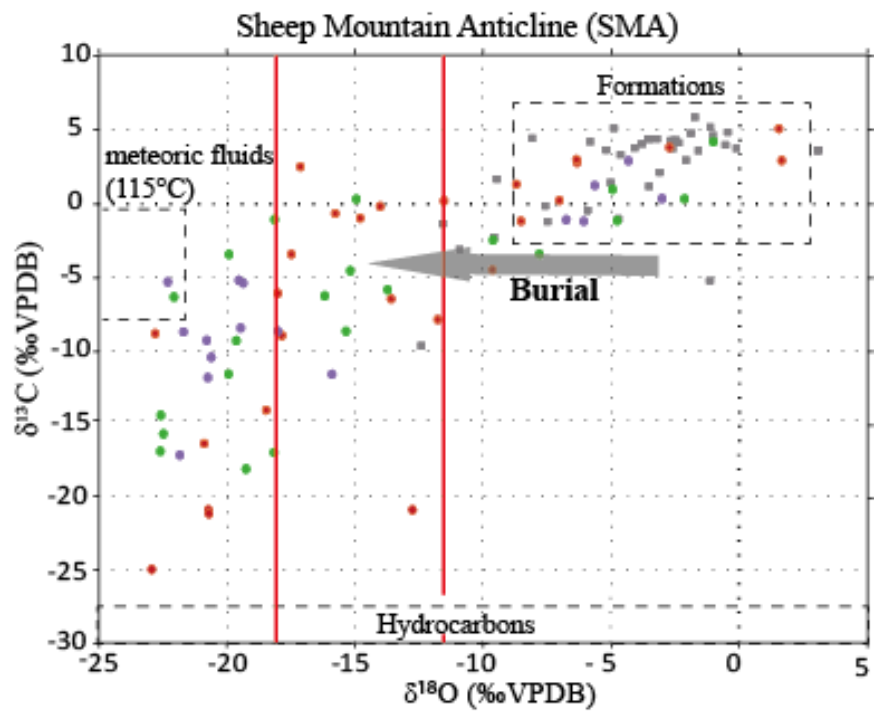
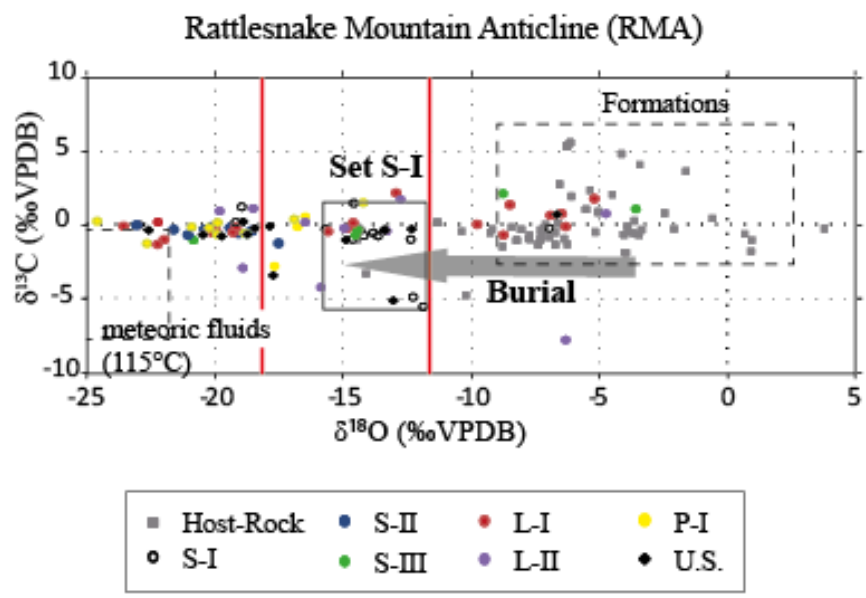




# Defining the fluid system

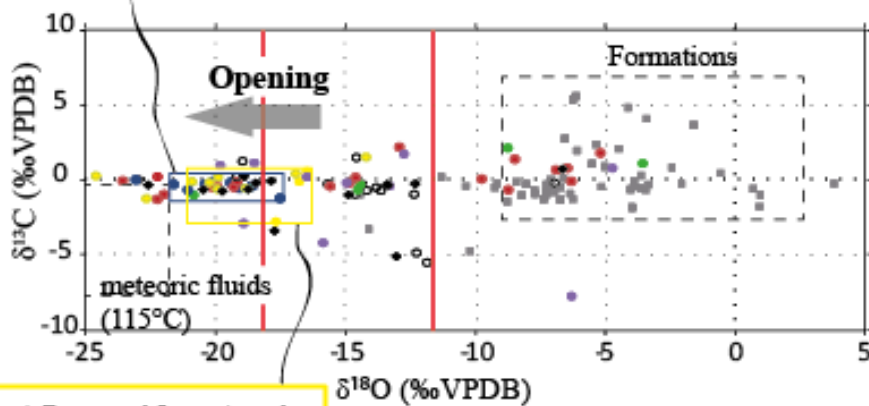
- \* Total isotopic and thermal equilibrium with host-rock
- \*  $\delta^{18}\text{O}$  depletion but thermal equilibrium with host-rock
- \* High  $\delta^{18}\text{O}$  depletion and thermal disequilibrium with host-rock





**Syn-flexure**

**Rattlesnake Mountain Anticline (RMA)**

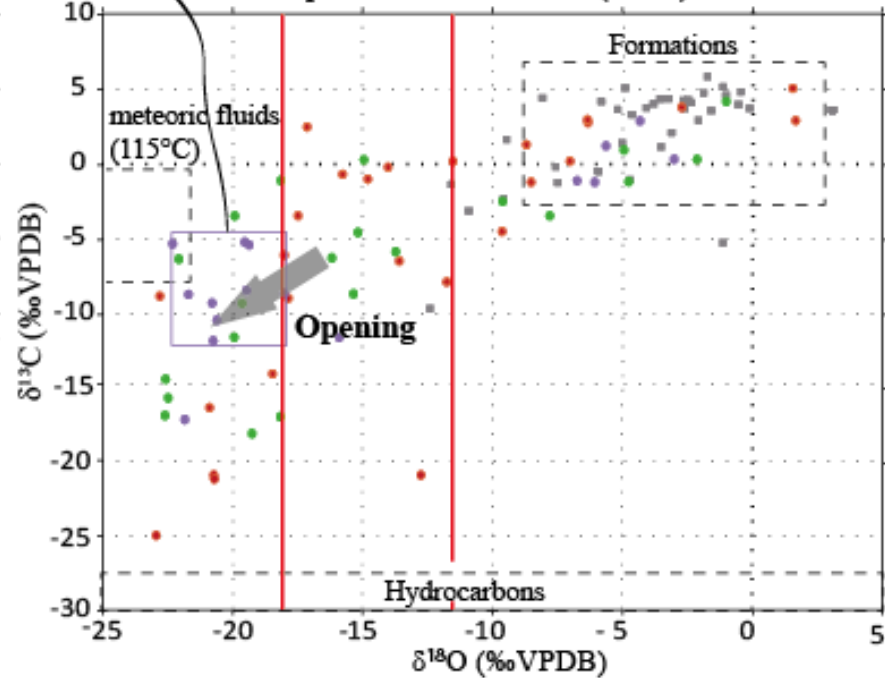


**Post-Laramide extension**



**Syn-folding**

**Sheep Mountain Anticline (SMA)**

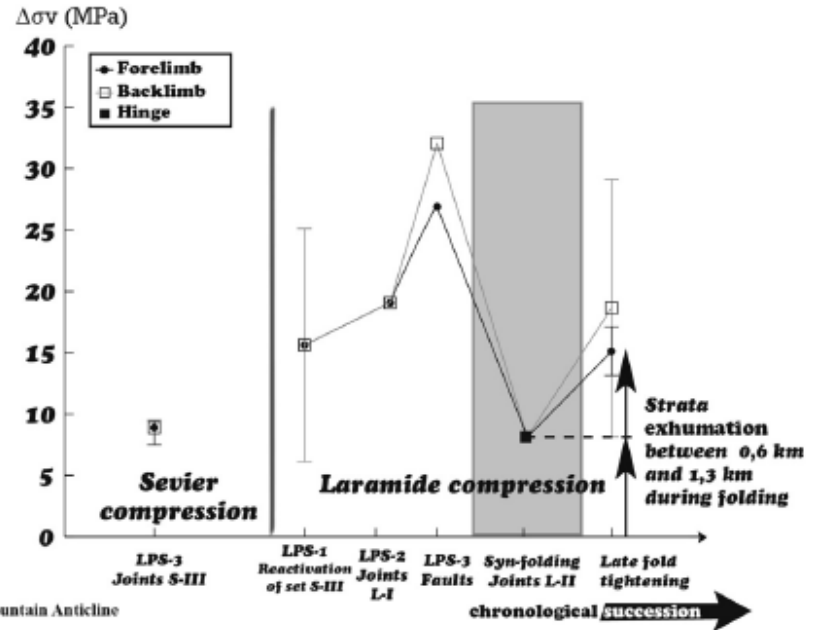




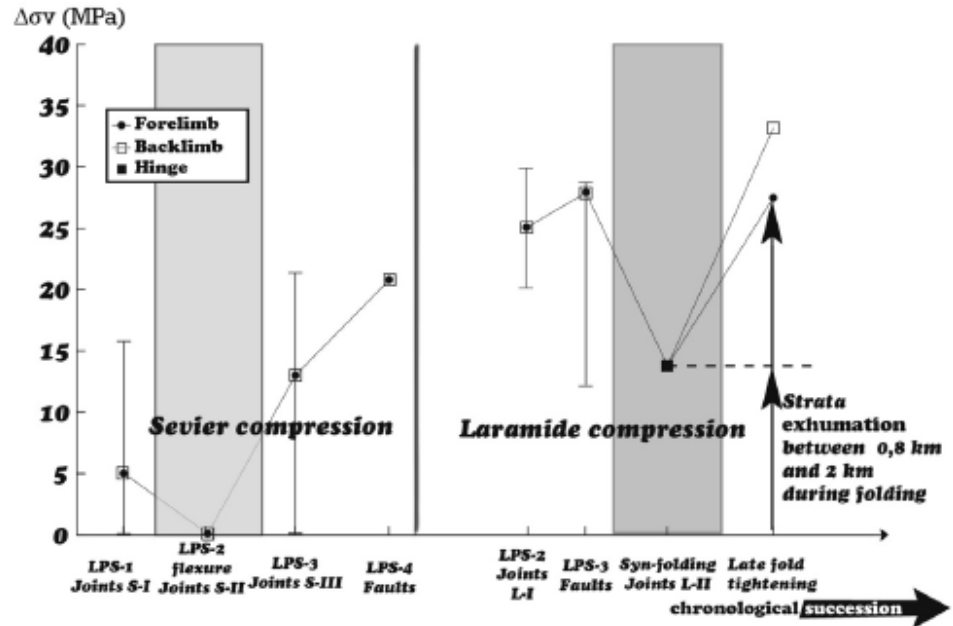
# Comparison of $\Delta\sigma_v$ evolution in SMA and RMA

- Coeval release of fluid overpressure during folding
- Same level of overpressure once normalized to depth

a) Sheep Mountain Anticline



b) Rattlesnake Mountain Anticline



# Some brief conclusions ...

## 1. General

Interest/requirement of a multi-source approach

Interest/requirement of a multi-scale approach  
(from micro-scale to fold scale, then to basin scale)

# Some brief conclusions ...

## 2. More specific

First integrated picture of the evolution of stress, strain and pore fluid (over) pressure during folding

Reliability and power of studies of sub-seismic fracture populations for paleo-hydrological reconstructions  
→ Complement fault zone paleo-hydrological studies

Feedbacks between deformation and paleo-hydrology, role of tectonic style (thick-skinned vs thin-skinned)

→ Next step : fluid flow modelling





Thank you for your attention...

### Suggested readings :

Amrouch K., Lacombe O., Bellahsen N., Daniel J.-M. & Callot J.P., 2010, Stress/strain patterns, kinematics and deformation mechanisms in a basement-cored anticline : Sheep Mountain anticline (Wyoming, USA). **Tectonics**, 29, TC1005

Amrouch K., Robion P., Callot J.-P., Lacombe O., Daniel J.-M., Bellahsen N. & Faure J.-L., 2010, Constraints on deformation mechanisms during folding provided by rock physical properties: a case study at Sheep Mountain anticline (Wyoming, USA). **Geophys. J. Int.**, 182, 1105-1123

Amrouch K., Beaudoin N., Lacombe O., Bellahsen N. & Daniel J.M., 2011, Paleostress magnitudes in folded sedimentary rocks. **Geophys. Res. Lett.**, 38, L17301

Beaudoin N., Bellahsen N., Lacombe O. & Emmanuel L., 2011, Fracture-controlled paleohydrogeology in a basement-cored, fault-related fold: Sheep Mountain anticline (Wyoming, USA). **Geochem. Geophys. Geosyst.**, 12, Q06011

Beaudoin N., Lacombe O., Bellahsen N., Amrouch K. & Daniel J.M., 2014. Evolution of fluid pressure during folding and basin contraction in overpressured reservoirs : insights from the Madison-Phosphoria carbonate formations in the Bighorn basin (Wyoming, USA). **Marine and Petroleum Geology**, 10.1016/j.marpetgeo.2013.12.009

Beaudoin N., Bellahsen N., Lacombe O., Emmanuel L. & Pironon J., 2014. Crustal-scale fluid flow during the tectonic evolution of the Bighorn Basin (Wyoming, USA). **Basin Research**, doi: 10.1111/bre.12032